N-I

AD

RSIC-820

ANALYSIS OF THERMAL STRESSES AND METAL MOVEMENT DURING WELDING

by

Koichi Masubuchi
F. B. Simmons
R. E. Monroe

Contract No. DA-01-021-AMC-14693(Z)
Battelle Memorial Institute
505 King Avenue
Columbus, Ohio 43201

July 1968

This document has been approved for public release and sale; its distribution is unlimited.

'O PRICE $ _____

STI PRICE(S) $ _____

Hard copy (HC) _ ____

Microfiche (MF) _____

3 July 65

REDSTONE SCIENTIFIC INFORMATION CENTER
REDSTONE ARSENAL, ALABAMA

JOINTLY SUPPORTED BY

U.S. ARMY MISSILE COMMAND

GEORGE C. MARSHALL SPACE FLIGHT CENTER

N68-37857

FACILITY FORM 602

(ACCESSION NUMBER)	(THRU)
155	1
(PAGES)	(CODE)
TMX 61300	15
(NASA CR OR TMX OR AD NUMBER)	(CATEGORY)

FORM AMSMI-R-78, 1 NOV 65

DISPOSITION INSTRUCTIONS

Destroy this report when it is no longer needed. Do not return it to the originator.

DISCLAIMER

The findings in this report are not to be construed as an official Department of the Army position unless so designated by other authorized documents.

10 July 1968 RSIC-820

ANALYSIS OF THERMAL STRESSES AND METAL MOVEMENT DURING WELDING

by

Koichi Masubuchi
F. B. Simmons
R. E. Monroe

Contract No. DA-01-021-AMC-14693(Z)
Battelle Memorial Institute
505 King Avenue
Columbus, Ohio 43201

Research Branch
Redstone Scientific Information Center
Research and Development Directorate
U. S. Army Missle Command
Redstone Arsenal, Alabama 35809

ABSTRACT

A literature survey on thermal stresses during welding and buckling after welding is described. From the analyses found, a computer program was developed to calculate thermal stresses and resulting residual stresses due to a moving heat source. This program is included in the appendix.

Studies at Marshall Space Flight Center on three-dimensional movement during welding of flat plate specimens are summarized and interpreted on the basis of the Battelle literature survey and computer analysis. It is concluded that local metal movement during welding appears to be caused by bending moment and that general metal movement is apparently caused by buckling. Future programs to improve the present analysis are recommended.

FOREWORD

This is the final report on a program to analyze weld distortion in Saturn V structures under Contract No. DA-01-021-AMC-14693(Z) for the Manufacturing Engineering Laboratory of the George C. Marshall Space Flight Center, Huntsville, Alabama.

Information in this report comes from documents and data supplied by the Marshall Space Flight Center of the National Aeronautics and Space Administration and presently available literature.

CONTENTS

CONTENTS (Concluded)

ILLUSTRATIONS

ILLUSTRATIONS (Continued)

ILLUSTRATIONS (Concluded)

Section I. INTRODUCTION

A major problem in the fabrication of space vehicle structures is distortion caused by welding. These structures include a number of structural components that must be fabricated to close dimensional tolerances. Unacceptable distortion that occurs during welding of joints in these structures is often impossible to correct without removing the weld joint. Distortion can also cause mismatch of weld joints, which results in reduction of the joint strength.

Empirical approaches to the problem of distortion have neither successfully prevented distortion nor given an understanding of thermal and mechanical causes of distortion. Yet, before this program no organized analytically oriented research had been conducted on distortion control of space vehicle structures.

Several aerospace companies have encountered distortion problems during fabrication of Saturn V components. Although production practices have been developed to overcome these problems, these again are empirical solutions. There has been no opportunity to develop theoretical knowledge of these problems. The objective of the Battelle study was to theoretically analyze certain distortion phenomena encountered during the fabrication of Saturn V structures and to correlate this analysis with empirical data developed during their production. The emphasis of this study was placed on the mathematical analysis of thermal stresses and on metal movement in the thickness direction during fusion welding. The study involved the following phases:

1) Identification of weld distortion problems
2) Literature survey and analysis of present data on the basis of presently available formulas
3) Formulation of experimental programs to improve the theoretical analysis
4) Recommendation of future programs on distortion control.

The objective of the first phase was to identify weld distortion problems in the Saturn V structures. During discussions with National Aeronautics and Space Administration (NASA) monitors on this research program, it was decided that the Battelle study would be focused on the analysis of metal movement around the arc during welding.

In the previous fabrication of Saturn V fuel tanks, mismatch of joints was experienced during the welding of girth joints, especially the joint between the cylindrical parallel section and the transition ring. Before the initiation of the Battelle study, an experiment was conducted at Marshall Space Flight Center (MSFC) to measure metal movement during girth welding of a cylinder 133 inches in diameter and 12 inches high. In this experiment it was found that there is metal movement in the thickness direction near the arc. A buckling distortion upon completion of the weld was also observed. Therefore it was decided to direct the Battelle research toward a study of these two problems, especially the metal movement during welding.

A literature survey was made to obtain useful information on thermal stresses during welding and buckling after welding. Section III presents the results of this survey as a state-of-the-art analysis of weld distortion. Following the survey, the existing distortion data on the Saturn V structure were analyzed on the basis of presently available analyses. Using these analyses, a computer program for analyses of thermal stress was developed. Section IV describes results of the computer analysis. The FORTRAN computer program is given in the appendix.

On the basis of the above survey, Battelle recommended that MSFC conduct studies on three-dimensional movement during welding of flat-plate specimens. Flat plates were recommended because they yield the most fundamental information on thermal stress during welding and buckling after welding. Section V of this report presents summaries of the experimental results. Section VI discusses how the experimental results can be interpreted on the basis of the literature survey and the analysis conducted at Battelle.

The entire program is summarized and pertinent conclusions are presented in Section VII. On the basis of the information obtained in this research, recommendations are made for future research programs. This discussion is given in Section VIII.

Section II. GENERAL DISCUSSION OF FABRICATION OF SATURN V

The Saturn V is a giant three-stage rocket designed to send the Apollo spacecraft toward the moon. It stands 362 feet high, weighs 6.1 million pounds, and has a maximum diameter of 33 feet. Its fabrication includes thousands of feet of welding and introduces many welding problems. Several articles have been written describing the fabrication and welding of the Saturn V structure. [1-5] The following is a very limited description of steps in the fabrication of the first stage (S-1C) that are most directly related to the Battelle study.

The S-1C is a semi-monocoque structure measuring 138 feet in length by 33 feet in diameter. The structure has various components including welded fuel and oxidizer tanks. These tanks are fabricated from two aluminum alloys, 2219 for the S-1C and 2014 for the S-II and S-IV stages.

The Battelle study was related primarily to these fuel and oxidizer tanks which are of all-welded construction. Either gas metal-arc (GMA) or gas tungsten-arc (GTA) welding is used on these assemblies except for the inside baffles. Both tanks are constructed by attaching skin cylinders to upper and lower head assemblies by means of a Y-shaped transition ring. The unit serves as a transition piece between bulkheads and skins and between the thrust structure and forward skirt. This design is illustrated in Figure 1.

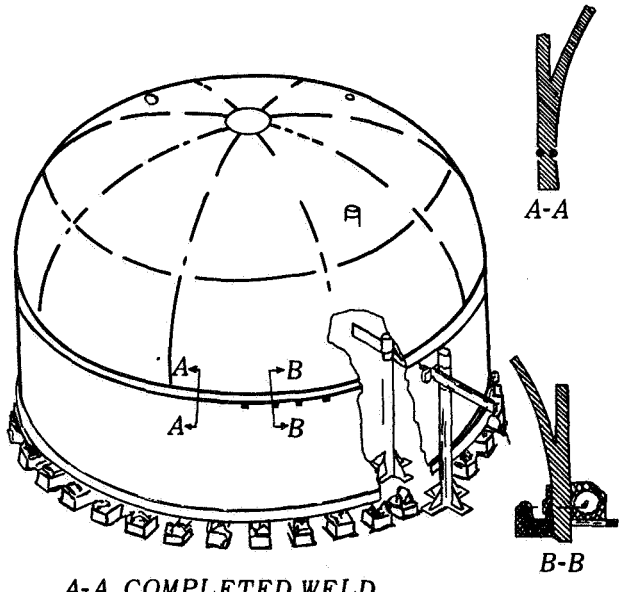

A-A COMPLETED WELD
B-B STRAP ALIGNMENT CLAMP

FIGURE 1. WELDING OF THE TRANSITION RING

Welding between the transition ring and cylindrical sections is probably the most critical on the S-1C stage and thus the most troublesome from a distortion viewpoint. Three vertical joints, 47 inches long, are automatically GMA welded to join three forged and rolled billets. An excess of 0.140 inch of metal is allowed for weld shrinkage at each joint. During final assembly of the tanks, the transition ring is joined to the cylindrical parallel section by a GMA or GTA weld made from both sides in the horizontal position.

Section III. PRESENT STATE OF THE ART OF THE ANALYSIS OF WELD DISTORTION

This section describes the state of the art of the analysis of weld distortion. Emphasis is placed on distortions that occur during butt welding of girth joints of a cylindrical tank.

1. Past Reviews on Weld Distortion and Residual Stresses

Residual stresses and distortion during fabrication of welded structures have been studied by many investigators. Although most studies have been experimental, some analytical studies have been made. Several reviews and books have been written on residual stresses and distortion in weldments and welded structures.

Spraragen and associates prepared a series of comprehensive reviews on residual stress and distortion in welds in 1937 through 1950.[6-8] In 1954, Osgood[9] edited a book on residual stresses in metals and metal construction. Masubuchi wrote a report on measurement of residual stresses in metals and metal structures in 1965.[10] His report emphasized residual stresses in structures in aluminum alloys.

Four books have been published in Japan on residual stresses and distortion in weldments by Naka, Kihara, Masubuchi, Watanabe, and Satoh.[11-14] In Russia several books have been written including one by Okerblom.[15] The Swede, Gunnert, has written a book that covers primarily the residual-stress measuring technique he developed.[16] A group of international authors, Hall, Kihara, Soete, and Wells,[17] published a book in 1967 that summarizes recent work on the effects of residual stresses on brittle fracture of welded steel plates.

Among these past reviews, those which were written by Spraragen et al,[6-8] Kihara and Masubuchi,[12,13] Watanabe and Satoh,[14] and Okerblom[15] contain considerable information on the analysis of weld distortion. However, most of the above reviews cover only welding of mild steel with covered electrodes. Very little is mentioned about other materials, such as high-strength ferrous and nonferrous alloys, or inert-gas metal or tungsten-arc welding processes.

Since 1 July 1967 Battelle has been conducting a 3-year program, supported by a group of industrial companies, to develop analytical methods for prediction of distortion in welded structures.[18] As a part of the program,

Battelle has recently compiled a very extensive and up-to-date bibliography on the subject of weld distortion. Battelle's review covers many materials and many processes and includes literature from eighteen different countries. This is probably the most extensive collection of references available on the subject of weld distortion. Direct access to this review is restricted to supporting companies.

a. General Discussion of Residual Stresses and Distortion in Welded Structures

Residual stresses are those stresses that would exist in a body if all external loads were removed. Residual stresses in metal structures occur for many reasons during various manufacturing stages, including rolling, casting, machining, flame cutting, and welding.

Because a weldment is locally heated by the welding heat source, the temperature distribution in the weldment is not uniform and changes as welding progresses. During the welding cycle, complex strains occur in the weld metal and base metal regions near the weld, both during heating and cooling. The strains produced during heating are accompanied by plastic upsetting.

The stresses resulting from these strains combine and react to produce internal forces that cause bending, buckling, and rotation. It is these displacements that are called distortion.

b. Typical Distributions of Residual Stresses in Weldments

The residual stresses in a welded joint are caused by the contraction of the weld metal and the plastic deformation produced in the base metal region near the weld. Residual stresses in a welded joint are classified as "residual welding stress," which occurs in a joint free from any external constraint, and "reaction stress" (or "locked-in stress"), which is induced by an external constraint. Most of the information on residual stresses has been obtained on arc-welded joints, especially on butt joints in mild steel. Rather limited information is available on residual stresses and distortions in weldments in aluminum alloys. [19-22]

A typical distribution of residual stresses in a butt weld is shown in Figure 2. The stresses of concern are those parallel to the weld direction, designated σ_x, and those transverse to the weld, designated σ_y.

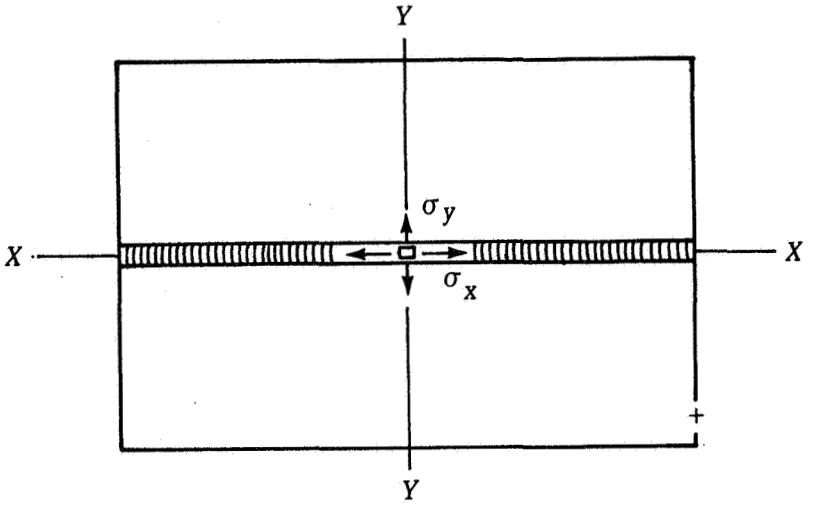

(a) BUTT WELD

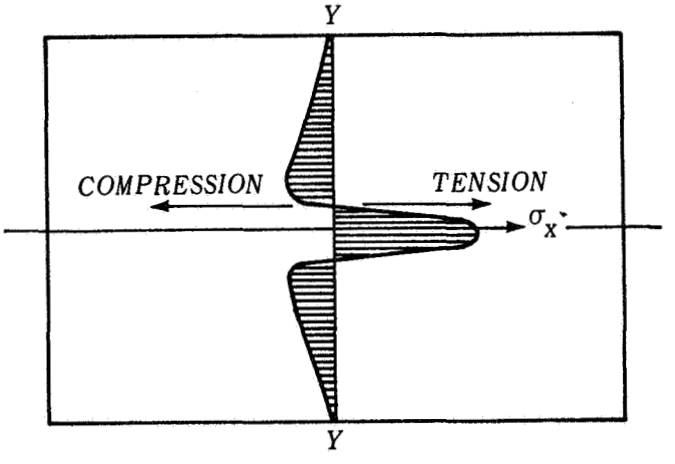

(b) DISTRIBUTION OF σ_x ALONG YY

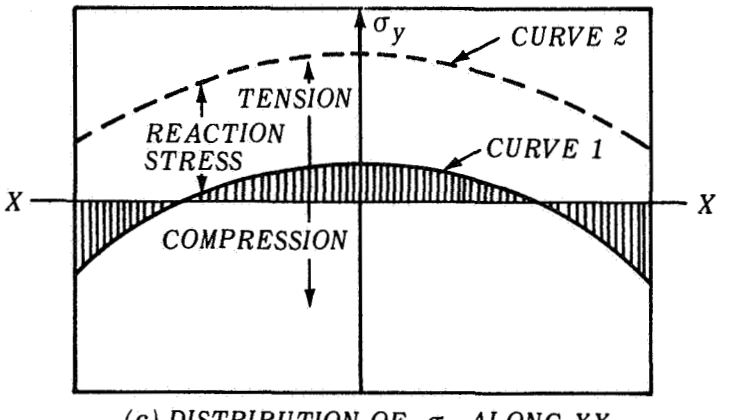

(c) DISTRIBUTION OF σ_y ALONG XX

FIGURE 2. TYPICAL DISTRIBUTION OF RESIDUAL STRESSES IN BUTT WELD

The distribution of the σ_x residual stress along a line transverse to the weld (YY) is shown in Figure 2(b). Tensile stresses of high magnitude are produced in the region of the weld; these taper off rapidly and become compressive at a distance of several times the width of the weld. The weld metal and heat-affected zone try to shrink in the direction of the weld, and the adjacent plate material prevents this shrinkage. The distribution of σ_y residual stress along the length of the weld XX is shown by Curve 1 in Figure 2(c). Tensile stresses of relatively low magnitude are produced in the middle of the joint, and compressive stresses are observed at the end of the joint.

If the contraction of the joint is restrained by an external constraint, the distribution of σ_y is as shown by Curve 2 in Figure 2(c). Tensile stresses, approximately uniform along the weld, are added as the reaction stress. An external constraint, however, has little influence on the distribution of σ_x residual stresses.

The magnitude and distribution of residual stresses in a weld are determined by (1) expansion and contraction characteristics of the base metal and the weld metal during the welding thermal cycle and (2) temperature versus yield-strength relationships of the base metal and the weld metal. Much research on carbon-steel weldments has shown that the maximum residual weld stress is as high as the yield stress of the weld metal. However, in a recent investigation conducted at Battelle,[23] the maximum stresses in high-strength-steel weldments were not as high as the yield strength of the weld metals. In weldments in heat-treated SAE 4340 steel, for example, the maximum residual stresses were around 50,000 to 80,000 pounds per square inch, considerably less than the yield strength of the weld metal (around 150,000 psi) and the base metal (224,000 psi).

Hill[20] investigated residual stresses in butt joints in Alloy 5456-H321 plates welded by the inert-gas-shielded arc-welding process with Alloy 5556 consumable electrodes. Figure 3 shows a typical distribution of longitudinal residual stresses in a 0.5- by 36- by 48-inch panel fabricated by welding two 0.5- by 18- by 48-inch plates. Variation in yield strength of the material with distance from the center line of weld is also shown. The residual tensile stresses in and adjacent to the weld approach the yield strength. These tensile stresses are confined to the region in which the heat of welding has lowered the yield strength of the material.

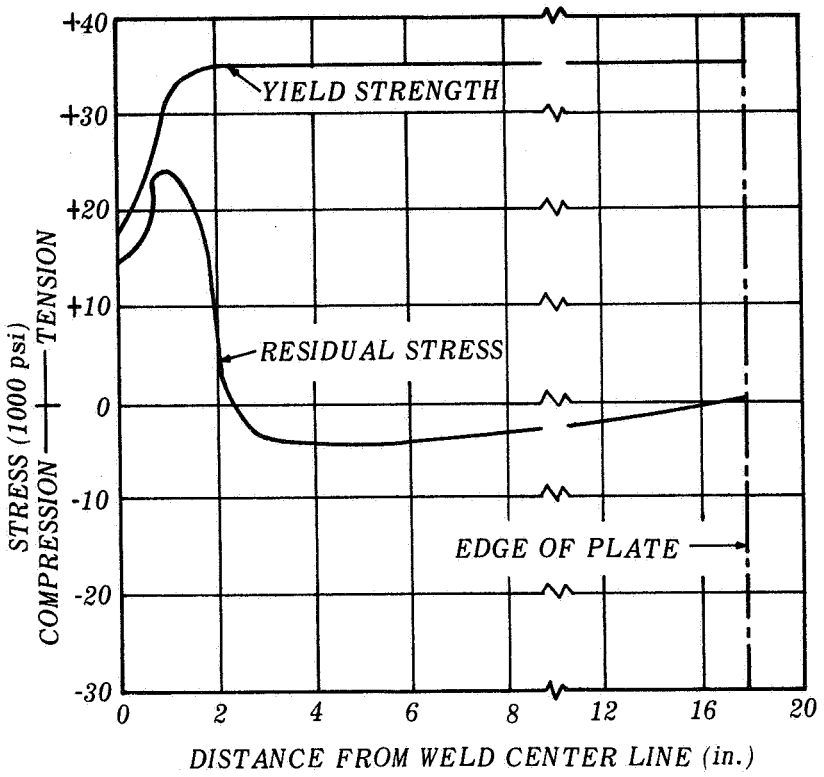

FIGURE 3. DISTRIBUTION OF YIELD STRENGTH AND LONGITUDINAL RESIDUAL STRESSES IN A WELDED 5456-H321 PLATE

c. Fundamental Types of Distortion

The distortion found in fabricated structures is caused by three fundamental dimensional changes that occur during welding, (1) transverse shrinkage that occurs perpendicular to the weld line, (2) longitudinal shrinkage that occurs parallel to the weld line, and (3) an angular change that consists of rotation around the weld line. All three of these dimensional changes are shown in the sketches in Figure 4.

Figure 4(a) shows transverse shrinkage in a simple butt weld. The distribution of the longitudinal residual stress σ_y is shown in Figure 4(b). This stress causes the longitudinal shrinkage shown in the figure. High tensile stresses exist in regions near the weld, and compressive stresses exist in regions away from the weld. This indicates that the longitudinal shrinkage of the weld metal and base metal regions adjacent to the weld are restrained by the surrounding base metal regions.

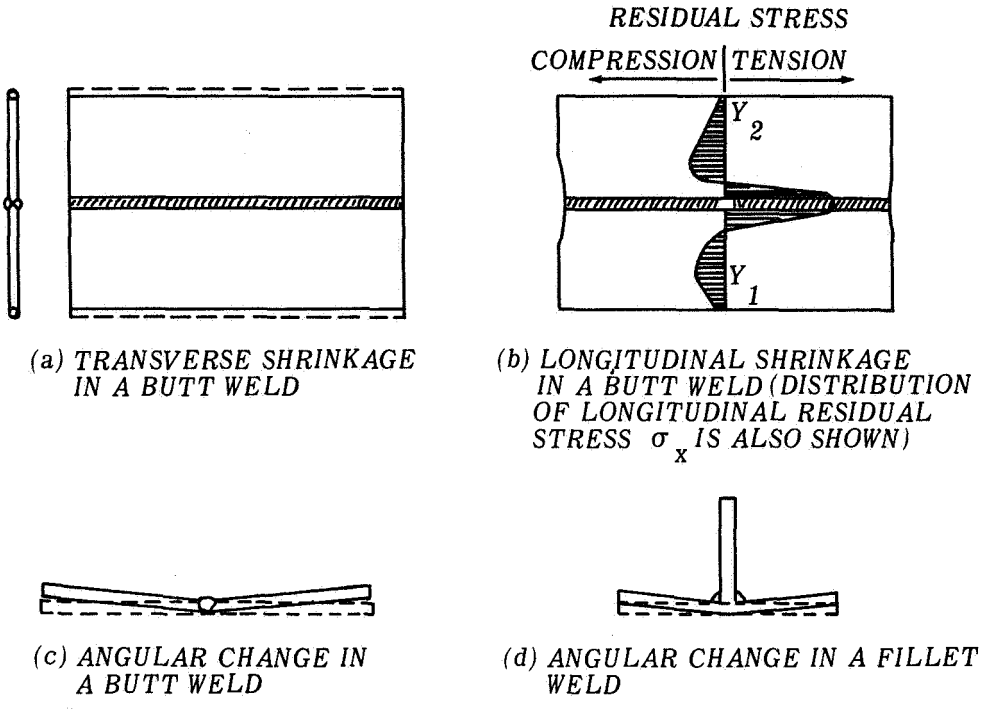

(a) TRANSVERSE SHRINKAGE IN A BUTT WELD

(b) LONGITUDINAL SHRINKAGE IN A BUTT WELD (DISTRIBUTION OF LONGITUDINAL RESIDUAL STRESS σ_x IS ALSO SHOWN)

(c) ANGULAR CHANGE IN A BUTT WELD

(d) ANGULAR CHANGE IN A FILLET WELD

FIGURE 4. FUNDAMENTAL DIMENSIONAL CHANGES THAT OCCUR IN WELDMENTS

Figure 4(c) shows the angular change that occurs in a butt weld. Non-uniformity of transverse shrinkage in the thickness direction is the cause of this rotation. Figure 4(d) shows the angular change that occurs in a fillet weld. Here, the angular change is caused by the unbalance of shrinkage on opposite sides of the flange member.

Distortions which occur in practical weldments are more complex than those shown in Figure 4. Figure 5 shows distortion induced by longitudinal shrinkage in various joints. Figure 5(a) shows distortion of a beam fabricated by welding. When the weld line is not located along the neutral axis of the joint, longitudinal shrinkage of the weld causes bending distortion. Figure 5(b) shows the distortion of a single-vee butt weld. The amount of weld metal, and consequently the amount of shrinkage, is not uniform in the thickness direction. The weldment deforms into a concave shape (looking from the top). When a thin plate is welded, residual compressive stresses, which occur in areas away from the weld, cause the buckling shown in Figure 5(c). In the cases shown in Figures 5(a), (b), and (c), distortions caused by angular changes are superimposed on those caused by longitudinal shrinkage.

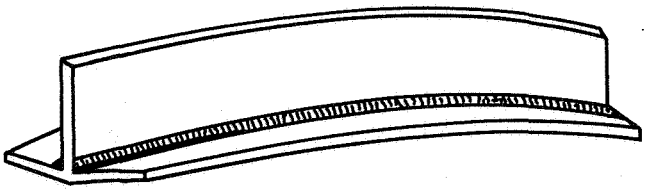

(a) LONGITUDINAL DISTORTION OF A BUILT-UP BEAM

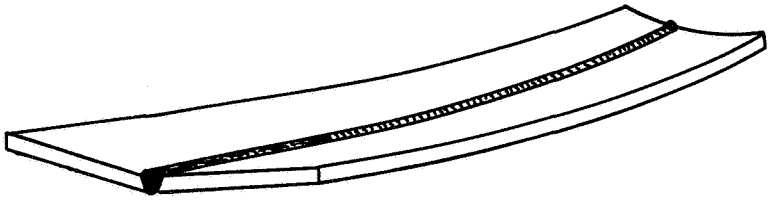

(b) LONGITUDINAL BENDING DISTORTION OF A SINGLE-VEE BUTT WELD

(c) BUCKLING DISTORTION

FIGURE 5. DISTORTIONS INDUCED BY LONGITUDINAL SHRINKAGE

Figures 4 and 5 show only a few examples of weld distortion. Shrinkage and distortion that occur during the fabrication of actual structures are far more complex than those shown. A recent paper by Masubuchi[18] covers various types of weld distortion.

2. Mathematical Analysis of Thermal Stresses During Welding and of Residual Stresses

a. Changes of Temperature and Stress During Welding

Figure 6 shows schematically how residual stresses are formed in a weld. Figure 6(a) shows a bead-on-plate weld in which a weld bead is being laid at a speed v. The coordinate axis is 0-xy, the origin 0 is on the surface underneath the welding arc, and the x direction lies in the direction of welding.

Figure 6 shows temperature distribution along several cross sections. Along Section A-A, which is ahead of the welding arc, the temperature change

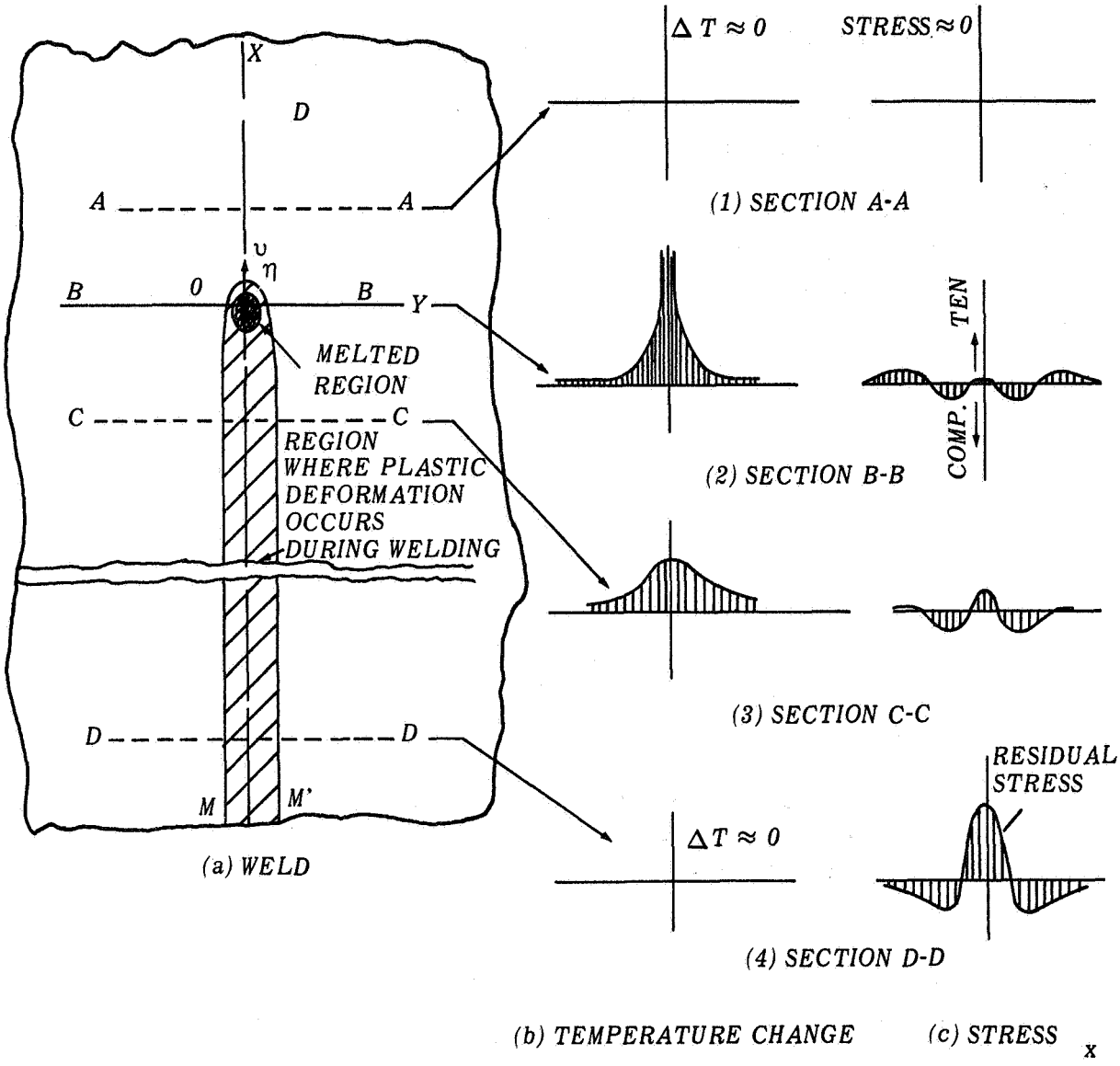

FIGURE 6. SCHEMATIC REPRESENTATION OF CHANGES OF TEMPERATURE AND STRESSES DURING WELDING

due to welding, ΔT, is almost zero. Along Section B-B, which crosses the welding arc, the temperature distribution is very steep. Along Section C-C, which is some distance behind the welding arc, the distribution of temperature change is shown in Figure 6(b). Along Section D-D, which is very far from the welding arc, the temperature change due to welding again diminishes.

Figure 6(c) shows the distribution of stresses along these sections in the x direction, σ_x. Stress in the y direction σ_y and shearing stress τ_{xy} also exist in a two-dimensional stress field [Figure 6(a)].*

Along Section A-A [Figure 6(c)], thermal stresses due to welding are almost zero. The stress distribution along Section B-B is shown in Figure 6(c)-(2). Stresses in areas underneath the welding arc are close to zero, because molten metal does not support loads. Stresses in areas somewhat away from the arc are compressive, because the expansion of these areas is restrained by surrounding areas which are heated to lower temperatures. Since the temperatures of these areas are quite high and the yield strength of the material is low, stresses in these areas are as high as the yield strength of the material at corresponding temperatures. The amount of compressive stress increases with increasing distance from the weld or with decreasing temperature. However, stresses in areas away from the weld are tensile and balance with compressive stresses in areas near the weld. In other words,

$$\int \sigma_x \cdot dy = 0 \qquad (1)$$

across Section BB.** The stress distribution along Section BB is shown in Figure 6(c)-(2).

Stresses which are distributed along Section C-C are shown in Figure 6(c)-(3). Since the weld metal and base metal regions near the weld have cooled, they try to shrink, which causes tensile stresses in areas close to the weld. As the distance from the weld increases, the stresses first change to compressive and then become tensile.

Figure 6(c)-(4) shows the stress distribution along Section D-D. High tensile stresses are produced in areas near the weld, while compressive stresses are produced in areas away from the weld. The distribution of residual stresses that remain after welding is completed is shown in the figure. The stress distribution is quite similar to that shown in Figure 1(a).

The cross-hatched area MM' in Figure 6(a) shows the region where plastic deformation occurs during the welding thermal cycle. The cross-hatched

---

*In a general three-dimensional stress field, six stress components, σ_x, σ_y, σ_z, τ_{xy}, τ_{zy}, τ_{zx}, exist.

**Equation (1) neglects the effect of σ_y and τ_{xy} on the equilibrium condition.

area near the origin 0 indicates the region where the metal is melted. The region outside the cross-hatched area remains elastic during the entire welding thermal cycle.

The above discussion shows that to analyze residual stress and distortion completely by mathematics, the following steps must be taken:

1) Analyze heat flow.

2) Analyze thermal stresses during welding and determine the distribution of incompatible strains that are produced during the welding thermal cycle.

3) Determine residual stresses and distortion produced by the incompatible strains.

A number of articles have been published on the subject of heat flow in weldments (Section IV). Although not an easy problem, it can be handled analytically.

The problem of determining the distribution of incompatible strains is extremely difficult, however. When the material undergoes plastic deformation, the stress-strain relationship is not linear. Furthermore, plastic properties of the material change with temperature.

When the distribution of incompatible strains is known, be it analytically or experimentally, the third step, determination of residual stress and distortion, can be handled analytically. Moriguchi developed a fundamental theory of stresses caused by incompatible strains.[24] Masubuchi has applied this theory to the study of residual stresses and distortion in weldments.[25]

Because of the difficulty in determining the distribution of incompatible strains, no analysis has yet been developed to trace the change of two-dimensional thermal stresses during welding and to determine distributions of three residual-stress components, σ_x, σ_y, and τ_{xy}. In other words, no analysis has been made in which both heat flow and stress fields are treated as two-dimensional problems. In all studies conducted so far, the problem has been simplified in some way.

b. Analysis of Stresses Caused by Longitudinal Welding in Strips and Rectangular Plates

In 1936, Boulton and Lance-Martin calculated the residual stresses produced by depositing weld metals on one or both edges of long, flat

plates, 9 feet by 6 inches by $^3/_8$ inch.[26] They assumed that the only stress component that existed was the longitudinal stress (σ_x in Figure 6) and that it was constant in the longitudinal direction. Rodgers and Fetcher in 1938 and Rosenthal and Zábrs' in 1940 conducted similar studies.[27,28] Since then many investigators have studied stresses due to longitudinal welding in strips and rectangular plates (including bead welding on plate edges, bead welding along the plate center, and butt welding) by making various assumptions concerning stress and temperature distribution.[13,19,29,30]

1) For stress distribution, consider the longitudinal stress only and neglect the transverse and shear stresses ($\sigma_y = \tau_{xy} = 0$ in Figure 6). In some cases, it is even assumed that the longitudinal stress is constant in the longitudinal direction; σ_x is a function of y only in Figure 6.

2) For temperature distribution, assume that temperature does not vary in the longitudinal direction. In some cases, it is even assumed that a narrow band in the weld area is heated to a constant temperature, while other areas are kept at the initial room temperature.

Both Tall[31,32] and Tsuji[33-36] conducted rather comprehensive analyses. Tall used the two-dimensional temperature distribution, but neglected transverse and shear stress ($\sigma_y = \tau_{xy} = 0$). Schematic curves shown in Figure 6 are drawn based on calculations by Tall.

Tsuji used a temperature-distribution constant in the longitudinal direction, as shown in Figure 7. He assumed that the central region (width 2a) of a rectangular plate is suddenly heated to temperature T_0 and that heat flows into other areas by conduction. He handled the plate as a two-dimensional, elastic-plastic field, i.e., he considered the three stress components, σ_x, σ_y, τ_{xy}. Tsuji studied the effects on residual stresses of various parameters including heat input and material properties.

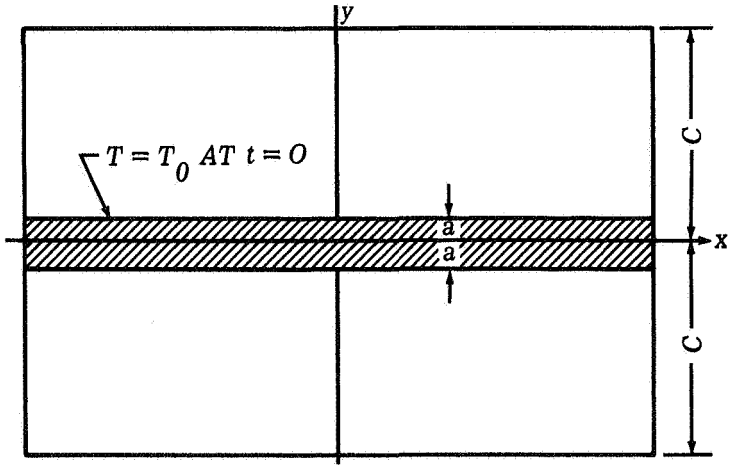

FIGURE 7. INITIAL TEMPERATURE CONDITION USED BY TSUJI FOR THE ANALYSIS OF RESIDUAL STRESSES IN A BUTT WELD

A recent trend is an increased use of computers for

analysis, especially digital computers. Tall and Tsuji both used computers for their calculations. N. N. Prokhorov and N. Nikol. Prokohorov used a digital computer for calculating distortion which develops when a bead is deposited on the edge of a strip.[37] Makhnenko and Velikowanenko used a computer for calculating stresses and distortion in structures made of welded narrow plates.[38]

During the present study, Battelle has developed a FORTRAN program for calculating both thermal stresses during welding and residual stresses in a butt weld. The analysis is essentially the same as that of Tall. Details of the Battelle analysis are described in Section V.

c. Analysis of Stresses Which Remain After Welding is Completed

A relatively simple analysis can be made if we are interested in stresses which remain after welding is completed and not necessarily in the stress change during welding. Based on Moriguchi's fundamental study of elasticity and plasticity, Kihara and Masubuchi proposed an approach that can be applied to a study of residual stresses in practical weldments.[39] Here, the problem is divided into the following two steps:

1) Determination of distribution of incompatible strains produced by welding
2) Determination of residual stresses due to the incompatible strains.

The first step can be achieved analytically or experimentally. The analytical achievement of the first step is extremely difficult, as described earlier. However, it is relatively easy to calculate residual stresses once the distribution of incompatible strain is determined. Masubuchi and associates have studied various problems related to residual stresses and distortion in weldments, which include the following:

1) Effect of welding procedures on residual stresses and transverse shrinkage of simple butt welds
2) Effect of welding sequence on residual stresses and transverse shrinkage of butt welds and circular patch welds.

Some of the results are described in a paper written by Masubuchi.[25]

The approach that Masubuchi and associates have taken is very similar to Prandtl's wing theory.[24,25,40,41] The following is an excerpt that compares equations describing distributions of residual stress and shrinkage of a welded joint and the phenomena that occur in the velocity distribution around the wing of an airplane.[25]

Theory of Residual Stress

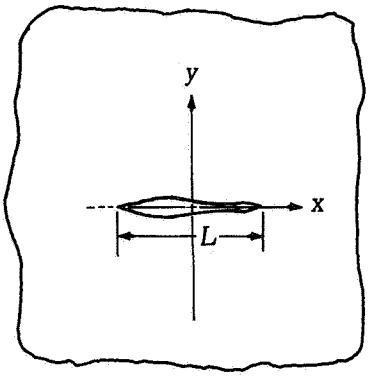

Stress: σ_x, σ_y, τ_a

Slit length (weld length): L

Transverse Stress on Slit: σ_{y0}

$$\sigma_{y0} = \frac{E}{4\pi} \int_{-L/2}^{L/2}{}' \frac{1}{x - x'} \left(\frac{d[v]}{dx}\right)_x dx' \qquad (1)$$

where:

E = Young's modulus.
[v] = dislocation.

$$[v] = \sum_{n=1}^{\infty} A_n \sin n\theta \qquad (2)$$

$$\sigma_{y0} = \frac{E}{2L} \sum_{n=1}^{\infty} nA_n \frac{\sin n\theta}{\sin \theta} \qquad (3)$$

$$x = \frac{L}{2} \cos \theta$$

Mean Dislocation: $[\bar{v}]$

$$[\bar{v}] = \frac{1}{L}\int_{-L/2}^{L/2} [v]dx$$

$$= \frac{1}{L}\int_{0}^{\pi} \frac{L}{2}\left(\sum_{n=1}^{\infty} A_n \sin n\theta\right) \sin\theta \cdot d\theta$$

$$= \frac{\pi}{4} A_1 \tag{4}$$

The magnitude of mean dislocation is determined only by the value A_1.

Strain Energy: U

$$U = \int_{-L/2}^{L/2} \frac{1}{2}\sigma_{y0}[v]dx$$

$$= \frac{\pi}{16} E\left(\sum_{n=1}^{\infty} n A_n^{\,2}\right)$$

$$= \frac{\pi}{16} E(1+\delta) A_1^{\,2} \tag{5}$$

where:

$$\delta = \frac{1}{A_1^{\,2}}\left(\sum_{n=2}^{\infty} n A_n^2\right) \tag{5'}$$

The magnitude of strain energy becomes minimum when $\delta = 0$ provided that the length of L and mean dislocation [v] remain constant. When $\delta = 0$, the form of dislocation [v] is elliptical and the distribution of transverse stress σ_{y0} is uniform along the slit.

Wing Theory

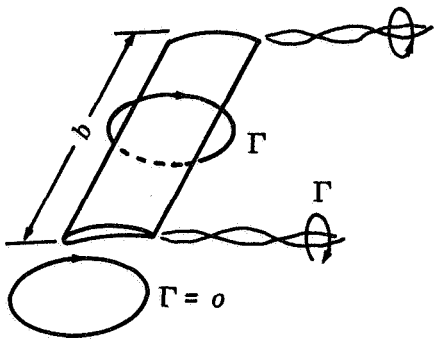

Velocity: u, v
Wing breadth: b

Down Wash: w

$$w = \frac{1}{4\pi} \int_{-b/2}^{b/2} \frac{1}{x - x'} \left(\frac{d\Gamma}{dx}\right)_{x'} dx'$$

where:

Γ = circulation.

$$\Gamma = 2bV \sum_{n=1}^{\infty} A_n \sin n\theta$$

$$w = V \sum_{n=1}^{\infty} nA_n \frac{\sin n\theta}{\sin \theta}$$

V = velocity at infinity

$$x = \frac{b}{2} \cos \theta$$

Lift: L

$$L = \rho V \int_{-b/2}^{b/2} (x)\, dx$$

$$= \frac{\pi}{2} \rho b^2 V^2 A_1$$

where:

ρ = density.

The magnitude of life is determined only by the value A_1.

Induced Resistance: D_i

$$D_i = \rho \int_{-b/2}^{b/2} \Gamma(x)\, w(x)\, dx$$

$$= \frac{\pi}{2} \rho b^2 V^2 \left(\sum_{n=1}^{\infty} n A^2 n \right)$$

$$= \frac{\pi}{2} \rho b^2 V^2 (1 + \delta) A_1^2$$

where:

$$\delta = \frac{1}{A_i^2} \left(\sum_{n=2}^{\infty} n\, A_n^2 \right)$$

The magnitude of induced resistance becomes minimum when $\delta = 0$, provided that the wing breadth and lift L remain constant. When $\delta = 0$, the distribution of circulation Γ is elliptical and the distribution of down wash is uniform along the wing.

Equation (1) in the above excerpt shows the relationship between the dislocation* which occurs along the part of the x-axis between (-L/2, 0) and (L/2, 0) and the transverse stress produced at that part of the x-axis designated as σ_{y0}. The physical meaning of this stress problem can be interpreted as follows. When transverse stress σ_{y0}, given by Eq. (3), is applied along both sides of the slit of length L located on the x-axis, the relative displacement of the sides of the slit is given by Eq. (2). The value of U given by Eq. (5) can indicate the elastic strain energy stored in the plate (per unit plate thickness) when transverse stress σ_{y0} is applied along the slit.

To determine the distribution of residual stress in a weld joint and to investigate the influence of welding procedures on stress distribution, it is not always necessary to trace the history of nonelastic deformations. The important thing in these problems is to determine the distribution of incompatibility. If the distribution of incompatibility is determined, residual stresses and distortions can be calculated theoretically. This approach makes it possible to study residual stresses and distortion analytically without becoming involved in complex calculations related to plastic behavior of the material.

3. Buckling Distortion in Weldments in Thin Plates

An excellent review of buckling distortion in thin welded plates is presented in Chapter 11 of a book by Kihara, Watanabe, Masubuchi, and Satoh, published by the Society of Naval Architects of Japan.[13] The following discussion is taken primarily from that chapter. Although the discussion is concerned with carbon steel welded with covered electrodes and with the submerged arc process, it is included in this report because no such comprehensive work on aluminum is available. Because this is taken from Japanese work, all measurements in this section of the report are in the metric system and temperatures are in centigrade.

---

*The term dislocation used here is not the same as the dislocation used in physical metallurgy, although their fundamental natures are closely related mathematically. As used here, dislocation means discontinuity in displacement such as opening of a crack in a residual-stress field. In this case, displacements are expressed in multivalued functions.

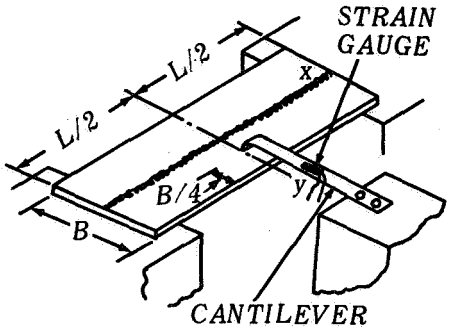

FIGURE 8. APPARATUS FOR DEFLECTION MEASUREMENT

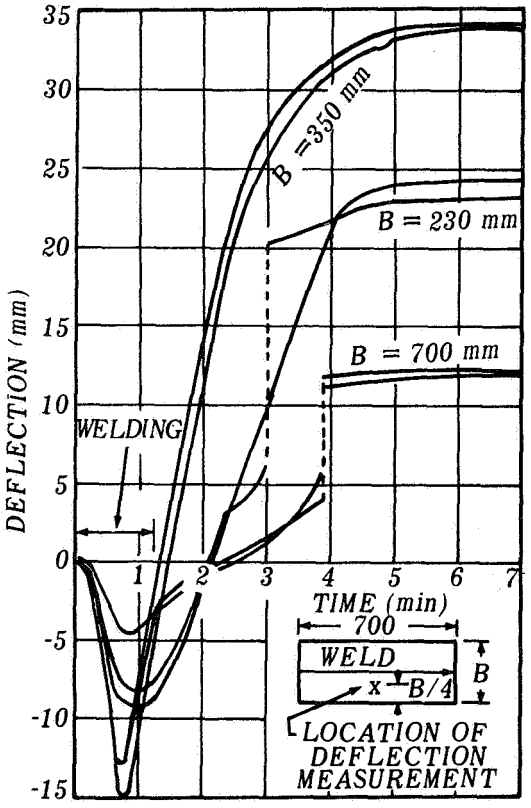

WELDING CURRENT 100 A
ARC VOLTAGE 25 V
TRAVEL SPEED 1.0 cm/sec
SIZE OF ELECTRODE 3.2 mm IN DIAMETER

FIGURE 9. DEFLECTION DUE TO WELDING VERSUS TIME CURVES

a. Distributing Features in the Distortion of Thin Plate Due to Welding

In welding of a thin plate, the plate may buckle due to compressive thermal stress during cooling, as shown in Figure 5(c). Fundamental investigations of buckling-type distortion were undertaken by Watanabe, Satoh,[42,43] Masubuchi,[44] and Mura.[45]

To obtain characteristics of distortion in thin plates. Watanabe and Satoh[42,43] observed the distortion produced when a single-pass, straight-bead weld is laid on the center line of a steel sheet 700 millimeters long and 1.6 millimeters thick. The apparatus used to measure deflection of the plate during welding and cooling is shown in Figure 8.[43] A cantilever of spring-steel sheet was set on a rigid station near a specimen and the edge was bent to be in contact with the specimen. Thus, deflection of the specimen was transmitted to the cantilever. The spring-steel sheet cantilever was made as thin as possible to minimize the effects of its rigidity on deflection of the specimen. As shown in the figure, an electric wire strain gauge was attached to the cantilever surface. Changes in reading of the gauge were measured by a dynamic wire-strain indicator. Then curves showing the relation between deflection of the specimen and time were obtained. The results are shown in Figure 9.[43]

As seen in the figure, an abrupt change in deflection in the 700-millimeter wide specimens occurred about 4 minutes after the start of welding. The change

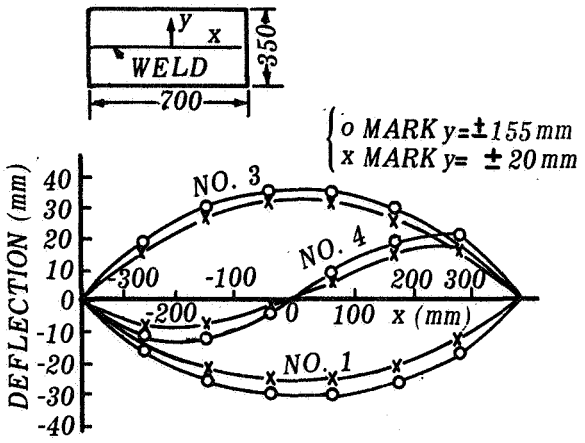

WELDING CURRENT 90 A
TRAVEL SPEED 0.60 cm/sec
SIZE OF ELECTRODE 2.6 mm

FIGURE 10. STATES OF DISTORTION PRODUCED AFTER BEAD WELDING IN A FEW SPECIMENS OF MILD-STEEL SHEET

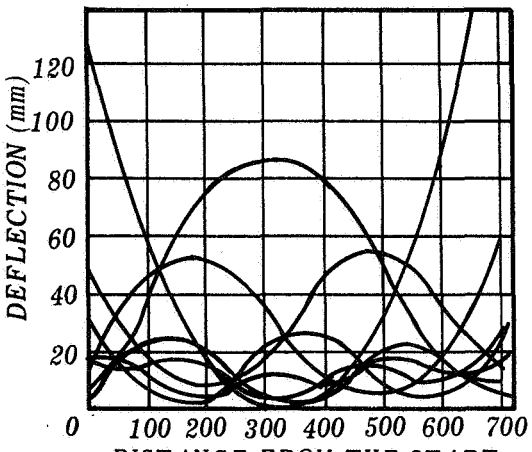

BEAD WELDING WAS MADE ON THE CENTER LINE OF THE PLATE BY SUBMERGED ARC WELDING AT 410 A, 30 V, AND 2.0 cm/sec TRAVEL SPEED.

FIGURE 11. SEVERAL STABLE TYPES OF LONGITUDINAL DISTORTION DUE TO WELDING IN A THIN PLATE

was so abrupt that it was accompanied by a loud noise. Measurement of temperature rise at the middle point of the welding bead indicated that that point had already cooled to 70° to 80° C at that instant. In the narrower specimens, the abrupt changes of deflection were not observed but the deflection was much increased after welding (Figure 9).

Figure 10 shows states of distortion produced after cooling of specimens 350 millimeters wide, 700 millimeters long, and 1.6 millimeters thick.[43] Three different states of distortion were observed despite the fact that almost the same welding conditions were applied. In Specimen No. 1, transverse distortion was concave and longitudinal distortion was convex to the side of the deposited bead. In Specimen No. 3, this relationship was reversed. A combined type of distortion was observed in Specimen No. 4, i.e., the states of distortion in transverse and longitudinal directions reverse themselves in the same plate.

Masubuchi[44] observed longitudinal distortions after cooling of submerged arc welded long rectangular plates. A weld bead was laid on the center line of the 720-centimeter long, 2.3-millimeter thick plates. Curves in Figure 11 show longitudinal deflections produced in a plate 40 centimeters wide.[44] Several stable states of distortion are observed in the same plate.

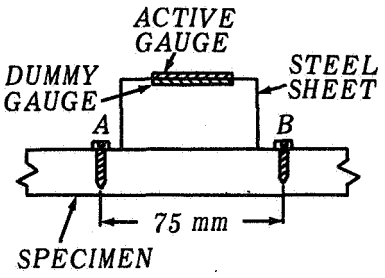

FIGURE 12. BRIDGE-TYPE STRAIN GAUGE USED FOR MEASUREMENT OF LONGITUDINAL STRAIN DUE TO WELDING

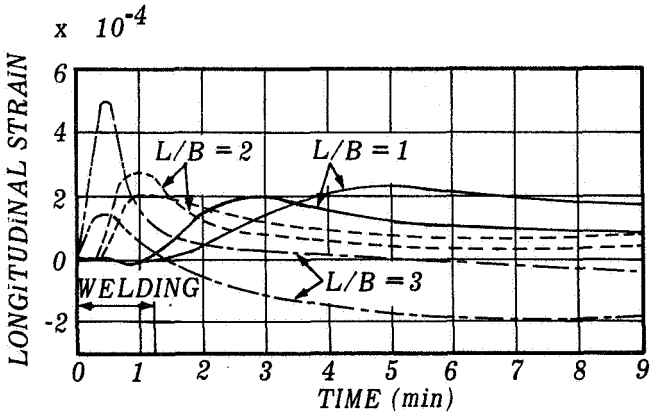

WELDING CURRENT 100 A
ARC VOLTAGE 25 V
TRAVEL SPEED 1.0 cm/sec
SIZE OF ELECTRODE 3.2 mm IN DIAMETER

FIGURE 13. LONGITUDINAL STRAIN DUE TO WELDING VERSUS TIME CURVES

b. Critical Buckling Stress When Welding Thin Plate

Fundamental problems relating to buckling distortion in thin plates due to welding are (1) critical buckling stress of a plate which has both a given aspect ratio and thickness and (2) the amount of deflection after buckling.

Watanabe and Satoh determined experimentally thermal stresses produced during welding on the specimens shown in Figures 7 and 8. In addition to the cantilever for measuring distortion, they attached a bridge-type strain-measuring unit on the specimen shown in Figure 12.[43] Active and dummy-strain gauges were mounted on a steel strip 0.3 millimeter thick and 7 millimeters wide, which was bent to the shape shown in Figure 12. Then the strip was attached to the specimen using Screws A and B which were 75 millimeters apart. The bridge-type unit was placed in the longitudinal direction of the specimen near the distortion measuring point shown in Figure 8. A thermocouple also was attached to the specimen to determine temperature change.

The strain determined by the bridge-type unit included thermal expansion in addition to strains that were related to thermal stresses; therefore, Watanabe and Satoh called the strain determined by the bridge-type unit apparent strain. Figure 13 shows changes of the apparent strain in the longitudinal direction ϵ_x during and after welding.[43] Figure 14 shows temperature change θ and resulting free thermal expansion $\alpha\theta$, where α is the

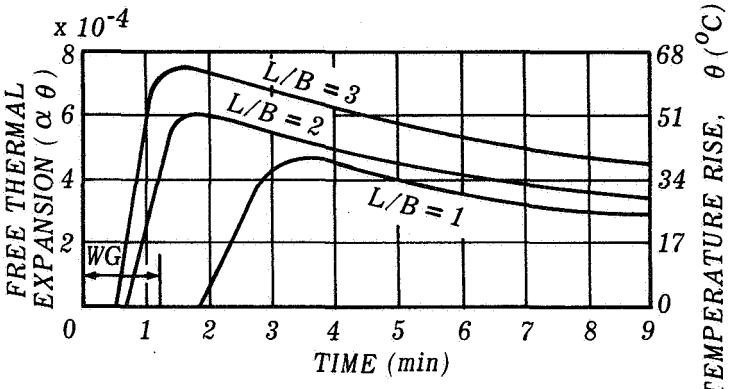

WELDING CURRENT 100 A
ARC VOLTAGE 25 V
TRAVEL SPEED 1.0 cm/sec
SIZE OF ELECTRODE 3.2 mm IN DIAMETER

FIGURE 14. TEMPERATURE RISE AND FREE THERMAL EXPANSION VERSUS TIME CURVES

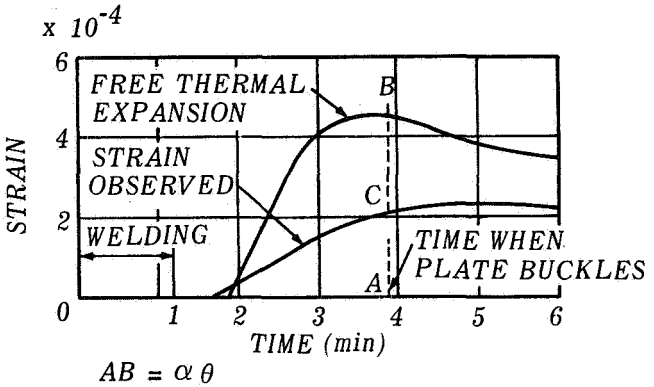

$AB = \alpha\theta$
$AC = \epsilon_x$ *(LONGITUDINAL STRAIN)*

$\sigma_{cr} = E \times BC,$

$= 21 \times 10^3 \, (0.160\text{-}0.459) \times 10^{-3}$

$= -6.3 \text{ kg/mm}^2$

FIGURE 15. AN EXAMPLE OF THERMAL STRESS CALCULATION

coefficient of linear thermal expansion.[43] The following equation was used to calculate thermal stress in the longitudinal direction σ_x:

$$\sigma_x = E\,(\zeta_x - \alpha\theta), \qquad (2)$$

where E equals Young's modulus. In the above calculation, transverse stress σ_y was neglected.

Figure 15 shows an example of the thermal stress calculation for a specimen 700 millimeters long and 700 millimeters wide.[43] The calculation was made at the point x = 0, y = 1/4B = 175 mm. The amount of compressive thermal stress at the instant of buckling σ_{cr} was determined as E × BC in Figure 15. In the particular case shown in Figure 15, σ_{cr} = -6.3 kg/mm = (9000 psi).

In the narrower specimens, no abrupt change of deflection, as was shown in Figure 9, was observed and the magnitudes of σ_{cr} were obtained on the assumption that buckling might have taken place at the instant shown in Figure 16. Values are shown in Table I.

Compressive thermal stress is considered to be caused by inherent shrinkage due

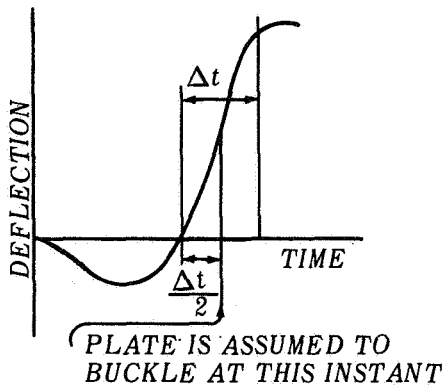

FIGURE 16. CHANGE OF DEFLECTION IN A NARROW PLATE INCREASING CONTINUOUSLY DURING COOLING

to welding. Thus, critical inherent shrinkage of buckling was obtained upon the assumption that compressive thermal stress is equivalent to stress in the plate produced by concentrated compressive forces $P = Eh\,(\xi_1)$ acting at the both ends of the weld line (Figure 17). When the force approaches the critical value P_{cr} the plate buckles. The stress at the measuring point ($x = 0$, $y = B/4$) due to the concentrated compressive forces can be obtained according to the theory of elasticity. When $L/B \geqq 1$, it is given by

TABLE I. CRITICAL VALUE OF INHERENT SHRINKAGE $(\xi_1)_{cr}$ FOR BEAD-ON-PLATE AND NUMERICAL FACTOR k

L (mm)	B (mm)	σ_{cr} (kg/mm^2)	P_{cr} (T)	$(\xi_1)_{cr}$ (mm)	k
700	700	6.3	7.45	0.222	67
		5.9	6.98	0.208	63
700	350	9.9	5.55	0.165	25
		8.8	4.94	0.147	22
700	230	14.7	5.41	0.161	16
		16.2	5.96	0.177	17.5

$$\sigma_x\left(\text{at } x = 0,\ y = \frac{B}{4}\right) = \frac{P}{Eh}\left[1 + 4\sum_{m=2,4,6}^{\infty}(-1)^{\frac{m}{2}}(m\pi\mu + 1)\,e^{-m\pi\mu}\right], \qquad (3)$$

where μ equals L/B. Critical values of P and (ξ_1) (= P/Eh) can be obtained (Table I) by substituting σ_{cr} in Table I in the left-hand side of Eq. (3).

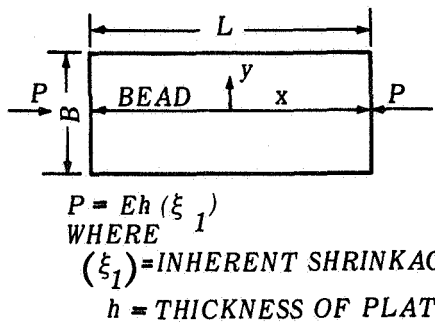

FIGURE 17. LONGITUDINAL DISTORTION AND STRESS IN THE PLATE

the following equation (Figure 18)[43]:

Watanabe and Satoh have expressed the critical inherent shrinkage as

$$(\xi_1)_{cr} = \frac{P_{cr}}{Eh} \frac{k\pi^2 h^2}{12(1-\nu^2)B}, \qquad (4)$$

where

h = plate thickness
ν = Poisson's ratio.

The term k is a numerical factor depending on the aspect ratio L/B of the plate. As seen in Table I, the magnitude of k decreases as L/B increases, and it is approximately represented by

$$k = 11 + 50\left(\frac{B}{L}\right)^2 \qquad (5)$$

and is independent of material.

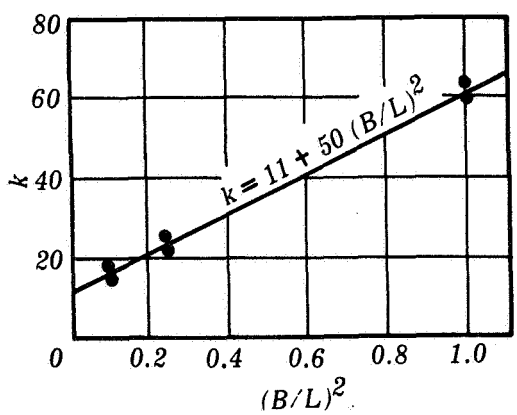

FIGURE 18. NUMERICAL FACTOR k

Watanabe and Satoh further analyzed the relationship between welding conditions and the inherent shrinkage (ξ_1). Based on their previous work, they proposed the following formula for welding carbon steel using ilmenite-type covered electrodes 4 millimeters (0.16 in.) in diameter:

$$(\xi_1) = 0.136 \times 10^{-6}\left(\frac{I}{h\sqrt{\nu}}\right)^2, \qquad (6)$$

where

(ξ_1) = inherent shrinkage (mm)
I = welding current (A)
ν = arc travelling speed (cm/sec)
h = plate thickness (cm).

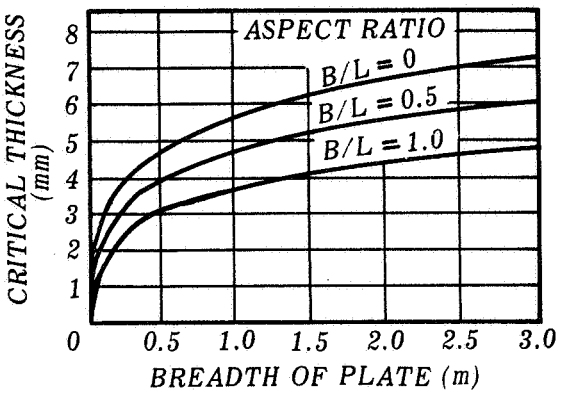

FIGURE 19. CRITICAL PLATE THICKNESS FOR LOW-CARBON STEEL FOR VARIOUS WIDTHS OF PLATE AND ASPECT RATIOS

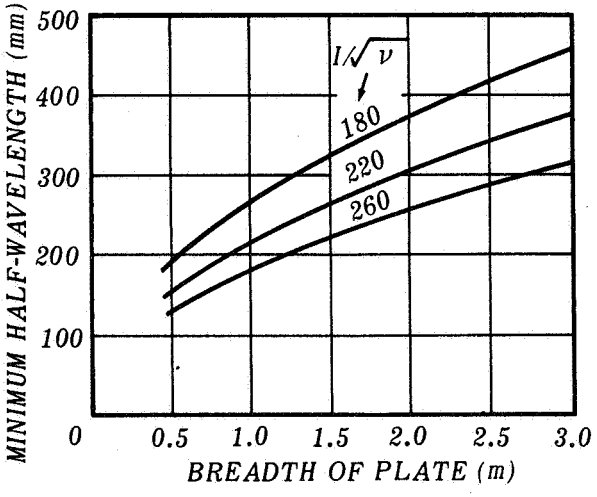

FIGURE 20. CRITICAL HALF WAVELENGTH FOR LOW-CARBON STEEL FOR VARIOUS WIDTHS OF PLATE AND WELDING CONDITIONS

It is considered that a plate will buckle in the longitudinal direction when the magnitude of (ξ_1) exceeds its critical value $(\xi_1)_{cr}$ obtained by Eq. (4) and (5). Figure 19 shows the relationship among the critical thickness of the steel plate, the aspect ratio, and the thickness of the plate under the condition of $I/\sqrt{\nu} = 260$, where I is welding current in amperes and ν is welding speed in centimeters per second.[43] Figure 20 shows the relationship among minimum half wavelength welding conditions and the width of the plate on plates 1.6 millimeters thick.

Mura[45] conducted a mathematical analysis of buckling-type distortion of a long strip due to welding (Figure 21). The width is 2a, the length is L, and the weld is made along the center of the strip. The following assumption is made regarding residual stress components:

$$\text{Longitudinal stress } \sigma_x = \begin{cases} -\sigma' & /y/ > C \\ \sigma'' & 0 < /y/ < C \end{cases}$$

$$\text{Transverse, } \sigma_y = 0$$

$$\text{Shear, } \tau_{xy} = 0. \qquad (7)$$

Since residual stress must be balanced,

$$\int_0^a \sigma_x \, dy = 0. \qquad (8)$$

Therefore,

$$\sigma' = \frac{c}{a - c} \sigma'' . \qquad (9)$$

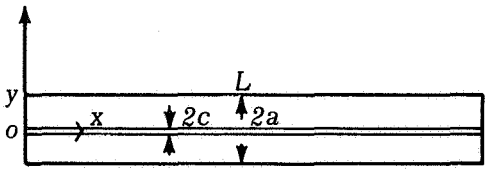

FIGURE 21. WELD SPECIMEN USED IN MURA'S ANALYSIS

If we denote the deformation in the z-direction as W, the equation of equilibrium is

$$D\left(\frac{\partial^4 W}{\partial x^4} + 2\frac{\partial^4 W}{\partial x^2 \partial y^2} + \frac{\partial^4 W}{\partial y^4}\right) = T_x \frac{\partial^2 W}{\partial x^2} \quad , \tag{10}$$

where

$$D = \text{rigidity of the plate} = \frac{Eh^3}{12(1-\nu^2)}$$

$$T_x = \sigma_x h$$

h = plate thickness.

For boundary conditions, it was assumed that the plate is simply supported at both ends, x = 0 and L, and that the plate is free along y = ±A.

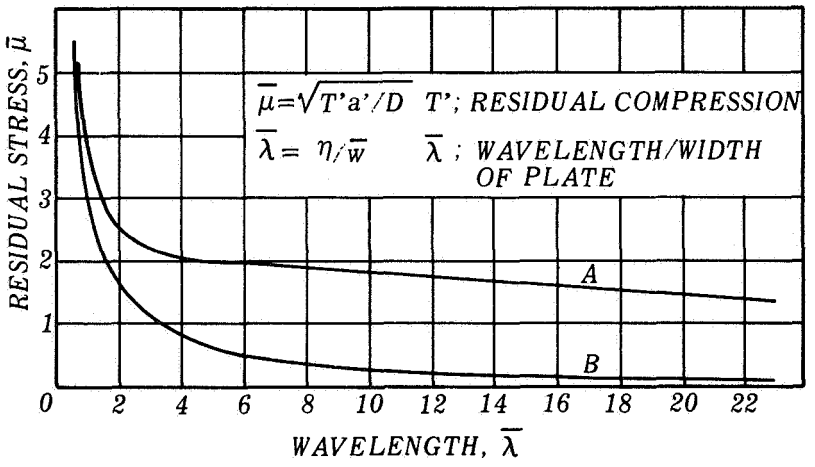

FIGURE 22. RELATIONSHIP BETWEEN WAVELENGTH AND RESIDUAL STRESS IN A LONG WELDED STRIP

Mura determined the stable wavelengths by solving Eq. (11). Curve A of Figure 22 shows the relationship between non-dimensional parameters, $\bar{\lambda}$ and $\bar{\mu}$, which express wavelength and residual stress,

$$\bar{\lambda} = \frac{2}{m}\frac{L}{2a}$$

$$\bar{\mu} = \left(\frac{a}{h}\right)\sqrt{\frac{12(1-\nu^2)\sigma_1}{E}} \tag{11}$$

where m is the integer.

The relationship is given as

$$\left[\bar{\mu}^2 - (1-\nu)^2\,\bar{\omega}^2\right] + \left[\bar{\mu}^2 + (1-\nu)^2\,\bar{\omega}^2\right] \cosh\sqrt{\bar{\mu}\,\bar{\omega} + \bar{\omega}^2}\cos\sqrt{\bar{\mu}\,\bar{\omega} - \bar{\omega}^2}$$

$$+ \frac{\bar{\omega}\,[(1-2\nu),\ \bar{\mu}^2 - (1-\nu)^2\,\bar{\omega}^2\,]}{\sqrt{\bar{\mu}^2 - \bar{\omega}^2}} \sinh\sqrt{\bar{\mu}\,\bar{\omega} + \bar{\omega}^2}\sin\sqrt{\bar{\mu}\,\bar{\omega}\,\bar{\omega}^2}$$

$$- \frac{\sqrt{\bar{\mu}\,\bar{\omega} - \bar{\omega}^2}}{\bar{\mu}\,\bar{\omega}}\left[\bar{\mu} + (1-\nu)\,\bar{\omega}\right]^2 \cosh\sqrt{\bar{\mu}\,\bar{\omega} + \bar{\omega}^2}\sin\sqrt{\bar{\mu}\,\bar{\omega} - \bar{\omega}^2}$$

$$- \frac{\sqrt{\bar{\mu}\,\bar{\omega} + \bar{\omega}^2}}{\bar{\mu}\,\bar{\omega}}\left[\bar{\mu} - (1-\nu)\,\bar{\omega}\right]^2 \sinh\sqrt{\bar{\mu}\,\bar{\omega} + \bar{\omega}^2}\cos\sqrt{\bar{\mu}\,\bar{\omega} - \bar{\omega}^2}$$

$$= 0\,. \qquad (12)$$

From knowing the residual stress σ_1, μ is determined. Then $\bar{\lambda}$ is determined. Wavelength values L_1, L_2, L_3 for $\mu = 1, 2, 3, \ldots$. The longest wave L_1 is obtained under $\bar{\mu} = 1$. For a given residual stress σ_1 and for width a, a plate longer than L_1 is going to buckle. Therefore, L_1 is considered as the critical size of the plate to cause buckling due to residual stress.

Curve B in Figure 22 shows the $\bar{\mu}$-$\bar{\lambda}$ relationship when the compressive stress σ_1 is applied across the entire width of the plate. For the same value of λ, the value of $\bar{\mu}$ for Curve A is considerably greater than that for Curve B. This is because the tensile stress in the region near the weld restricts the tendency to buckle caused by compressive stress and the compressive stresses must be much higher to cause buckling.

c. Deflection of Plate After Buckling

Attempts were made to analyze the amount of deflection of a plate after buckling. Masubuchi[44] investigated the relation between the wavelength of the longitudinal deflection curve and the amplitude in rectangular plates 720 centimeters long and 2.3 millimeters thick where the welding bead was deposited on the surface by submerged arc welding. Several stable states of distortion are observed in this specimen, and generally the amplitude increases as the wavelength increases, or as the number of waves decreases (Figure 10).

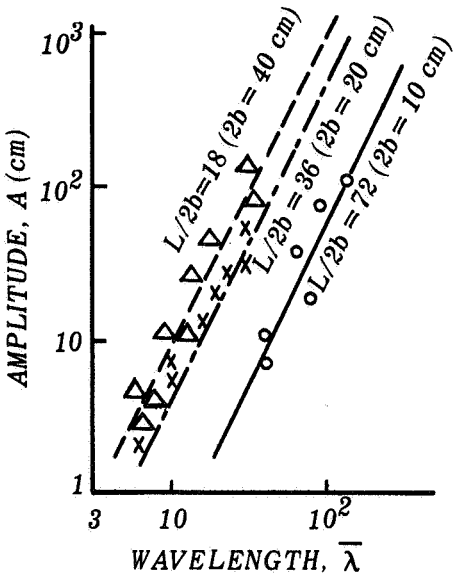

FIGURE 23. EFFECT OF WAVELENGTH IN LONGITUDINAL DEFLECTION CURVES ON THE AMPLITUDE

TABLE II. NUMERICAL CONSTANTS n AND C

L/2b	n	C (cm)
72	2.08	0.0041
36	2.06	0.036
18	2.02	0.076

Figure 23 shows the relation between the amplitude A and ratio of the wavelength and the width of the specimen.[43] The term $\bar{\lambda}$ is the ratio of wavelength versus width of the specimen, L is length of the specimen, and 2b is the width of the specimen. Bead welds were made by submerged arc welding. Figure 23 is approximately represented by

$$A = C\,\bar{\lambda}^{n} , \qquad (13)$$

where C and n are constants.

The magnitudes of the constants obtained from Figure 23 are shown in Table II. Accordingly, it is understood that the amplitude is almost proportional to the square of the wavelength.

Watanabe and Satoh[43] have expressed the deflection after buckling as follows: The curve of deflection along the half wavelength after buckling is expressed by a sine curve such as

$$y = y_0 \sin \frac{\pi x}{L} , \qquad (14)$$

where L is the half wavelength after buckling and y_0 is the maximum deflection in the half wave. Maximum curvature A at x = L/2 is given by

$$A = \frac{y_0 \cdot \pi^2}{L^2}$$

or

$$y_0 = \frac{A}{\pi^2} L^2 . \qquad (15)$$

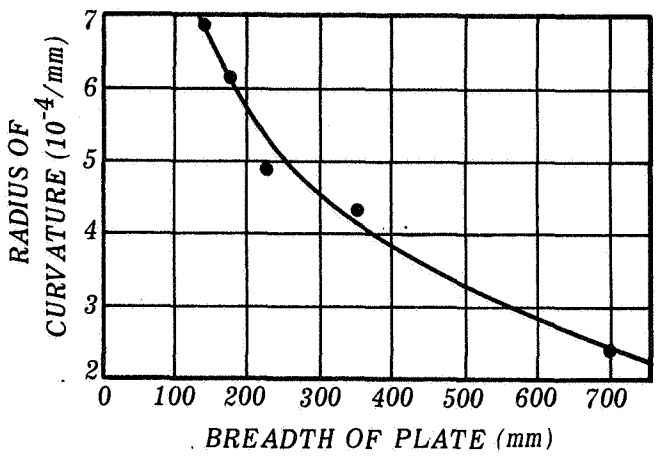

FIGURE 24. MAXIMUM RADIUS OF CURVATURE OF BUCKLED PLATE

estimated by using Eq. (15) and Figure 24.[43]

Hence, y_0 is proportional to the square of the half wavelength. Equation (15) is of the same type as the experimental formula (13) presented by Masubuchi. Referring to curves of distortion due to bead welding on a center line of rectangular plates 700 millimeters long and 1.6 millimeters thick, maximum curvatures in the longitudinal direction or the magnitudes of A in Eq. (15) are obtained as in Figure 24. As the magnitude of A decreases the width of the plate increases. Deflection after buckling of a rectangular plate of a given size can be

Section IV. COMPUTER ANALYSIS OF THERMAL STRESSES DURING WELDING AND RESULTING RESIDUAL STRESSES

In an attempt to obtain a better understanding of stress buildup and distortion resulting from welding, a computer program (written in FORTRAN digital-computer language) has been developed to simulate the welding process. This program uses present theoretically derived mathematical relationships that were already available. Although, realizing that these existing equations relied on certain assumptions, Battelle felt that they were sufficiently reliable to develop a useful analysis through correlation with good experimental data.

The computer program consists of three basic sections and several subprograms. The main sections of the program are

1) The calculation of temperature distribution created in a plate by a moving heat source, which simulates making a butt or edge weld
2) The calculation of the resulting thermal and residual stress distributions
3) The development of tables and graphs relating time, temperature, stress distributions, and position on the plate as direct computer printer and plotter output.

Although the basic relationships and equations used in the first two sections come primarily from the doctorial dissertation of Lambert Tall at Lehigh University,[31] the Battelle study includes the following modifications and advancements:

1) It is fully computerized and mechanized, including printing of numerical results and machine plotting of graphs.
2) The program is designed for any material.
3) The effects of temperature on material properties, including thermal conductivity, yield strength, modulus of elasticity, coefficient of thermal expansion, and specific heat, are considered to some extent.

1. Calculation of Heat Flow During Welding

Heat flow during arc welding has been studied analytically and experimentally by many investigators including Rosenthal,[46] Adams,[47,48] Masubuchi,[49] Christensen et al.,[50] and Rykalin.[51] Rykalin prepared an extensive

review on this subject. Battelle Defense Metals Information Center Report 172 presents the state of the art of this subject and discusses some shortcomings of the present analysis.[52]

This section presents a brief summary of the state of the art of the analysis of heat flow during welding as it is related to the computer program developed in this study.

a. Generation and Dissipation of Welding Heat

(1) Heat Generated by a Welding Arc. The electric power of the welding arc H* contributes by far the largest amount of heat to the arc. The term H is defined by

$$H = VI\ W\ (J/sec)\ , \tag{16}$$

where

V = arc voltage (V)
I = arc current (A).

The thermal equivalent of the electric power is 0.24 VI calories per second.

The energy input (or heat input) of the welding arc, which is given in terms of joules per inch of weld, is commonly used to express the intensity of the welding heat source

$$60 \times \frac{VI}{v}\ , \tag{17}$$

where v is the travel speed of the welding arc in inches per minute.

(2) Dissipation of Welding Heat. Most of the heat generated by the welding arc is supplied to the workpiece under the welding arc and then dissipates into further portions of the workpiece. The remainder of the heat is dissipated into the electrode by thermal conduction and is lost to the surrounding atmosphere by radiation. It is customary to express the amount of heat

*Other heat sources include the heat caused by chemical reactions in the arc atmosphere and the heat caused by transformation of metal.

supplied to the workpiece Q, calories per second, as a portion of the thermal equivalent of the electric power of the welding arc (or arc energy) 0.24 VI as

$$Q = \eta \times 0.24\ VI\ , \tag{18}$$

where η is called arc efficiency, and Q may be called the net heat or effective thermal power of the welding arc.

Figure 25, presented by Christensen et al.,[50] shows measured values of arc efficiency for various welding processes and materials including GTA and GMA welding of aluminum.[52] A logarithmic presentation is used so as to cover the range of energies from 300 to 12,000 calories (1 to 50 kVA). Accordingly, the efficiency is given by the position of the curves or bands representing each process, while the slope of these bands by definition will remain constant at 45 degrees. Values of η range 66 to 85 percent for the GMA process and 21 to 48 percent for the GTA process for welding of both steel and aluminum. However, according to the information obtained at Marshall Space Flight Center, the values of η for welding aluminum with GTA and GMA processes are about 80 to 90 percent.

b. General Discussion on Mathematical Analysis of Heat Flow in Weldments

Figure 26 shows schematically the temperature distribution in a plate on whose surface a weld bead is being laid at a speed v. Curves 1 to 6 represent isothermal curves on the surface, while the dotted curves represent isothermal curves on the transverse section ABCD. The coordinate axis is 0-xyz; the origin 0 is on the surface underneath the welding arc, the x-axis lies in the direction of welding, and the z-axis is placed in the thickness of the plate, downward.

The fundamental expression for heat conduction is given by the Fourier heat-flow equation,[51,52]

$$\frac{\partial \theta}{\partial t} = \kappa \left(\frac{\partial^2 \theta}{\partial x^2} + \frac{\partial^2 \theta}{\partial y^2} + \frac{\partial^2 \theta}{\partial z^2} \right) , \tag{19}$$

where

$\theta = (H) - \theta_0$ = temperature change
(H) = temperature

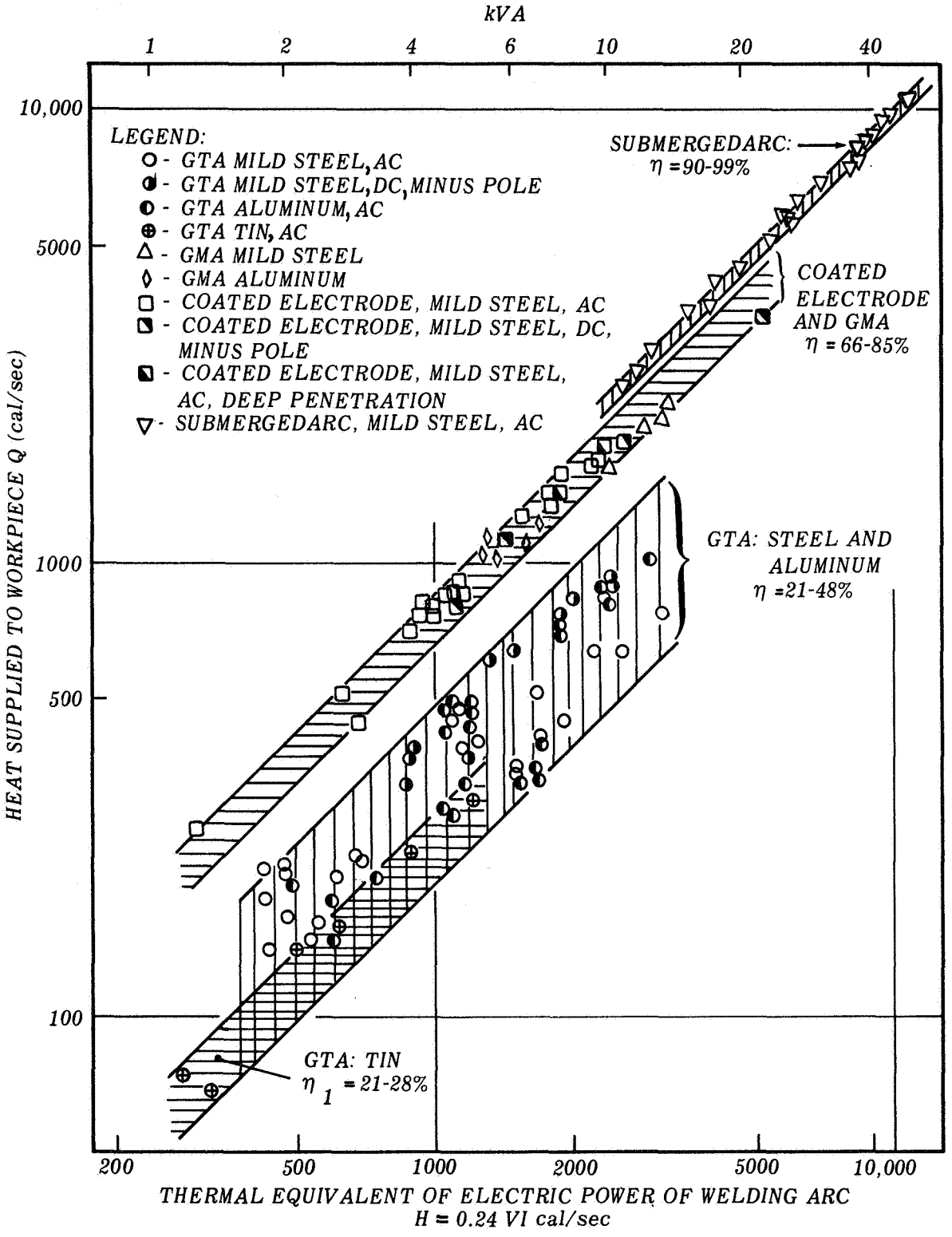

FIGURE 25. MEASURED VALUES OF ARC EFFICIENCY FOR VARIOUS PROCESSES AND MATERIALS

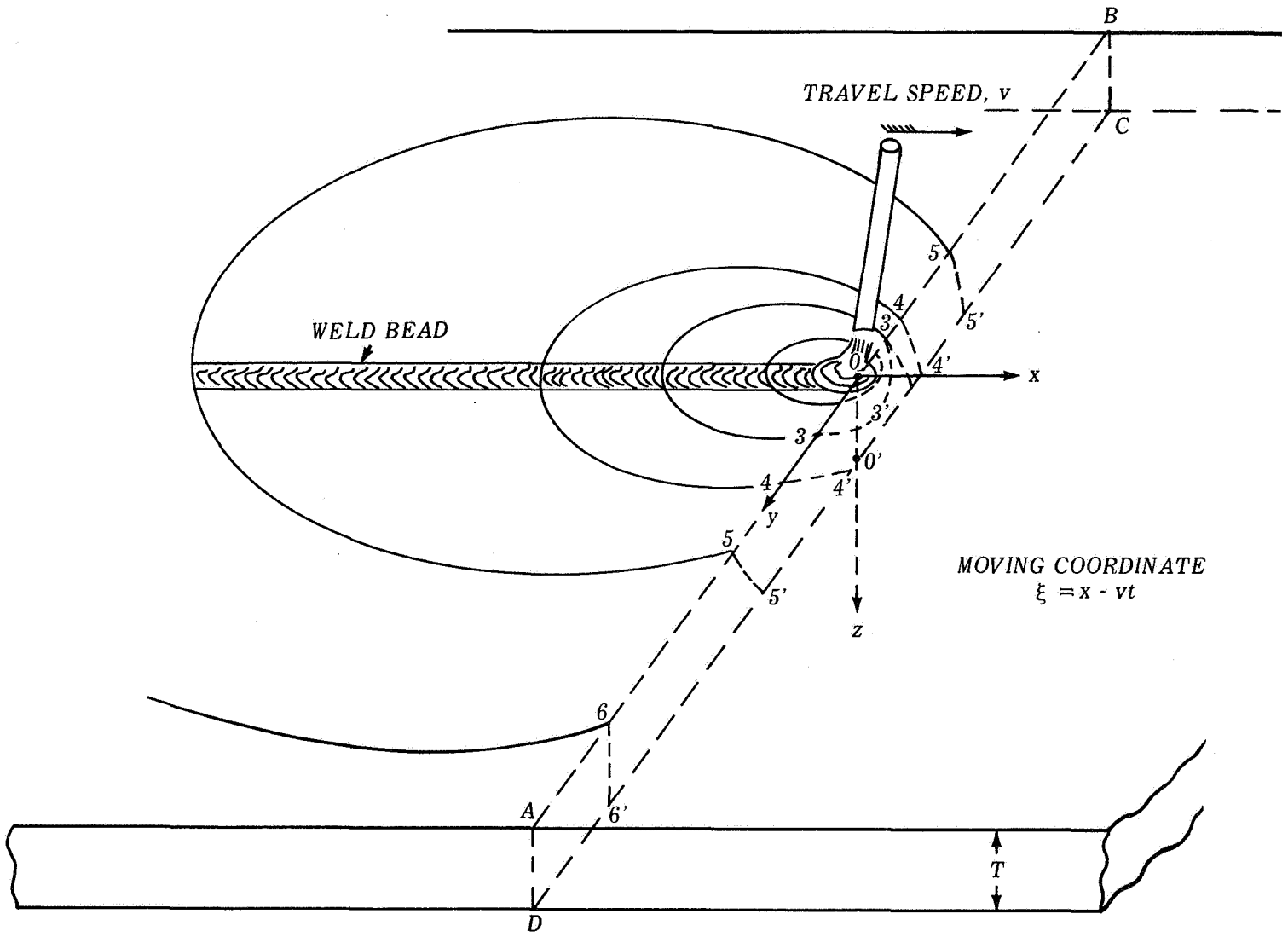

FIGURE 26. TEMPERATURE DISTRIBUTION IN A PLATE WHEN A WELD BEAD IS LAID ON THE SURFACE

θ_0 = initial temperature
t = time
$\kappa = \frac{\lambda}{c\rho}$ thermal diffusivity
C = specific heat
ρ = density
λ = thermal conductivity.

The mathematical analysis of heat flow in a weldment is essentially a solution of Eq. (19) for a given initial condition (initial temperature distribution) and a boundary condition (shape and intensity of the heat source, geometry of the weldment, etc.).

Two features of the heat flow during metal-arc welding are

1) The heat source moves, usually at a constant speed, on or near the surface of the workpiece.
2) The size of the heat source (welding arc) is small compared to the size of the workpiece.

(1) Quasi-Stationary State and Nonstationary State. The process of heat flow in arc welding is divided into three stages.

1) Heat saturation process in which the temperature in the field, moving together with the heat source, continues to rise
2) Quasi-sationary state in which the temperature distribution is stationary for a coordinate system that moves with the heat source
3) Temperature leveling-off process after the welding arc is extinguished.

In the quasi-stationary state the mathematical analysis is simple, since the problem can be treated as a steady-heat-flow problem for a moving coordinate. The quasi-stationary state takes place at a point close to the weld that is continued for a long period. Most of the mathematical analyses conducted so far on heat flow in weldments have been on the temperature distribution in the quasi-stationary state.

Heat flow is in the nonstationary state in areas near the start (Stage 1) and the end (Stage 3) of a weld, even when the weld is made over a considerable length. When welding is performed over a short length, the quasi-stationary state is never reached. Mathematical analysis of heat flow in the nonstationary state is much more complex than that in the quasi-stationary state.

(2) Effect of the Shape of the Heat Source. The local effect principle of the heat-conduction theory shows that the pattern of heat distribution of a local source has a substantial effect upon the temperature distribution only in the region adjacent to the source. Therefore, the temperature distribution of the workpiece in a region reasonably far from the welding arc can be calculated with sufficient accuracy by schematizing the pattern of the heat-flux distribution. In Figure 26, for example, temperature distribution in areas outside, say, Curve 4 can be calculated with sufficient accuracy by assuming that the heat source is concentrated in an elementary volume (point source) located at Point 0. The difference in temperature at a corresponding point on the top and the bottom surface becomes less pronounced as the point is located farther away from the welding arc (Curves 5 and 6). In such cases, the temperature calculation may be made on the assumption that the heat source is concentrated along Line 00' (line source); the temperature distribution is reduced to a two-dimensional plane problem.

(3) Physical Constants (Linear and Nonlinear Theories). Physical properties, including thermal diffusivity κ, specific heat c, density ρ, and thermal conductivity λ, are not really constants but change with temperature, and the extent of the change depends upon the metal concerned.[53] Almost all of the mathematical analyses conducted so far on heat flow in weldments have been made on the linear theory in which thermal properties[54] are assumed to be constants. Such solutions give approximate results. When values of thermal properties are considered to change with temperature, Eq. (19) becomes nonlinear and the mathematical analysis becomes extremely complex. Grosh et al.[55] analyzed heat flow in weldments assuming that thermal properties change linearly with temperature. However, only limited work has been done on the nonlinear analysis of heat flow in weldments.

c. Temperature Distributions in the Quasi-Stationary State

Mathematical analyses of heat flow in welding in the quasi-stationary state have been made by Boulton and Lance-Martin,[56] Rosenthal and Scherbes,[57] and many other investigators.

Using a coordinate (ξ, y, z) that is moving at the same speed as the welding arc shown in Figure 26,

$$\xi = x - vt \ . \tag{20}$$

The temperature undergoes no change in the moving coordinate system, thus Eq. (19) is expressed as[46,51,52]

$$\frac{\partial^2\theta}{\partial\xi^2} = \frac{\partial^2\theta}{\partial y^2} = \frac{\partial^2\theta}{\partial z^2} = -\frac{y}{\kappa}\frac{\partial\theta}{\partial\xi} \ . \tag{21}$$

Now θ is a function of position (ξ, y, z) only.

Solutions have been obtained for various cases including:

Case 1, three-dimensional case, semi-infinite plate (for very thick plate)

Case 2, three-dimensional case, finite thickness

Case 3, two-dimensional case, infinite plate (for large thin plate)

Case 4, two-dimensional case, finite size (for thin plate with finite size).

In most cases, solutions are obtained for a point or line-heat source with a given intensity. In other words, the size of the heat source is considered to be infinitely small. Solutions for a finite-sized heat source can be obtained by integrating solutions for a point or line-heat source.

Complexity of a solution varies, depending upon the boundary condition. Solutions for Case 1 due to a point source and Case 3 due to a line source are rather simple. Solutions for a finite-sized plate due to a finite-sized heat source are very complex.

After the complexity and usefulness of these solutions were evaluated, it was decided that the solution for Case 3 (two-dimensional) due to a line source be used for the Battelle computer program. The specimens analyzed in this study (aluminum plates 0.25 by 30 by 144 in.) are considered to be large enough that (1) temperature is quite uniform in the thickness direction in most areas where analyses are made and (2) the size effect of the plate can be neglected. More complex solutions may be used in future programs to improve the accuracy of calculations. The solution for Case 3, which is used in the Battelle program, is described in the following pages.

The temperature change caused by a line source (intensity: $q = Q/h$, where h is plate thickness) which moves along the x-axis of an infinite plate is given by Eq. (22),

$$\theta = \frac{q}{2\pi\lambda} e^{\frac{-v}{2\kappa}\xi} \cdot K_0\left(\frac{v}{2\kappa} r\right) \quad , \tag{22}$$

where

$r = \sqrt{\xi^2 + y^2}$

$K_0(z)$ = modified Bessel function of the second kind and zero order.*

2. Calculation of Thermal and Residual Stresses

The present state of the art of the analysis of stresses caused by longitudinal welding in strips and rectangular plates is described in Section III. After usefulness of available solutions for analyzing the problems being investigated in this study was evaluated, it was decided to use the analysis by Tall.[31,32] This analysis (Section III) uses the two-dimensional temperature distribution but it only considers the longitudinal stress σ_y and neglects transverse stress σ_x and shear stress τ_{ny}. Compressive stresses in the longitudinal direction that exist in areas near the moving arc are believed to be the primary factor causing lateral metal movement. Consequently, it was felt that Tall's analysis would be good enough at least for an initial analysis. It is strongly recommended, however, that the analysis be further developed in a future program to include all three stress components.

---

*Detailed descriptions on the modified Bessel functions are given by Watson and McLochlan[58,59]

$$K_0(z) = \int_{-1}^{\infty} \frac{e^{-zt}}{\sqrt{t^2 - 1}} dt \ .$$

When z is large enough, $K_0(z)$ can be expressed

$$K_0(z) \simeq \sqrt{\frac{\pi}{2z}} \cdot e^{-z} \ .$$

Tall's analysis employs a step-by-step method for calculating thermal and residual stresses that result when a plate is arc welded at either the center line or edge by a moving electrode, assuming that the bead is deposited at a uniform rate. At each step, the plastic deformation is considered and equilibrium accounted for.

First the temperature distribution around the moving arc is calculated by using Eq. (22). Then the stress field is divided into a set of transverse strips (Figure 27). The time interval represented by the strip width must be short enough that the temperature and thermal stress for each increment may be regarded as being constant. Since the greatest changes in temperature occur immediately after the onset of welding, the time increments should be short at first and comparatively long for the time approaching infinity.

The calculation starts on a strip some distance ahead of the welding arc where the temperature change is negligible and stresses are purely elastic. Time zero is fixed on the strip. For example, in the calculation shown in the fourth section of the appendix, the heat source is located at T = 9 seconds. In this particular case, the welding speed is 0.233 inch per second, as shown in the third section of the appendix. In other words, the calculation started at a strip 2.1 inches (0.233 × 9) ahead of the arc.

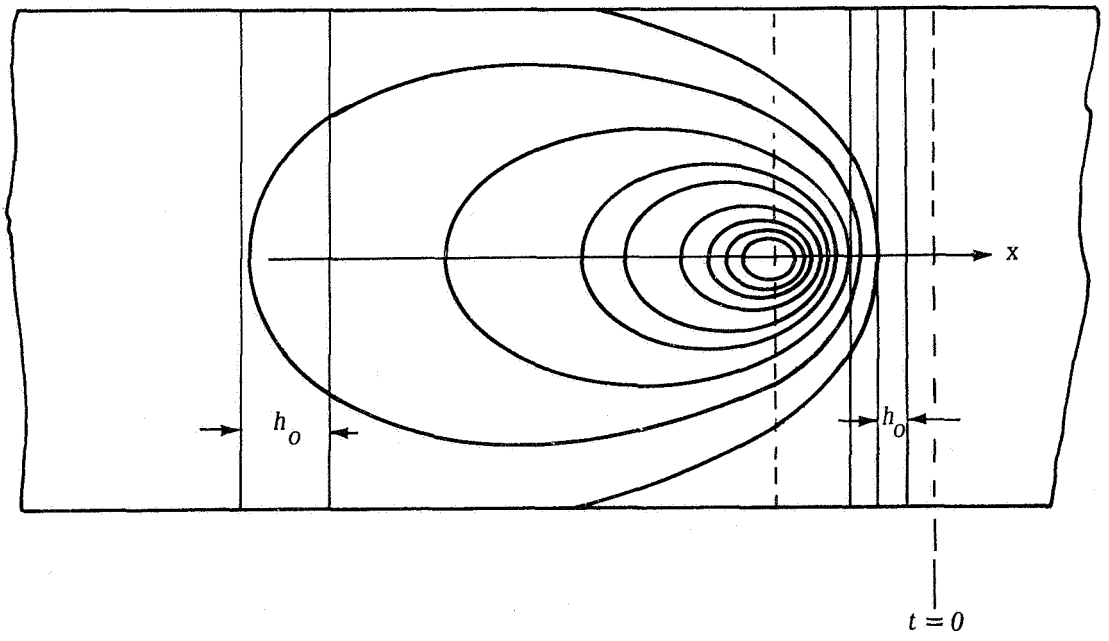

FIGURE 27. DIVIDING THE STRESS FIELD INTO TRANSVERSE STRIPS FOR CALCULATING THERMAL AND RESIDUAL STRESSES

Thermal stresses along the strip are calculated by the following equation:

$$\sigma = \alpha E \theta \ , \tag{23}$$

where

σ = stress
α = coefficient of linear thermal expansion
E = Young's modulus
θ = change in temperature.

The relation $\sigma = \alpha \cdot E \cdot \theta$ is derived by equating the equations for expansion; thermal expansion of the strip $\Delta H = h_0 \alpha \theta$, where h_0 is the width of the strip is equal to the expansion due to stressing $\Delta H = h_0 \frac{\sigma}{E}$. The temperature increment for the next time interval, or the next strip, is calculated and the thermal stress increment corresponding to it determined. This thermal stress increment is added to that existing at zero time, and this addition is limited by the yield stress of the material at the actual temperature under consideration. At each step, the stresses should be in equilibrium; i.e., the summation of compressive and tensile stresses must be zero and the moment of these forces must total zero across the total plate,

$$\int \sigma \cdot dy = 0 \tag{24}$$

$$\int \sigma \cdot y \cdot dy = 0 \ . \tag{25}$$

Since temperature distribution is symmetric with respect to y, Eq. (25) is automatically satisfied. In order to satisfy Eq. (24), a constant stress (compressive or tensile) across the plate is added (Figure 28).

It is also assumed that the amount of stress at a given point does not exceed the yield stress of the material at the temperature of that point. In areas near the welding arc, temperatures are high but stresses are low because values of the yield stress are low at high temperatures. In fact, liquidus areas very close to the arc hold no stress.

Each increment has its thermal stress added to that already accumulated from the preceding steps with the limitations that the addition must satisfy both equilibrium conditions and that the maximum yield stress existing at that temperature may not be exceeded. The stress distribution at time infinity gives residual stress after welding is completed.

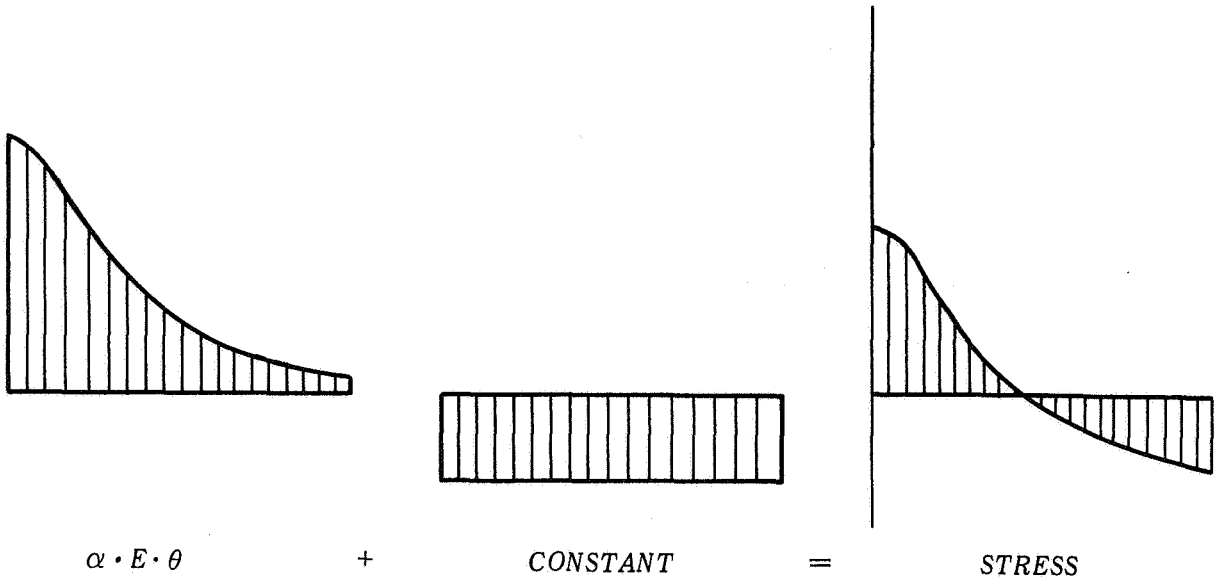

FIGURE 28. CALCULATION OF THERMAL STRESSES IN A TRANSVERSE STRIP

In conducting the analysis, the time increments, or the widths of the strip, need to be small enough to give a reasonably continuous thermal-stress pattern. For example, the time intervals used in the calculation given in the fourth section of the appendix follow:

a) 1-second interval for time 0 to 50 seconds

b) 50-second interval for time 50 to 1000 seconds

c) 5000-second interval for time 1000 to 3600 seconds and infinity.

3. The Battelle Computer Program and Results of Computation

The program developed in this study is to calculate temperature distribution and resulting thermal and residual stresses due to a moving heat source. The program is written in FORTRAN IV computer language for use on a Control Data Corporation (CDC) 6400 computer system including a CalComp plotter. The FORTRAN language is common in computer programming and can be adapted readily to any other computer that has a FORTRAN compiler program. The appendix presents the program and examples of calculation in the following order:

a) Main program

b) Subprogram

c) Listing of input

d) Sample listing of output data

e) Examples of graphical computer-output plots.

a. The Battelle Computer Program

(1) Materials and Welding Parameters. To facilitate a broad coverage of possible parameter values, the program is written to be quite general. Computations can be made readily for any material (if the material properties are known) and for any welding parameters (arc voltage, welding current, arc efficiency, and arc travel speed). These values are fed to the program as input data, as described in the third section of the appendix.

A single value for any of the required material properties (density, specific heat, thermal conductivity, coefficient of thermal expansion, Young's modulus, and maximum yield stress) is all that is required. However, to improve the accuracy of the analysis, a table of up to ten values of each property as a function of temperature may be entered as data. The temperature range used is in equal increments from 0°F to some value near the melting point. A given material property value can thus be determined for any temperature by means of a special interpolating subroutine (appendix, second section).

The program also allows the width of the plate to be subdivided into two areas of different increment spacing to allow smaller numerical integration areas close to the heat source. In addition, the length of the plate can be divided into three separate time spacings of different increments to allow more accurate calculations in the area of rapidly changing temperatures.

The entire set of input values, requiring nine IBM cards, is listed and each separate input value is explained at the beginning of the computer program description in the appendix. A typical listing of these input values for a run is also listed in the appendix.

After the program has read in and processed all the input values, the time and position spacings are calculated along with limiting values and spacings to be used on graphical outputs.

(2) Computation of Temperature Distribution. The next program step is to calculate a temperature value at a particular point by the method previously described using parameter values for either a temperature of a previous calculation or for ambient temperature (0°F temperature difference). The property values at the newly calculated temperature are determined and another new temperature is calculated. This process repeats in an interpretive fashion until the latest temperature calculated is within 0.1° of the previous temperature value. The temperature is calculated in this fashion at each point in the plate as specified by the input spacings. These temperature values are printed out in table form in the appendix. They are stored for use in other calculations and for graphical outputs.

The actual equation used to calculate each temperature value is of the form

$$T = K' e^{-a} K_0 (b) \quad . \tag{26}$$

Since K' is essentially a constant for any single calculation and a and b are functions of distance away from the heat source, the time since the heat source passed over any given point on a plate will eventually approach a large value, ∞. As the distance away from the moving heat source increases, the parameters a and b approach an infinitely large value. This results in an increasingly small value of e^{-a} multiplied by an increasingly large value K_0 (b) to yield a finite value. Since the computer only handles finite numbers (x) in the range $10^{-247} < x < 10^{+347}$, it was necessary to incorporate a routine to approximate, by series summation, the product $e^{-a} K_0$ (b) for large values of a and b.

(3) Computation of Stresses. After all the temperatures at a cross section have been calculated, the stress distribution is calculated as described previously. This involves computing both the change in temperature from the previous cross section and an average temperature over the increment to determine the values of limiting material properties, namely yield stress and modulus of elasticity. This stress distribution, if totaled across the plate, must equal zero to fulfill the required equilibrium conditions, Eq. (24) and (25), especially Eq. (24).

First, the values of $\alpha E\theta$ along the transverse line are calculated. Since the temperature change is greater near the center line of the plate and decreases away from the center line, values of $\alpha E\theta$ will tend to follow the same pattern

and hence not total zero across the plate. Thus, a constant stress is added to satisfy the equilibrium condition (Figure 28). If the stress value in any region is higher than the yield stress at the temperature of that region, the stress value is further adjusted so that the stress does not exceed the yield stress.

This analysis, however, has an obvious shortcoming regarding the effect of plate width on the stress distribution.* Since the equilibrium amount is spread out equally over the width, the stress distribution is directly dependent upon the plate width. When the width is infinitely large, as an extreme case, the stress becomes zero. There is a definite need for improving this analysis; the problem is discussed further in Section VII.

b. Trial Calculations to Improve the Program and to Establish Computation Procedures

In the initial stages of developing the program, different computer runs were made incorporating a range of values for heat-input energy, welding speed, material thickness, type of material, plate widths, and increment spacing between points across the plate (y-axis in this analysis) and time intervals along the length of the plate (x-axis in this analysis). In addition, modifications in the logic of the program, as well as some analysis changes, were made to improve the program's output results. It was determined that the cost of drawing a graph on the computer was as low as $0.75 and seldom over $1.50 per complete labelled plot. Thus, a major emphasis was placed on developing graphical computer output in a highly descriptive visual form. As can be seen from the graphical computer output shown in the fifth section of the appendix, a clear understanding of the complexities of the analyses is attained, especially in stress-distribution change during a welding cycle.

To check the validity of the computer program, calculations were made on mild steel welds and compared with results obtained by Tall.[31,32]

To check the accuracy of the numerical integration part of the analysis, tests were run to determine minimum spacing intervals along both the x- and y-axes. It was found that spacings in the y-direction as wide as 0.5 inch made

*In the present Battelle analysis, a plate with a finite width is used to calculate the stress distribution, while the solution for an infinite plate is used to calculate the temperature distribution. It was felt that the solution for the infinite plate is good enough for the present study. In future studies, a solution for a finite-sized plate may be recommended.

little difference in the calculations. Spacings in the x-direction of up to 10 seconds for the first 50 seconds, 100 seconds for 1000 seconds, and extremely large thereafter, only slightly affect the final residual-stress calculation. It was subsequently discovered that in spite of the fact that the final calculations change insignificantly during these intervals, the local thermal-stress distribution changes significantly and can thus hide the instantaneous effects. Thus a lead time ahead of the heat source and a 1-second interval to 50 seconds, a 50-second interval on to 1000 seconds, and a 5000-second interval thereafter to any desired stopping point were used.

c. Examples of Calculations

To study effects of welding parameters on the temperature and stress distributions, this report presents results of calculations for bead-on-plate welds in 2014-T6 aluminum made under six different conditions (Table III).

TABLE III. WELDING PARAMETERS USED FOR SAMPLE CALCULATIONS

Condition Number	Voltage (V)	Current (A)	Efficiency Factor	Speed (in./sec)	Thickness (in.)
1*	10	254	0.8	0.233	0.25
2	25	250	0.9	0.3	0.25
3	25	250	0.5	0.3	0.25
4	25	250	0.1	0.3	0.25
5	25	250	0.5	0.6	0.25
6	25	250	0.5	0.3	0.5

*Simulates the conditions used for experiments performed at NASA.

Condition 1 simulates the conditions used for experiments performed at the Marshall Space Flight Center, NASA. For Conditions 2 through 6, changes were made in thermal power of the welding arc, arc travel speed, and plate thickness. The effective thermal power of the welding arc is changed by varying any or all of the values of arc voltage, welding current, and arc efficiency [Eq. (18)]. In this study, a moderately high voltage and amperage for actual welding conditions were selected and held constant. Only the efficiency value

was changed to vary the effective thermal power of the welding arc. It was assumed that the weld was made along the longitudinal center line of a plate 8 inches wide and infinitely long.

(1) Temperature and Stress Distributions Across the Plate. Figures A-1 through A-10 illustrate the temperature and stress distributions across the plate at the instantaneous time given on each pair of figures for Condition 1. For this time sequence of figures, the heat source is located at the 9-second time position. Numerical values of temperature and stress at various times are listed in the appendix. Similar results for Conditions 2 through 6 were obtained but are not presented in this report.

Figures A-1 and A-2 show the temperature and stress distributions, respectively, at 7 seconds, or along a cross section slightly ahead of the moving heat source. The temperature increase above ambient is 277°F at the center line, y = 0. Compressive stresses are produced in regions near the center line because the expansions of these areas are restrained by the surrounding areas. Tensile stresses exist in areas away from the weld. The maximum compressive stress is about 27,000 pounds per square inch, which is smaller than the yield stress.* Consequently, the entire cross section is still in the elastic condition.

Figures A-3 and A-4 show the temperature and stress distributions, respectively, at 9 seconds, or along the cross section passing the heat source. The amount of stress at the center line is almost zero, because the temperature is very high. As the distance from the center line increases, the absolute value of the compressive stress increases since the temperature of the point decreases.

At the time increment 15 seconds, the temperature change spreads outward (Figure A-5). Stresses in areas near the center line change to tensile as these areas start to cool (Figure A-6). Compressive stresses exist in areas between y = 0.6 and 2 inches.

At the time increment 1000 seconds, the temperature change is quite uniform across the entire section (Figure A-9). Figure A-10 shows that high tensile stresses are produced in areas near the weld while compressive stresses exist in areas away from the weld.

---

*According to the input data on Card 5, the yield stress of 2014-T6 alluminum alloy is 62,000 pounds per square inch at room temperature, and it is as high as 50,000 pounds per square inch at a temperature increase of 300°F (appendix).

The fourth section of the appendix lists temperature and stress values for times up to infinity. The stress distribution at infinity represents the residual stress after welding is completed. The computer readouts in this section show that the stress values do not change significantly after some time increment, say 500 seconds. If we take the stress value at the weld center, for example, the stress value at infinity is 7.29 kips per square inch. The stress at the center reaches 99 percent of the residual stress, or 7.22 kips per square inch, at 500 seconds, and 95 percent (6.93 psi) at 200 seconds.

Figures A-11 and A-12 show changes of temperature and stress, respectively, of the center line (y = 0), y = 1 inch, and the plate edge (y = 4 in.). The temperature at a point on the center line starts to decrease rapidly as soon as the arc passes the point, while the temperature at a point on the plate edge continues to rise for a long time. Figure A-12 illustrates that a point on the center line is subjected to a complex stress change. First compressive stresses are produced as the heat source approaches the point. The absolute value of the compressive stress first increases as the heat source approaches and then decreases as the temperature rises and the yield stress decreases. As the heat source passes the point and the temperature begins to decrease, the stress changes to tensile and the value increases again. The stress at y = 1 inch remains compressive during the entire period, and the stress at the plate edge remains tensile.

(2) Isotherm and Isostress Curves Around the Heat Source. Figures A-13 and A-14 show curves for equal temperature and equal stress around the moving heat source under Condition 1. Figures A-15 through A-24 show isotherm and isostress curves around the heat source under Conditions 2 through 6. Figures A-15, A-17, A-19, A-21, and A-23 show isotherm curves, while Figures A-16, A-18, A-20, A-22, and A-24 show isostress curves.

The general pattern of the isostress curves is schematically shown in Figure 29. Portions of a plate start to experience significant stress changes when the heat source approaches them. There is a high compressive stress area shortly ahead of the heat source; however, values of compressive stresses are very low in high-temperature areas very close to the heat source. There is a narrow tensile-stress zone along the center line behind the heat source, and the compressive-stress zone expands outwards from this (Figure 29).

From the standpoint of metal movement in the thickness direction during welding, with which the present study is primarily concerned, the compressive-stress zone appears to be of particular importance. If the plate is thin, or the

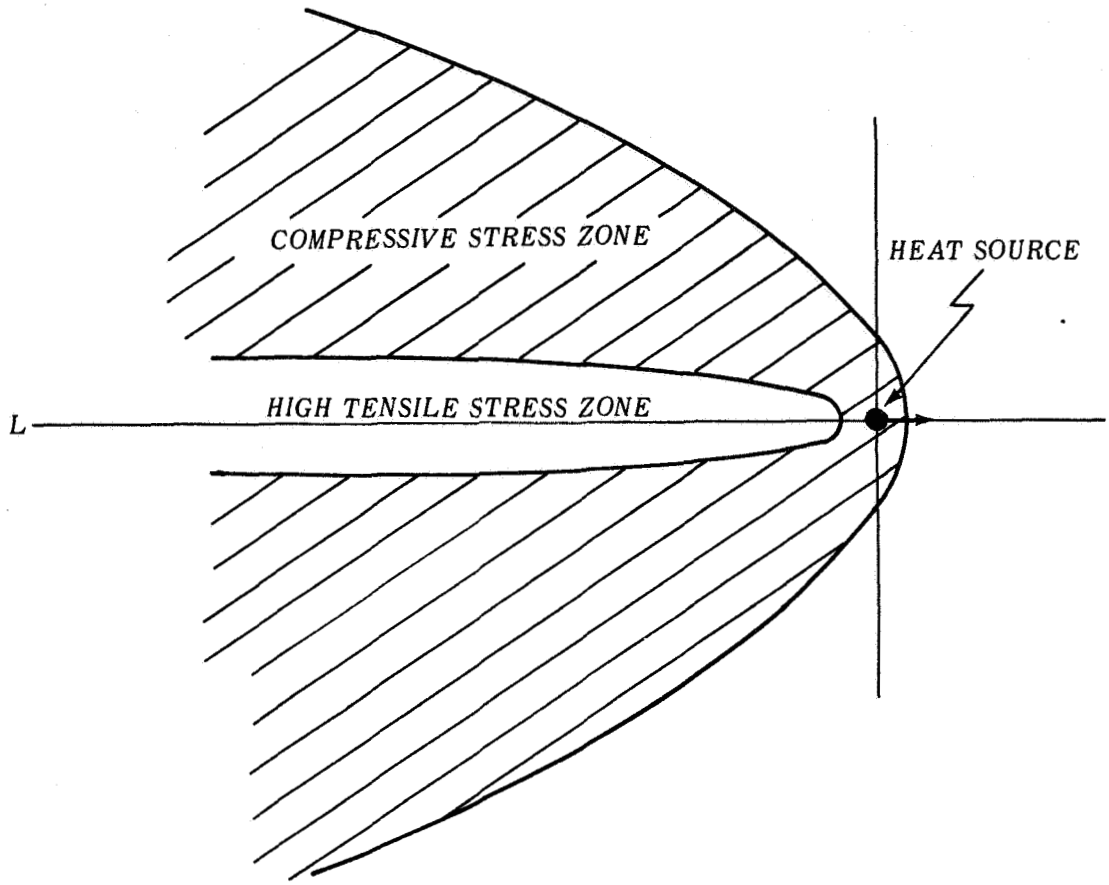

FIGURE 29. TENSILE- AND COMPRESSIVE-STRESS ZONES AROUND THE MOVING HEAT SOURCE

compressive-stress zone is large, the plate may buckle during welding. Distortion in the thickness direction also may be caused if the temperature and stress distributions are not uniform in the thickness direction. This problem will be further discussed in Section VI.

d. Effects of Welding Parameters on Temperature and Stress Distributions

As described previously, the current analysis has several shortcomings, one of which is the way in which the effect of plate width is handled. Another shortcoming is that no experimental verification of stress values has been obtained. Consequently, results of calculations presented in Figures A-1 through A-24 should be regarded as showing trends.

Figures A-16, A-18, and A-20 show isostress stress curves under Conditions 2 (high heat energy), 3 (medium heat energy), and 4 (low heat energy). By comparing these figures, one could deduce that the following phenomena would take place when the heat energy is reduced:

1) Maximum tensile residual stress in the weld center may not be reduced significantly, but the width of the tensile-stress zone would be reduced.

2) Consequently, the amount of compressive stresses and the size of the compressive-stress zone could be reduced.

e. Assumptions and Limitations Inherent in the Present Battelle Program

The presently available information regarding thermal stresses during arc welding is very scarce. Consequently, the Battelle program provides valuable information on this subject. However, the present program involves several assumptions, thus the usefulness of the program is still limited. It is hoped that the program can be further developed in the future and its usefulness expanded. The following are assumptions inherent in the present program:

1) The thermal constants and the material properties at elevated temperatures are known. (Actually, the data available are very limited.)

2) The temperature and stress changes in the thickness direction can be neglected. (Actually, bending distortion due to the stress changes in the thickness direction could be very important for causing lateral metal movement.)

3) The effects of transverse stress can be neglected. (Actually, the weld while melting and cooling causes changes not only in the longitudinal direction, but also transversely, i.e., a moment exists due to the transverse forces which is neglected in the computation. This moment can be increased or decreased if adjoining parts cause a nonuniform restraint, for example, at the junction of a flange and web. The effect, however, is of secondary importance.)

4) The fiber has no further resistance to load when its stress reaches the yield-point value. This assumes an idealized elastic-plastic stress-strain relationship at all temperatures. The stress-strain curve at elevated temperatures is not of the idealized elastic-plastic type, but rather a nonlinear curve. The yield point is therefore defined by an offset so that considerable resistance to load can exist past the specified yield point.

5) The heat input is known. (Actually, heat input for this investigation was not determined experimentally. The heat input has an effect on the thermal and residual stress distribution.)

In the present analysis, it was also assumed that any transverse sections remain plane during the entire process. It was necessary to simplify the analysis so that a two-dimensional stress field is replaced by a one-dimensional field system. The equilibrium condition also is simplified. Instead of using an ordinary equilibrium condition in a two-dimensional stress field, simple conditions [Eq. (24) and (25)] are used. The equilibrium force is distributed evenly over the cross section. Consequently, the residual stresses could be zero when the plate width becomes infinite.

Section V. EXPERIMENTAL INVESTIGATIONS CONDUCTED AT THE MARSHALL SPACE FLIGHT CENTER

Experimental investigations were conducted at the Welding Branch, Manufacturing Engineering Laboratory (MEL) of George C. Marshall Space Flight Center, NASA, on metal movement during welding of aluminum plates. The experiments are described in two reports prepared by R. W. Jackson, Welding Development Group of Hayes International Corporation MEL Operations.[60,61] The MEL Technical Report WD-70-67[60] describes the results on the first test (Panel No. 1), while the MEL Technical Report WD-79-68[61] describes the results on the second test (Panel No. 2).

This section presents the results from these reports that are important to the Battelle study.

1. Experimental Methods

Metal movements during welding were measured on two plates of 2014-T6 aluminum alloy in the horizontal position. The movements were determined by 32 dial indicators and recorded on 17 time-sequence photographs. The test conditions including welding conditions of the two panels were essentially the same.

a. Test Panels

Figure 30 shows the test panels and locations of dial indicators. The test plates were 144 inches long, 30 inches wide, and 0.25 inch thick. The panels were suspended lengthwise in an upright position between two stanchions. The end nearest the weld starting point was securely attached to the stanchion. Two cables, two ratchet action puller hoists, "come-alongs," and two dynanometers were used in securing the end near the weld stopping point to the other stanchion. This permitted free movement of the panel during welding. A tension preload of 3500 inch-pounds was applied to the panel with the come-alongs as measured in inch-pounds by the dynanometers (capacity of 0 to 20,000 in.-lb). Tension was maintained throughout the welding cycle.

b. Welding

The weld extended for 90 inches along the horizontal center of the panel, beginning and ending 27 inches from the ends (Figure 30). The panel

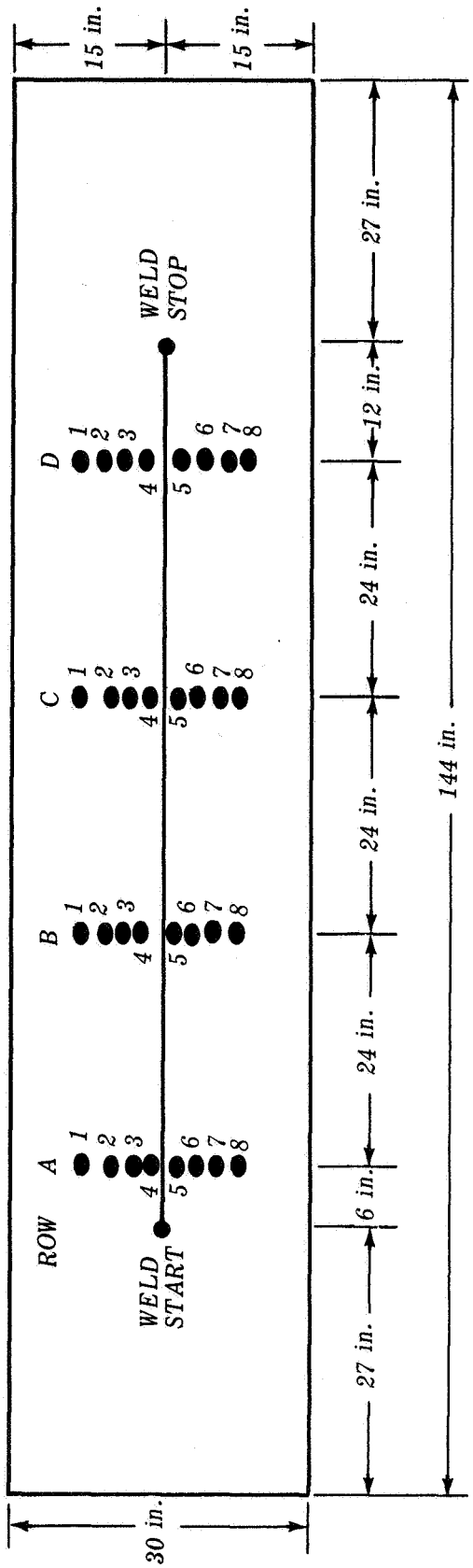

FIGURE 30. LOCATIONS OF DIAL INDICATOR CONTACT POINTS IN RELATION TO THE WELD

was welded with a bead-on-plate technique using the gas tungsten-arc process. The following welding conditions were used:

1) Arc current 254 A
2) Arc voltage 10 V
3) Arc travel speed 14 in./min (0.233 in./sec).

The weld was made on the side away from the dial indicators.

c. Measurement of Metal Movement

Metal movement was measured with 32 dial indicators mounted on a stationary frame in 4 vertical rows of 8 each so that the probes were in intimate contact with the surface of the panel opposite the torch. These rows, designated A, B, C, and D, intersected the horizontal or weld center line at points 6, 30, 54, and 78 inches from the weld starting point (Figure 30). The dial indicators were arranged vertically along these rows at points 1, 2, 4, and 8 inches on each side of the weld center line. These points were designated 1 through 8 from the top to the bottom. For example, Point 5 is 1 inch below the weld center line.

Data were collected during tests by time-sequence photographs beginning at the time the arc was struck and continuing at intervals until torch shut-off. The time interval between frames was about 30 seconds. Another photograph was taken approximately 10 minutes after torch shut-off. Each photograph simultaneously recorded 32 measurements. The visual reading of the dial indicators was made approximately 3 hours after the test with the panel at room temperature.

2. Test Results

Data obtained by the 32 dial indicators were analyzed to determine the metal movement during welding. The following pages describe typical results pertinent to the Battelle study.

a. Metal Movement on Panel No. 2

Figure 31 shows how points at dial indicators No. 5 (1 in. below the weld center line) on Rows A through D moved as welding progressed on Panel No. 2. Positive values indicate movement toward the welding torch;

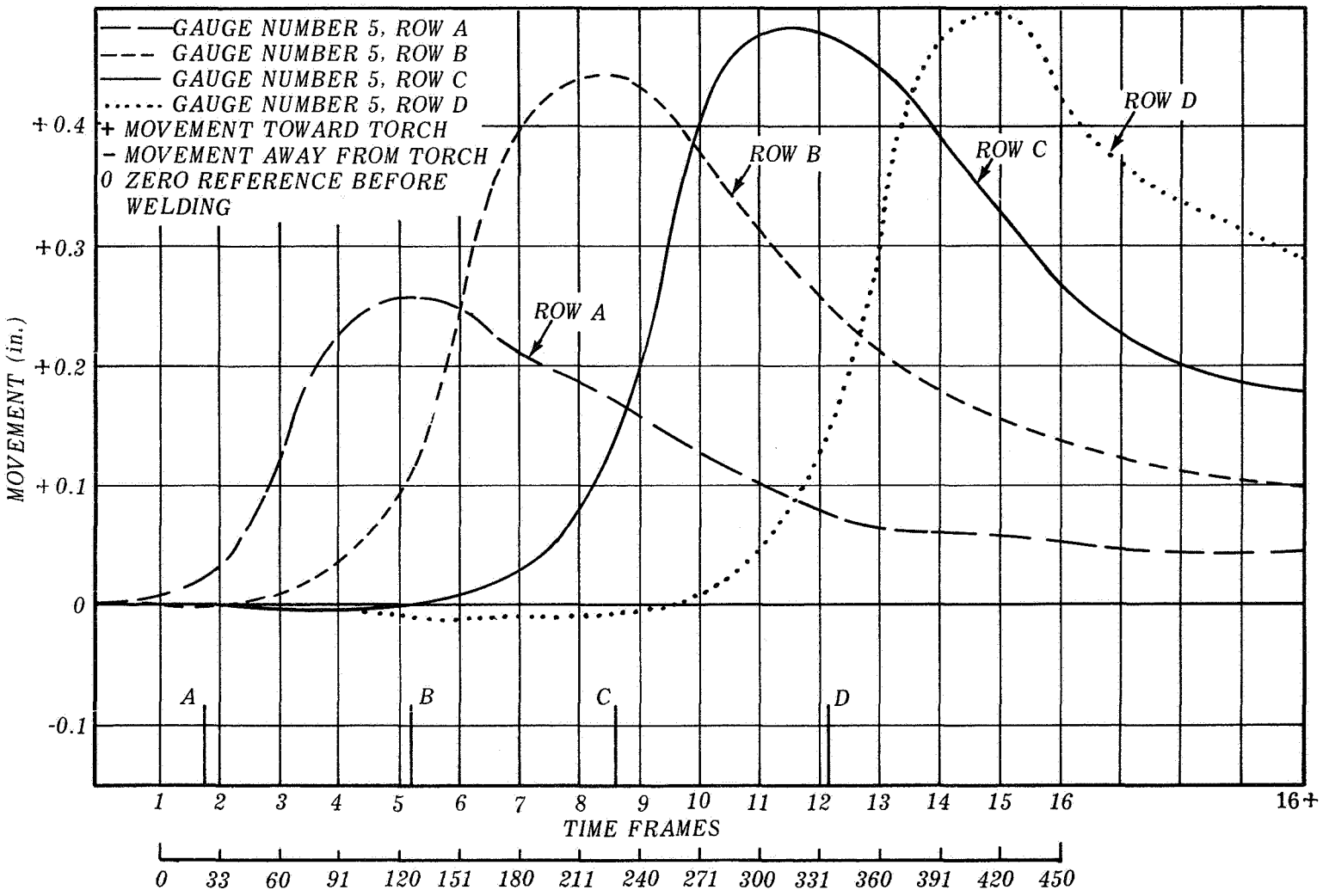

FIGURE 31. TYPICAL PROFILES OF METAL MOVEMENT IN THE HORIZONTAL PLATE

negative values indicate movement away from the welding torch. Four marks, A, B, C, and D, in the figure indicate the time when the welding torch passed Rows A, B, C, and D, respectively.

Values of metal movement first increased and then decreased gradually as welding progressed. This is shown by curves for Rows A through D. There was a definite time lag between a curve for a certain row and that of the next row. This indicates that there was a local metal movement near the welding torch that traveled with the welding torch.

The figure also shows that there was a gradual increase in the amount of metal movement as the welding progressed from Row A toward Row D.

Figure 32 shows profiles of vertical axes along Rows A through D at time frame 9. At this time the welding torch was located just beyond Row C. The metal movement along Row B was quite significant, while little metal movement occurred along Row D.

These figures indicate two types of metal movement; (1) local metal movement around the welding arc and (2) general metal movement of the entire panel.

The local metal movement is insignificant in areas ahead of the welding arc. It reaches the maximum some distance behind the arc and then decreases gradually. In the particular case shown in Figure 31, the local metal movement reduced to an insignificant value about 300 seconds after the arc had passed. Or, stated differently, the local movement occurs in areas around 7 inches long. It is believed that the local metal movement is associated primarily with the thermal stresses around the moving arc. The local movement occurs toward the welding torch. This might mean that the plate surface near the torch is heated to a higher temperature compared to the other surface; thus the expansion of the torch-side surface is greater than the other surface.

The general movement of the panel increases as welding progresses, or as the total heat input to the panel increases.

b. Metal Movement on Panel No. 1

Figures 33 and 34 show typical profiles of movement in the horizontal line and vertical lines, respectively, of Panel No. 1. Figures 33 and 34 are presented in the same way as Figures 31 and 32.

PROFILE OF MOVEMENT ON THE VERTICAL AXIS AT TIME FRAME 9, COINCIDENTAL WITH INDICATOR POSITIONS A, B, C, AND D.

0 ZERO REFERENCE VERTICAL PROFILE BEFORE WELDING.
A, B, C, AND D VERTICAL PROFILE CHANGE AT TIME FRAME 9.
+ MOVEMENT AWAY FROM TORCH.
− MOVEMENT TOWARD TORCH.

FIGURE 32. TYPICAL PROFILES OF MOVEMENT IN THE VERTICAL AXIS

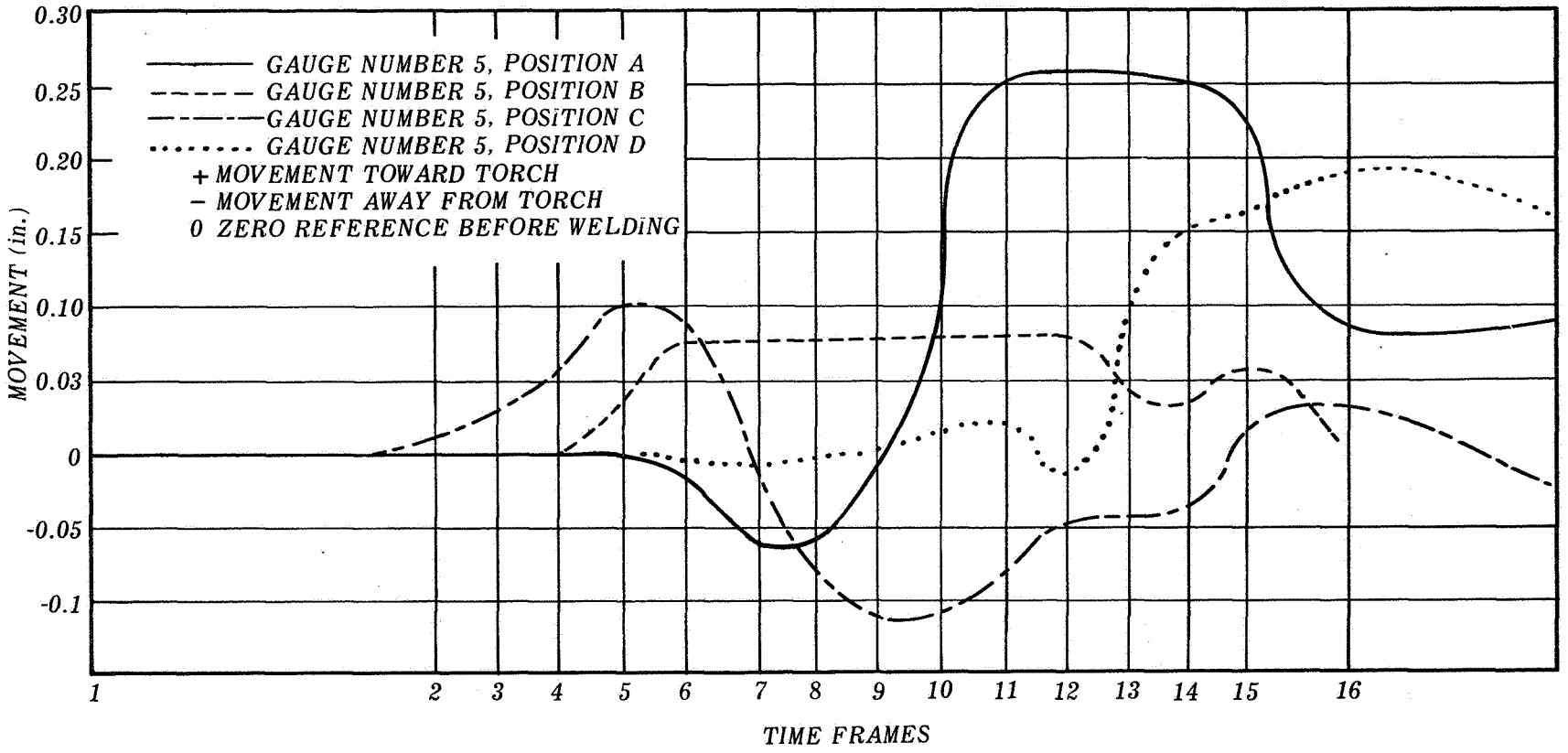

FIGURE 33. TYPICAL PROFILES OF METAL MOVEMENT IN THE HORIZONTAL PLANE

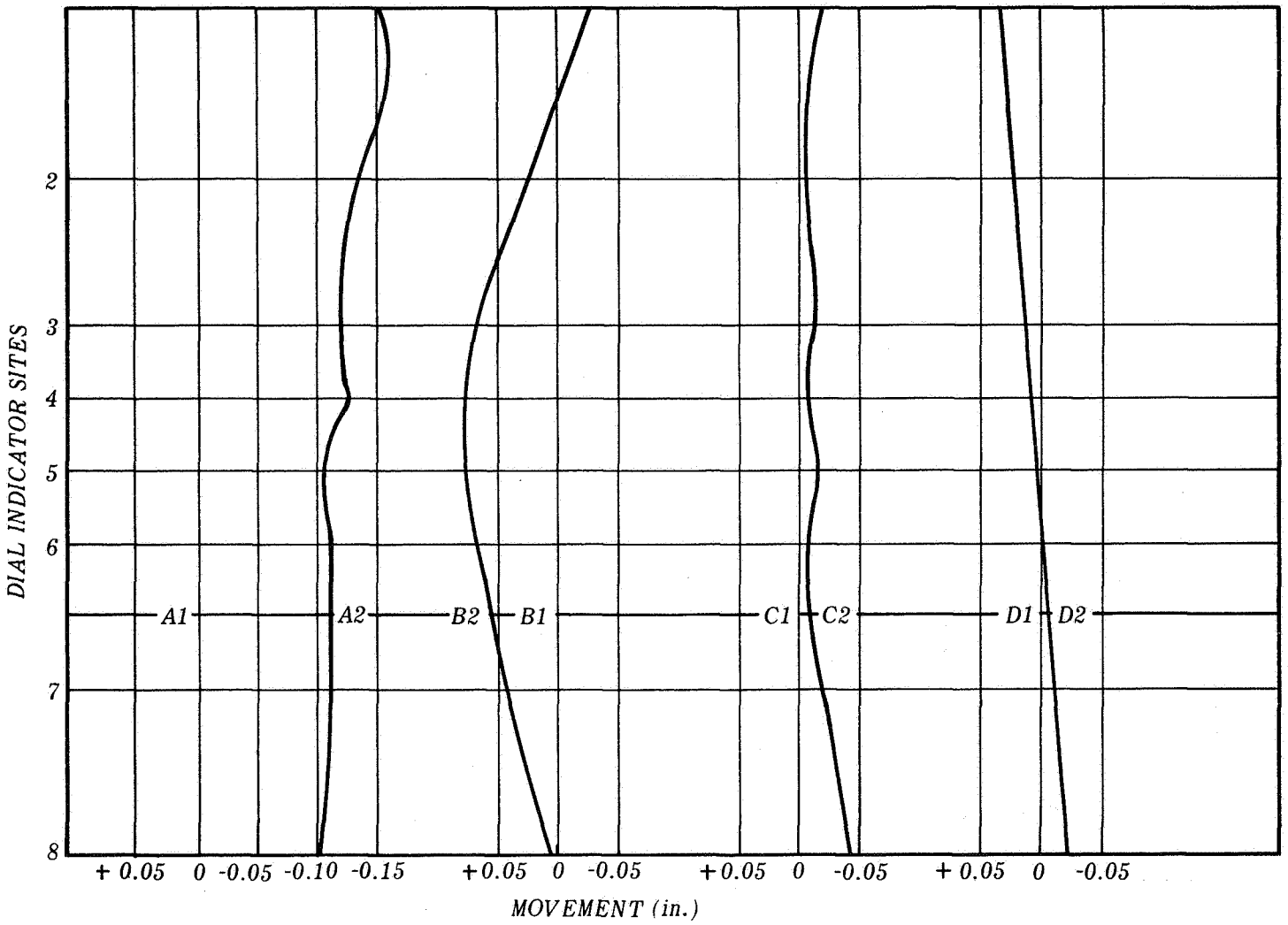

A1, B1, C1, AND D1 ZERO REFERENCE BEFORE WELDING
A2, B2, C2, AND D2 VERTICAL PROFILES AT TIME FRAME 9
+ MOVEMENT AWAY FROM TORCH
– MOVEMENT TOWARD TORCH

FIGURE 34. TYPICAL PROFILES OF MOVEMENT IN THE VERTICAL AXIS

Results shown in Figures 33 and 34 are similar to those shown in Figures 31 and 32, except that results shown in Figure 33 fluctuate considerably compared with those shown in Figure 31 and the amount of metal movement on Panel No. 1 was somewhat less than that on Panel No. 2.

During the experiment on Panel No. 1, experimental procedures, including techniques for measuring metal movement, were not completely established. Consequently, results on Panel No. 1 may contain more error than those on Panel No. 2, or the amount of metal movement may actually vary from one panel to another. Further study is needed to clarify these differences.

By using the data obtained on Panel No. 1, a series of figures was drawn at the Marshall Space Flight Center showing the shape of the panel at various instances during the welding cycle.

Figure 35 is an example of these figures. The x mark shows the location of the welding torch at this instance. The torch is moving from left to right. The broken lines show the original shape of the panel and reference lines. This figure shows that two types of metal movement exist, (1) the local metal movement toward the torch in areas near the torch and (2) the wavy-shaped general movement of the entire panel.

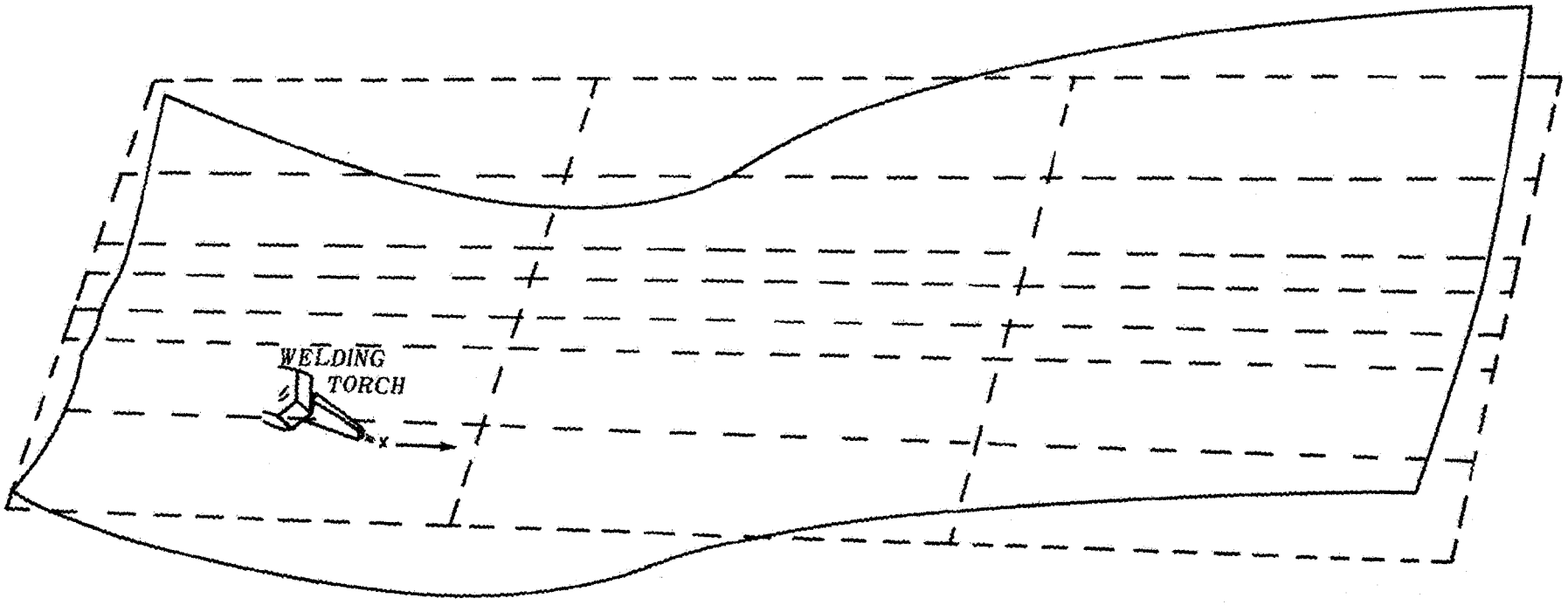

FIGURE 35. SHAPE OF PANEL DURING WELDING

Section VI. EXPLANATION OF EXPERIMENTAL RESULTS ON THE BASIS OF ANALYTICAL STUDIES

Metal movement, as described in Section V, is a complicated dynamic phenomenon, and no analytical information has been developed which is capable of quantitatively analyzing it. As a part of the present Battelle study, an attempt was made to study the mechanisms of metal movement in a semiquantitative manner, based on the present analysis.

The analysis was made on the following two subjects:

1) Local metal movement in areas near the welding arc, to determine if the local metal movement can be explained on the basis of thermal stresses around the moving heat source

2) General metal movement of the entire panel, to determine if the panel may buckle due to residual stresses.

Areas near the welding arc experience complex stress changes as the arc travels. A computer program has been developed in this study to calculate temperature and stress distributions around a moving heat source. Figures A-1 through A-14, for example, show results for welding parameters of Condition 1 in Table III, which simulates the experimental conditions of Panels No. 1 and 2.* These results, although they neglect stress changes in the thickness direction, are useful for studying the general trend.

The following are two logical possible causes of the local metal movement:

1) The local metal movement by bending. The temperature and stress distributions are not uniform in the thickness direction, thus bending movement is created.

2) The local metal movement by buckling. The compressive-stress zone near the heat source is large, or the compressive stresses are high, thus the panel buckles locally.

*In the calculation, the arc efficiency was estimated to be 0.8. The plate width for the calculation is 8 inches.

1. Possibility of Local Metal Movement Due to Bending

The possibility of local metal movement due to bending appears to be high.

According to Figure 31, metal movement increased significantly when the welding arc approached the point of interest and it took about 300 seconds for this movement to decrease. Computer-calculated stress changes around the heat source show a similar trend. The calculated stresses start to change significantly when the heat source approaches the point of interest, and it takes about 300 seconds for the stress distribution to become almost equal to the residual stress at time infinity (Figure A-12).

Figure 26 shows that temperature distribution around the welding arc is not uniform in the thickness direction, especially in areas close to the arc. Consequently, if stress calculations were made using temperature distributions shown by Curves 1, 2, 3, ... of Figure 26, the bending moment resulting from nonuniform thermal stresses may be large enough to cause local bending of the plate around the arc. It is recommended that further analysis be made on this subject.

2. Possibility of Local Metal Movement Due to Buckling

The analysis of local buckling of a plate due to thermal stresses caused by a moving heat source is extremely difficult. Consequently, only a simple analysis was made in the present study to see whether or not local metal movement due to buckling is a possibility. As it has turned out, the possibility of local metal movement due to buckling is remote.

A compressive-stress zone exists on both sides of the weld line (Figure 29). According to Figure A-14, the compressive-stress zone extends from y = 0.6 to 3.6 inches, and the stress values are around 7000 pounds per square inch. Therefore, an analysis was made to determine if a simply supported panel, 3 to 7 inches wide, would buckle under a uniform compressive load on the order of 7000 pounds per square inch.

The critical compressive stress σ_{cr} of a simply supported panel under uniaxial loading (Figure 36) is[62]

$$\sigma_{cr} = K \cdot \frac{E\pi^2}{12\ (1-\nu^2)} \left(\frac{h}{B}\right)^2 \qquad (27)$$

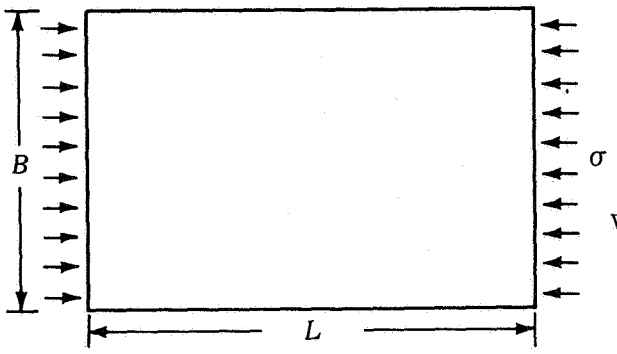

FIGURE 36. SIMPLY SUPPORTED RECTANGULAR PLATE UNDER UNIAXIAL COMPRESSIVE STRESSES

$$K = \left(\frac{\beta}{m} + \frac{m}{\beta}\right)^2 \qquad (27\text{-a})$$

$$\beta = \frac{L}{B} \qquad (27\text{-b})$$

where,

h = plate thickness
L = panel length
B = panel width
m = number of wave
E = Young's modulus
ν = Poisson's ratio.

For a narrow panel ($\beta > 4$), K = 4; therefore,

$$\sigma_{cr} = \frac{E\pi^2}{3\,(1-\nu^2)} \cdot \left(\frac{h}{B}\right)^2 . \qquad (28)$$

for 2014-T6 aluminum plate 0.25 inch thick ($E = 10^7$ psi for temperatures up to about 400°F and $\nu = 0.3$)

B (in.)	σ_{cr} (psi)
3	250,000 (well over the yield stress)
7	46,000

In other words, extremely high compressive stresses must be present to cause the local buckling. Consequently, the possibility of lateral movement due to buckling is considered to be remote.

3. Buckling of The Entire Panel

The buckling of the entire panel after welding can be analyzed by Mura's method described in Section III [Eq. (11) and Figure 22].

For a panel where L = 144 inches and 2a = 30 inches, the value of λ for m = 1 is 9.6. Using Curve A in Figure 22, the critical $\overline{\mu}$ is about 1.8. Then

the value of σ_1 is only 830 pounds per square inch. The compressive residual stresses in areas from the weld of an 8-inch wide plate is about 7000 pounds per square inch (Figure A-10). The mean value of the compressive stresses of a 30-inch wide plate is considered to be on the order of 1800 pounds per square inch, which is much higher than the above critical value of 830 pounds per square inch. Consequently, it is believed that the general metal movement of the entire panel is caused by buckling due to compressive residual stresses that exist in the base plate region away from the weld line.

Section VII. SUMMARY AND CONCLUSIONS

After identifying weld distortion problems in Saturn V structures, a literature survey was conducted to obtain useful information on thermal stresses during welding and buckling after welding. Using this information, a computer program was developed to calculate the temperature distribution and resulting thermal stress created by a moving heat source such as exists when making a butt or edge weld in a plate. The computer program is a mathematical model of a simple welding process as it affects material properties, temperature, and stress distributions in a plate.

The program is written in FORTRAN IV computer language for use on a CDC 6400 computer system including a CalComp plotter. Computations can readily be made for any material (provided that the material properties are known) and for any welding parameters (arc voltage, welding current, arc efficiency, and arc travel speed). The program is so designed that output results are printed and figures are plotted.

To study effects of welding parameters on the temperature and stress distributions, calculations were made for bead-on-plate welds in 2014-T6 aluminum alloy under six different conditions. Computer-plotted results are shown in Figures A-1 through A-34.

An attempt also was made to study the mechanisms of the metal movement observed during bead-on-plate welding of a flat panel in 2014-T6 aluminum alloy. The experiments were conducted at the Marshall Space Flight Center. The following conclusions have been drawn:

1) The local metal movement appears to be due to bending moment induced by nonuniformity in the thickness direction of thermal stresses in areas near the weld. The local metal movement does not appear to be due to buckling induced by compressive thermal stresses.

2) The general metal movement of the entire panel is believed to be caused by buckling due to compressive residual stresses which exist in the base plate region away from the weld.

It is also recognized that the computer program developed during this study could be profitably used in other stress-oriented programs. In addition, the success of this program indicates that the general idea of a computer aided analytical approach to experimental work has considerable merit and should be considered in other areas.

Section VIII. RECOMMENDED FUTURE PROGRAMS

Although the present analysis provides only an indicative picture of stress distribution, the development of such a program is in itself an advancement in the welding technology. It is recommended that further studies be conducted to experimentally verify the program, obtain additional experimental data needed for the analysis, and improve the accuracy of analysis.

1) Experimental Verification. First of all, it is important to conduct a series of experiments to study the validity of the present analysis, which has not been compared with experimental results. Most urgently needed is information on thermal stresses during welding.

2) Assessment of Data Needed for Analysis. The analysis requires accurate data on properties of metals (thermal conductivity, yield stress, specific heat, ... , etc., at various temperatures) and on arc efficiency. However, such data are scarce. It is recommended that experimental studies be made to obtain this type of information.

3) Improvement of Analysis. As described in the last part of Section IV, the present analysis involves several assumptions that limit the program's usefulness. It is recommended that future studies be made to improve the analysis. For example, temperature and stress changes in the thickness direction need to be included to analyze the metal movement during welding. The effects of local transverse stress near the heat source also need to be considered.

Figure 37 outlines a possible specific study drawn along these lines to further develop the present computer program.

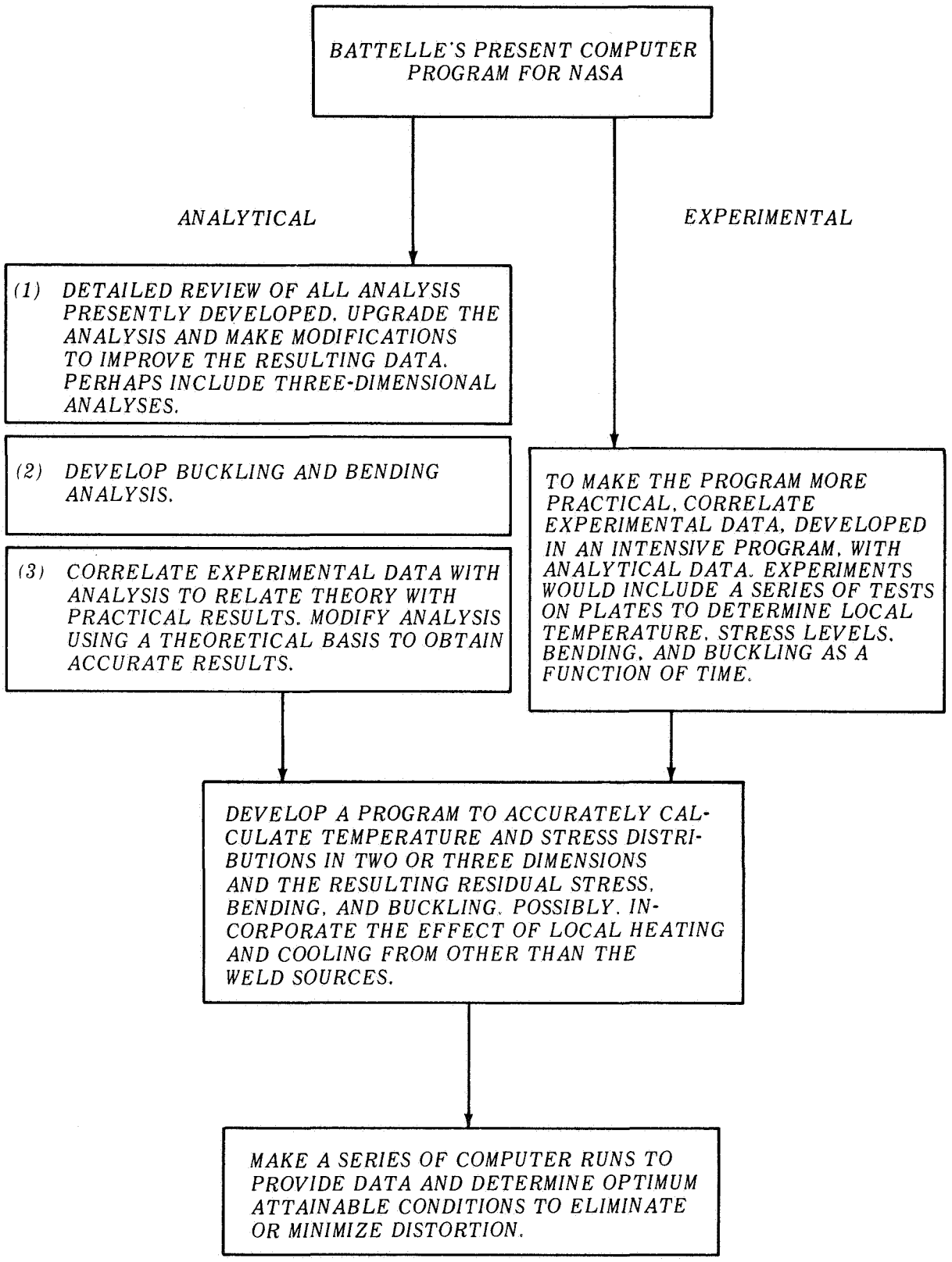

FIGURE 37. SUGGESTED STUDY TO FURTHER DEVELOP COMPUTER PROGRAM

Appendix
FORTRAN PROGRAM TO CALCULATE TEMPERATURE DISTRIBUTION AND RESULTING THERMAL AND RESIDUAL STRESSES DUE TO A MOVING HEAT SOURCE WHICH SIMULATES WELDING

MAIN PROGRAM

The FORTRAN program as listed directly by the computer is given. At the beginning of the program is a write-up of all the input cards required and the parameter associated with each value on an input card. In all, nine cards are required per run, but for this listing a repeating loop (in computer language a "DO" loop) was added to process up to six runs at a time.

It is important to note that this listing was run on a CDC 6400 computer system, and although FORTRAN is a generally used computer language, this program may have to be modified slightly to run on a different type computer system.

The program, as run on the CDC 6400 computer system, requires 60,000 octal-core storage positions. Depending on the number of spacings used and the number of output graphs to be drawn, it can process an average set of data in 30 to 45 seconds of central processor (CP) time and 50 to 120 seconds of peripheral processing time. The cost of each graph as drawn by the computer ranges from 75 cents to a few dollars depending on the complexity and number of data points involved.

Special subroutines or subprograms written especially to be used with this program are listed in "Subprograms."

```
      PROGRAM WELD(INPUT,OUTPUT,PLOT,TAPE99=PLOT)
C     CALCULATION OF RESIDUAL STRESS FROM A COMPUTED TEMPERATURE DISTRIBUTION
C     METHOD OF  L TALL
C     THIS PROGRAM REQUIRES 9 INPUT DATA CARDS. THESE CARDS ARE NUMBERED
C     FROM 1 THRU 9  IN THE FIRST COLUMN  OF EACH  CARD. THE CARDS LABELED
C     1,2, AND 3 ARE INPUT AND CONTROLL CARDS,  WHILE CARDS 4,5,6,7,8,
C     AND 9  CONTAIN DATA OF PARAMETER VARIATION WITH TEMPERATURE START-
C     ING FROM ZERO DEGREES FAHRENHEIT.
C     CARDS 4-9 EACH CONTAIN TEN VALUES OF THE PARAMETER OVER A RANGE
C     OF ZERO TO SOME VALUE NEAR THE MELTING POINT OF THE MATERIAL.
C     THESE VALUES ARE SPACED AT EQUAL INTERVALS OVER THE RANGE.  THIS,
C     THE SPACING INCREMENT USED,SHOULD BE LISTED IN COLUMNS 41-48 ON
C     CARD NUMBER 2.
C     CARD NUMBER 4 IS THERMAL CONDUCTIVITY (WATTS/IN-F)
C     CARD NUMBER 5 IS MAXIMUM ALLOWABLE YEILD STRESS (KSI)
C     CARD NUMBER 6 IS YOUNGS MODULES (E) (KSI)
C     CARD NUMBER 7 IS TH COEFFICIENT OF THERMAL EXPANSION (1/F)
C     CARD NUMBER 8 IS THE SPECIFIC HEAT (WATT-SEC/LB-F)
C     CARD NUMBER 9 IS THE DENSITY (LB/CU IN)
C     CARD NUMBER 1 CONTAINS  THE VALUES IN ORDER AS FOLLOWS (THE NUMBER
C     OF PLOTS OF TEMPERATURE VS LENGTH, THE SPACING IN INCHES BETWEEN
C     EACH PLOT FROM THE CENTERLINE,  11 TIME VALUES IN INCREASING
C     ORDER FOR WHICH PLOTS OF TEMPERATURE AND STRESS ARE TO  BE PLOTTED
C     - IF A DECREASING VALUE IS FOUND NO MORE PLOTS WILL BE MADE,
C     THE MATERIAL IDENTIFICATION IS WRITTEN OUT FROM COLUMN 57-77).
C     CARD 2 CONTAINS IN ORDER THE FOLLOWING VALUES (VOLTAGE,AMPERAGE,
C     EFFICIENCY FACTOR, WELDING SPEED IN INCHES PER SECOND, THICKNESS,
C     TEMPERATURE INCREMENT SPACING OF PARAMETERS IN CARDS 4-9, MELTING
C     TEMPERATURE , A FACTOR TO INCREASE THE YEILD STRENGTH IN THE
C     PLASTIC ZONE, AND THE MAXIMUM TIME TO BE PLOTTED ON THE CONTOUR
C     TYPE GRAPHS),
C     CARD 3 CONTAINS VALUES TO DETERMINE THE SPACING ACROSS THE WIDTH
C     OF THE SPECIMEN FOR NUMERICAL INTIGRATION, AND VALUES TO SET UP
C     THE TIME INTERVAL SPACING AS FOLLOWS (WIDTH INCREMENT IN INCHES,
C     MAXIMUM WIDTH FOR INCREMENT  IN INCHES, A SECOND SPACING INCREMENT
C     STARTING FROM THE LAST VALUE, THE MAXIMUM VALUE FOR THE SECOND
C     SPACING INCREMENT, THE FIRST TIME SPACING INTERVAL IN SECONDS,
C     THE MAXIMUM VALUE FOR THE FIRST TIME INTERVAL, A SECOND TIME
C     SPACING INTERVAL, THE MAXIMUM VALUE OF THE SECOND TIME INTERVAL,
C     A THIRD TIME SPACING INTERVAL, THE MAXIMUM VALUE OF THE THIRD
C     TIME INTERVAL).  ONLY ONE VALUE EACH OF AN INCREMENT AND A MAXIMUM
C     ARE NEEDED FOR BOTH  THE WIDTH AND TIME.
000003      COMMON RA(6,11),TMPI,TMPMX
000003      DIMENSION ITP(11),ENT(10),TY1(50),TY2(50),XX(50),DT(50),TAV(50)
000003      DIMENSION EAV(50),SIGAV(50),DSIG(50),DSIG2(50),DB(50),DP(50)
000003      DIMENSION YUK(50),XTT(99),YTT(99),ALAV(50),ITLE(2)
```

```
000003          DIMENSION XYZ(1100),YZX(1100),ZXY(1100),T1(300),T2(300),T3(300)
000003          DIMENSION T4(300),T5(300),T6(300),IARY(300)
000003          DIMENSION XXX(1100),YYY(1100),ZZZ(1100),YTTT(99),YTTTT(99),XA1(2)
000003          DIMENSION STT(99),STTT(99),STTTT(99),YA1(2)
000003          REAL LMDA
000003          XA1(1)=0.
000004          YA1(1)=0.
000005          YA1(2)=0.
000006          DO 1000 II=1,6
000007          JJ=2
000010          KZ=1
000011          IJK=1
000012          KYT=1
000013          ICUT=1
000014          MCHK=0
000015          D=0.
000016          SIGEQ=0.
000017          TE=1000.
          C     READ IN AND SET UP INPUT DATA
000020          READ 1,ICHK,NOX,XSPACE,(ITP(I),I=1,11),ITLE
000042        1 FORMAT(I1,I3,F4.1,10I4,I8,2A10)
000042          PRINT 2
000046        2 FORMAT(1H1,5X,*INPUT DATA CARDS*//)
000046          PRINT 3,ICHK,NOX,XSPACE,(ITP(I),I=1,11),ITLE
000070        3 FORMAT(2I4,F10.2,11I8,5X,2A10)
000070        4 READ 5,ICHK,(ENT(I),I=1,10)
000104        5 FORMAT(I1,F7.3,9F8.3)
000104          PRINT 6,ICHK,(ENT(I),I=1,10)
000120        6 FORMAT(/I4,10F10.3)
000120          GO TO (100,12,13,14,14,14,14,14,14)ICHK
000135       12 VOLT=ENT(1)
000137          AMP=ENT(2)
000140          EF1=ENT(3)
000142          VEL=ENT(4)
000143          THIK=ENT(5)
000145          TMPI=ENT(6)
000146          TMPMX=ENT(7)
000150          YSFACT=ENT(8)
000151          TMAX=ENT(9)
000153          GO TO 20
000153       13 DELY1=ENT(1)
000155          Y1MX=ENT(2)
000156          IF(ENT(3))100,44,45
000160       44 DELY2=1.
000162          Y2MX=Y1MX
000163          GO TO 46
000164       45 DELY2=ENT(3)
```

```
000166          Y2MX=ENT(4)
000167       46 TI1=ENT(5)
000171          T1MX=ENT(6)
000172          IF(ENT(7))100,40,41
000174       40 TI2=1.
000176          TI3=1.
000177          T2MX=T1MX
000200          T3MX=T2MX
000201          GO TO 20
000202       41 TI2=ENT(7)
000204          T2MX=ENT(8)
000205          IF(ENT(9))100,42,43
000207       42 TI3=1.
000211          T3MX=T2MX
000212          GO TO 20
000213       43 TI3=ENT(9)
000215          T3MX=ENT(10)
000216          GO TO 20
000217       14 ICH=ICHK-3
000221          IF(ENT(2))100,15,17
000223       15 DO 16 I=1,11
000225       16 RA(ICH,I)=ENT(1)
000233          GO TO 20
000234       17 DO 18 I=1,10
000236       18 RA(ICH,I)=ENT(I)
000245          RA(ICH,11)=ENT(10)
000247       20 MCHK=MCHK+1
000251          IF(MCHK-8)4,21,100
000254       21 QP=EF1*VOLT*AMP/(THIK*6.2831853)
000261          TGMAX=TMPMX*.15
000263          ISS0=RA(2,2)/4.+.9
000266          SS0=-ISS0*4.
000270          SSI=ISS0
000272          FRS=.5/1.2**Y2MX
000276          T=-TI1
000277          Y=-DELY1
000301          RHO=RA(6,5)
000302          SPHT=RA(5,5)
000304          COND=RA(1,5)
000305          KT=T1MX/TI1+(T2MX-T1MX)/TI2+(T3MX-T2MX)/TI3+1.2
000317          KY=Y1MX/DELY1+(Y2MX-Y1MX)/DELY2+1.2
000326          KZ=KT
000327          PRINT 222,ITLE,DELY1
000337      222 FORMAT(1H1,* TIME VS TEMPERATURE AND THERMAL STRESS*,10X,2A10,10X,
               1*SPACING EVERY*,F4.2,*INCHES STARTING WITH ZERO*)
            C     CALCULATE THE TEMPERATURE DISTRIBUTION
000337          IX=1.+2./VEL
```

```
000343          X=IX*VEL
000344          PRINT 223,IX
000352      223 FORMAT(10X,*HEAT SOURCE LOCATED AT T =*,I5//)
000352          DO 32 J=1,KY
000354          DSIG2(J)=0.
000355          TY2(J)=0.
000356          IF(Y-Y1MX+.0001)29,31,31
000362       29 Y=Y+DELY1
000364          GO TO 32
000365       31 Y=Y+DELY2
000367       32 XX(J)=Y
000374          XA1(2)=Y2MX
000375          YDIST=XX(KY)*.166666
000377          DB(1)=(XX(2)-XX(1))*.5
000402          XX(KY+1)=XX(KY)
000404          DO 30 K=2,KY
000406          DB(K)=(XX(K+1)-XX(K-1))*.5
000411       30 CONTINUE
000413          DO 999 I=1,KT
000415          IF(T-T1MX)22,23,24
000417       22 T=T+TI1
000421          GO TO 28
000422       23 T=T1MX+TI2
000424          GO TO 28
000425       24 IF(T-T2MX)25,26,27
000430       25 T=T+TI2
000432          GO TO 28
000433       26 T=T2MX+TI3
000435          GO TO 28
000436       27 T=T+TI3
000440       28 ETA=X-VEL*T
000443          DO 499 J=1,KY
000445          R=SQRT(ETA*ETA+XX(J)*XX(J))
000453       33 LMDA=RHO*SPHT*.5/COND
000457          Z=-LMDA*VEL*ETA
000462          ZZ=LMDA*VEL*R
000463          IF(Z-670.)331,331,330
000466      330 Q=2./ZZ
000470          QQ=Q*Q
000471          QQQ=QQ*Q
000472          EK=EXP(Z-ZZ)*(1.25331414-.07832358*Q+.02189568*QQ-.01062446*QQQ+.0
               10587872*QQ*QQ-.0025154*QQQ*QQ+.00053208*QQQ*QQQ)/SQRT(ZZ)
000520          GO TO 34
000520      331 EK=EXP(Z)*BESMK0(ZZ)
000526       34 TEMP=EK*QP/COND
000531          IF(TEMP-.01)37,35,39
000533       37 TEMP=0.
```

```
000534          GO TO 35
000535       39 IF(TEMP-TMPMX)35,35,332
000540      332 TEMP=TMPMX
000542       35 AB=ABS(TEMP-TE)
000545          IF(AB-.1)38,38,36
000547       36 TE=TEMP
000551          RHO=VART(TEMP,6)
000554          SPHT=VART(TEMP,5)
000557          COND=VART(TEMP,1)
000562          GO TO 33
000562       38 TY1(J)=TEMP
000564      499 CONTINUE
000567          PRINT 997,T
000574      997 FORMAT(/8H  TIME =,F6.0,10H   SECONDS)
000574          PRINT 998,(TY1(M),M=1,KY)
000607      998 FORMAT(/8X,5HTEMP ,13F9.2/13X,13F9.2/13X,13F9.2/13X,13F9.2/13X,13F
               19.2/13X,13F9.2/13X,13F9.2/13X,13F9.2)
000607          XTT(I)=T
000611          YTT(I)=TY1(1)
000613          YTTT(I)=TY1(6)
000614          YTTTT(I)=TY1(KY)
          C     CALCULATE THE STRESS DISTRIBUTION
000616          DO 67 K=1,KY
000620          DT(K)=TY2(K)-TY1(K)
000623          TY2(K)=TY1(K)
000624          TAV(K)=TY2(K)+DT(K)*.5+70.
000631          SIGAV(K)=VART(TAV(K),2)
000635          IF(DT(K))66,65,66
000636       65 DSIG(K)=0.
000640          GO TO 67
000640       66 ALAV(K)=VART(TAV(K),4)
000645          EAV(K)=VART(TAV(K),3)
000651          DSIG(K)=DT(K)*ALAV(K)*EAV(K)*.001
000655       67 CONTINUE
000660       70 DO 75 K=1,KY
000662          YUK(K)=DSIG(K)+DSIG2(K)+SIGEQ
000666          IF(ABS(YUK(K))-SIGAV(K))74,74,71
000671       71 IF(YUK(K))73,100,72
000673       72 YUK(K)=SIGAV(K)
000675          GO TO 74
000676       73 YUK(K)=-SIGAV(K)
000700       74 DP(K)=DB(K)*YUK(K)
000703       75 D=D+DP(K)
000707          IF(ABS(D)-.5)77,77,76
000712       76 SIGEQ=SIGEQ-D*FBS
000715          D=0.
000716          GO TO 70
```

```
000716      77 DO 78 K=1,KY
000720      78 DSIG2(K)=YUK(K)
000724         SIGEQ=0.
000725         D=0.
000726         STT(I)=YUK(1)
000730         STTT(I)=YUK(6)
000731         STTTT(I)=YUK(KY)
000733         PRINT 80,(YUK(K),K=1,KY)
000745      80 FORMAT(/7X,6HSTRESS,13F9.2/13X,13F9.2/13X,13F9.2/13X,13F9.2/13X,13
              1F9.2/13X,13F9.2/13X,13F9.2/13X,13F9.2)
            C  SET UP TABLES OF DATA TO BE PLOTTED
000745         IT=T+.05
000750         IF(IT-ITP(IJK))51,50,51
000752      50 CALL QIKSET(6.,0.,YDIST,8.,0.,TGMAX)
000756         CALL QIKPLT(XX,TY1,KY,12H*Y DISTANCE*,13H*TEMPERATURE*,ITLE)
000762         CALL HEDPLT(T,VOLT,AMP,VEL,THIK,EF1)
000766         IJK=IJK+1
000770         CALL QIKSET(6.,0.,YDIST,8.,SSO,SSI)
000774         CALL QIKPLT(XX,YUK,KY,12H*Y DISTANCE*,16H*THERMAL STRESS*,ITLE)
001000         CALL PLOT(-7.,1.,-3)
001003         CALL QLINE(XA1,YA1,2,0)
001006         CALL PLOT(7.,-1.,-3)
001011         CALL HEDPLT(T,VOLT,AMP,VEL,THIK,EF1)
001015      51 GO TO (52,999)ICUT
001023      52 DO 55 M=1,KY
001025         ZXY(KYT)=YUK(M)
001027         ZZZ(KYT)=TY1(M)
001031      55 KYT=KYT+1
001034         IF(T-TMAX)999,53,54
001037      53 KZ=I
001041         ICUT=2
001042         GO TO 999
001042      54 KZ=I-1
001044         ICUT=2
001045     999 CONTINUE
001050         GO TO (777,778)JJ
001056     778 JJ=1
001057         DO 767 K=1,KY
001061         DT(K)=TY2(K)-70.
001064         TAV(K)=70.
001065         ALAV(K)=VART(TAV(K),4)
001071         EAV(K)=VART(TAV(K),3)
001075         SIGAV(K)=VART(TAV(K),2)
001101     767 DSIG(K)=DT(K)*ALAV(K)*EAV(K)*.001
001107         PRINT 776
001113     776 FORMAT(/12H  T=INFINITY)
001113         GO TO 70
```

```
001114      100 PRINT 101,ICHK,MCHK,KT,KY,I,J,QP,T,Y,R,Z,ZZ,RHO,SPHT,COND,LMDA,EK
001162      101 FORMAT(//10X,6I8/11E11.4/)
001162      777 CONTINUE
001162          T=KZ-1
001165          TMAX=TMAX*.1
001166          CALL QIKSET(10.,0.,TMAX,8.,0.,TGMAX)
001172          CALL QIKPLT(XTT,YTT,KZ,16H*TIME OR X AXIS*,13H*TEMPERATURE*,25H*CE
                1NTER-LINE TEMPERATURE*)
001176          CALL PLOT(-11.,1.,-3)
001201          CALL QLINE(XTT,YTTT,KZ,-3)
001204          CALL QLINE(XTT,YTTTT,KZ,-4)
001207          CALL PLOT(11.,-1.,-3)
001212          CALL HEDPLT(T,VOLT,AMP,VEL,THIK,EF1)
001216          XA1(2)=T
001220          CALL QIKSET(10.,0.,TMAX,8.,SSO,SSI)
001224          CALL QIKPLT(XTT,STT,KZ,16H*TIME OR X AXIS*,8H*STRESS*,20H*CENTER-L
                1INE STRESS*)
001230          CALL PLOT(-11.,1.,-3)
001233          CALL QLINE(XTT,STTT,KZ,-3)
001236          CALL QLINE(XTT,STTTT,KZ,-4)
001241          CALL QLINE(XA1,YA1,2,0)
001244          CALL PLOT(11.,-1.,-3)
001247          CALL HEDPLT(T,VOLT,AMP,VEL,THIK,EF1)
001253          JDV=200
001254          KYT=KY*KZ
001257          L=1
001260          K=1
001261          KYZ=KY
001262          IF(KYT-1100)549,549,548
001264      548 KZ=1100/KY
001267          KYT=KY*KZ
001271          T=KZ-1
001273      549 CONTINUE
001273          DO 500 I=1,KYT
001275          XYZ(I)=XTT(K)
001277          XXX(I)=XTT(K)
001301          YZX(I)=XX(L)
001303          YYY(I)=XX(L)
001304          IF(I-KYZ)560,550,100
001307      550 K=K+1
001311          L=1
001312          KYZ=KY*K
001314          GO TO 500
001315      560 L=L+1
001317      500 CONTINUE
001322          YDIST=XX(KY)*.125
001324          CALL QIKSET(10.,0.,TMAX,8.,0.,YDIST)
```

```
001330          CALL QIKPLT(XTT,YTT,-1,16H*TIME OR X AXIS*,12H*Y DISTANCE*,23H*TEM
               1PERATURE ISOTHERMS*)
001334          CALL HEDPLT(T,VOLT,AMP,VEL,THIK,EF1)
001340          CALL PLOT(-11.,1.,-3)
001343          CALL CNTOUR(XXX,YYY,ZZZ,KYT,0.,0.,TMAX,YDIST,100.,0,0,T1,T2,T3,T4,
               1T5,T6,IARY,JDV)
001366          CALL PLOT(11.,-1.,-3)
001371          CALL QIKSET(10.,0.,TMAX,8.,0.,YDIST)
001375          CALL QIKPLT(XTT,YTT,-1,16H*TIME OR X AXIS*,12H*Y DISTANCE*,17H*ISO
               1STRESS LINES*)
001401          CALL HEDPLT(T,VOLT,AMP,VEL,THIK,EF1)
001405          CALL PLOT(-11.,1.,-3)
001410          CALL CNTOUR(XYZ,YZX,ZXY,KYT,0.,0.,TMAX,YDIST,10.,00,0,T1,T2,T3,T4,
               1T5,T6,IARY,JDV)
001433          CALL PLOT(11.,-1.,-3)
001436     1000 CONTINUE
001440     1001 CONTINUE
001440          END
```

SAMPLE LISTING OF OUTPUT DATA

This section of the appendix gives a sample output listing from the computer program. Temperature and stress distributions across the plate at different time intervals in the process are listed. The temperature values listed are a change from ambient conditions and are always positive. The stress values are positive for tensile stresses and negative for compressive stresses. These values form a table of temperature and stress that a particular point in a plate undergoes over a complete welding cycle or the values at a specific point at any instant during the welding process.

The values of temperature and stress start at the center line and continue out from it at the increments listed at the start of the program. Although it takes more than one line to list the values, each succeeding line is just a continuation of the preceding line for values extending out across the plate.

An infinite time (after the heat source has passed a plane) computation of stress is listed and is the resulting residual stress created by the welding cycle.

```
                      FUNCTION VART(TEMP,N)
                C     SUBROUTINE TO INTERPOLATE BETWEEN  DATA POINTS
000004                COMMON RA(6,11),TMPI,TMPMX
000004                IF(RA(N,1)-RA(N,10))2,1,2
000007              1 VART=RA(N,10)
000011                RETURN
000011              2 IF(TEMP-TMPMX)3,1,1
000014              3 IT=TEMP/TMPI
000016                VART=(RA(N,IT+2)-RA(N,IT+1))*(TEMP-IT*TMPI)/TMPI+RA(N,IT+1)
000030                RETURN
000031                END
```

```
                FUNCTION BESMKO(X)
          C     BESSEL FUCTION GENERATOR
000003          DIMENSION A1(6),A5(6),A7(6)
000003          DATA((A1(L),L=1,6) =  .0360768, .2659732,1.2067492, 3.0899424,
               1   3.5156229, 1. )
000003          DATA( ( A5(L),L=1,6) = 1.049804687E-7 , 1.026164062E-5,
               1   5.45092187E-4, 1.44185975E-2, .10569605, -.5772156  )
000003          DATA( (A7(L),L=1,6 ) =-.0804928, .09405952,-.08499568, .08758272,
               1  -.15664716, 1.25331414)
000003          IF( X ) 11, 10, 20
000005       10 BESMKO = 10.
000007          RETURN
000007       11 X=-X
000010       20 IF( X - 2.) 30, 50, 50
000013       30 XLN = LOGF(.5 * X )
000017          XW = X * X
000020          XWA = XW / 14.0625
000022          S1 = .0045813
000023          S5 = 1.806640625E-9
000025          DO 35 L = 1,6
000027          S1 = S1 * XWA+ A1(L)
000032          S5 = S5 * XW + A5(L)
000035       35 CONTINUE
000037          C = S5 - S1 * XLN
000042          GO TO 75
000042       50 XSR = SQRT ( X ) * EXP (X)
000050          S7 = 3.405312E-2
000052          XW = 1. / X
000054          DO 55 L = 1, 6
000055          S7 = S7 * XW + A7(L)
000060       55 CONTINUE
000062          C = S7 / XSR
000064       75 BESMKO = C
000066          RETURN
000066          END
```

```
                SUBROUTINE HEDPLT(T,VOLT,AMP,VEL,THIK,EF1)
          C     SUBROUTINE TO LABEL GRAPHS
000007          CALL PLOT(-7.,1.,-3)
000012          CALL SYMBOL(2.,8.,.14,18HT =          SECONDS,0.,18)
000016          CALL NUMBER(2.3,8.,.14,T,0.,4HF6.0)
000026          CALL SYMBOL(4.,7.4,.11,8HVOLTS = ,0.,8)
000032          CALL NUMBER(4.75,7.4,.11,VOLT,0.,4HF6.0)
000042          CALL SYMBOL(4.1,7.2,.11,7HAMPS = ,0.,7)
000046          CALL NUMBER(4.75,7.2,.11,AMP,0.,4HF6.0)
000056          CALL SYMBOL(4.,7.,.11,8HSPEED = ,0.,8)
000062          CALL NUMBER(4.75,7.,.11,VEL,0.,4HF6.3)
000071          CALL SYMBOL(3.62,6.8,.11,12HTHICKNESS = ,0.,12)
000075          CALL NUMBER(4.75,6.8,.11,THIK,0.,4HF6.3)
000105          CALL SYMBOL(3.53,6.6,.11,13HEFFICIENCY = ,0.,13)
000111          CALL NUMBER(4.75,6.6,.11,EF1,0.,4HF5.2)
000121          CALL PLOT(7.,-1.,-3)
000124          RETURN
000125          END
```

LISTING OF INPUT DATA CARDS

This section presents a list of input-data values as read into the program for one specific run and an example of typically used values.

The parameter associated with each value is listed at the beginning of the FORTRAN program at the beginning of this appendix.

Cards 1 and 3 contain limits, spacings, and parameters for graphing.

Card 2 contains, in order, the following parameters: voltage; amperage; efficiency factor; welding speed; plate thickness; temperature-spacing increment for tables of material properties; melting temperature; a factor to increase the yield-stress limit in the plastic zone; and the maximum time to be plotted on the contour graphs.

Cards 4 through 9 contain material-property variation with temperature data from 0°F to some incremental value near the melting temperature. Each of these cards contain ten values spaced at equal temperature intervals. For example, for aluminum the melting temperature is 950° to 1100°F. Therefore, the temperature increment may be 100°F, ranging from 0° to 900°F.

The properties on cards 4 through 9 in order are

Card 4: thermal conductivity (W/in.-°F)

Card 5: maximum yield stress (ksi)

Card 6: modulus of elasticity (ksi $\times 10^3$)

Card 7: coefficient of thermal expansion (1/°F)

Card 8: specific heat (W-sec/lb-°F)

Card 9: density (lb/in.^{3}).

The card number is punched in the card in column 1, the next parameter in the next 7 columns, and one parameter in every 8 columns to the end of the card (card number plus 10 parameter values).

An example of these input data cards is shown on the following page.

INPUT DATA CARDS

1	2	1.00	7	9	15	50	1000	0	-0	-0	-0	-0	-0	*ALUMINUM 2014 T6*
2	10.000	254.000	.800	.233	.250	100.000	950.000	1.200	30.000	-0.000				
3	.200	4.000	-0.000	-0.000	1.000	50.000	50.000	1000.000	5000.000	36000.000				
4	2.067	2.481	2.687	2.894	3.062	3.219	3.278	3.337	3.367	3.367				
5	62.000	59.000	56.500	50.000	39.000	25.000	10.000	5.000	2.000	0.000				
6	10.800	10.600	10.400	10.200	9.500	8.600	7.400	5.300	2.100	0.000				
7	11.780	12.160	12.500	12.800	13.100	13.370	13.630	13.880	14.100	14.300				
8	242.620	-0.000	-0.000	-0.000	-0.000	-0.000	-0.000	-0.000	-0.000	-0.000				
9	.102	-0.000	-0.000	-0.000	-0.000	-0.000	-0.000	-0.000	-0.000	-0.000				

SUBPROGRAMS

The three subroutines listed in this section are used frequently by the main program and may be called on from any point in the main program.

The first subprogram (UART) determines the value of a given material property (N) at a given temperature value (Temp). The routine selects two values in the input table, between which the given temperature lies, and performs a linear interpolation. This method was selected over many others, including fitting an equation to the data, because of the discontinuities of actual material properties as a function of temperature. These discontinuities generally result from phase changes and change in crystal structure during temperature change.

The second subprogram (BESMKO) calculates the value of a Bessel function and is used in the temperature calculation.

The third program simply labels the computer drawn graphs with a legend of descriptive values for the specific calculation.

Other mathematical and plotter routines were used but these were called directly from the computer's library. Since these programs are industry standards or company private, they are not listed.

TIME VS TEMPERATURE AND THERMAL STRESS *ALUMINUM 2014 T6* SPACING EVERY .20INCHES STARTING WITH ZERO
HEAT SOURCE LOCATED AT T = 9

TIME = 0 SECONDS												
TEMP	1.32	1.30	1.24	1.15	1.04	.91	.79	.66	.55	.45	.37	.30	.23
	.19	.15	.11	.09	.07	.05	.04	.03					
STRESS	-.17	-.17	-.16	-.15	-.13	-.12	-.10	-.09	-.07	-.06	-.05	-.04	-.03
	-.02	-.02	-.01	-.01	-.01	-.01	-.01	-.00					
TIME = 1 SECONDS												
TEMP	2.68	2.64	2.50	2.30	2.04	1.77	1.50	1.25	1.02	.82	.66	.52	.41
	.32	.25	.19	.15	.11	.09	.07	.05					
STRESS	-.22	-.21	-.20	-.17	-.14	-.10	-.07	-.04	-.01	.02	.04	.06	.07
	.08	.09	.10	.10	.11	.11	.12	.12					
TIME = 2 SECONDS												
TEMP	5.56	5.45	5.12	4.63	4.05	3.44	2.86	2.33	1.87	1.48	1.16	.90	.70
	.54	.41	.32	.24	.18	.14	.11	.08					
STRESS	-.47	-.46	-.41	-.35	-.28	-.20	-.12	-.05	.00	.05	.10	.13	.15
	.18	.19	.20	.21	.22	.23	.23	.23					
TIME = 3 SECONDS												
TEMP	11.80	11.50	10.67	9.46	8.08	6.69	5.42	4.30	3.38	2.62	2.02	1.55	1.18
	.90	.68	.51	.39	.29	.22	.17	.13					
STRESS	-1.04	-1.00	-.89	-.74	-.56	-.38	-.22	-.07	.05	.14	.22	.28	.33
	.36	.39	.41	.43	.44	.45	.46	.46					
TIME = 4 SECONDS												
TEMP	25.87	25.05	22.75	19.60	16.19	12.97	10.17	7.85	6.01	4.56	3.45	2.59	1.95
	1.46	1.10	.82	.62	.46	.34	.26	.19					
STRESS	-2.37	-2.27	-1.97	-1.57	-1.13	-.71	-.35	-.05	.18	.37	.51	.62	.70
	.77	.81	.85	.88	.90	.91	.92	.93					
TIME = 5 SECONDS												
TEMP	59.17	56.63	49.90	41.23	32.56	25.00	18.85	14.08	10.46	7.75	5.74	4.25	3.15
	2.33	1.73	1.28	.95	.71	.53	.39	.29					
STRESS	-5.68	-5.36	-4.49	-3.37	-2.25	-1.27	-.48	.13	.60	.95	1.20	1.39	1.54
	1.64	1.72	1.78	1.82	1.85	1.87	1.89	1.90					
TIME = 6 SECONDS												
TEMP	132.76	125.80	108.45	86.04	64.47	47.13	34.08	24.57	17.73	12.83	9.31	6.78	4.96

	3.63	2.67	1.96	1.45	1.07	.79	.59	.43					
STRESS	-13.23	-12.33	-10.07	-7.17	-4.38	-2.14	-.45	.77	1.65	2.28	2.74	3.06	3.29
	3.47	3.59	3.68	3.75	3.79	3.83	3.86	3.88					
TIME = 7	SECONDS												
TEMP	276.76	255.22	207.66	158.23	117.12	84.11	58.82	41.16	28.95	20.51	14.63	10.50	7.58
	5.50	4.00	2.93	2.14	1.58	1.16	.86	.63					
STRESS	-28.44	-25.62	-19.41	-12.97	-7.62	-3.34	-.07	2.21	3.79	4.87	5.63	6.16	6.54
	6.80	7.00	7.13	7.24	7.31	7.36	7.40	7.43					
TIME = 8	SECONDS												
TEMP	558.31	475.84	353.51	255.92	183.63	131.54	93.81	64.87	44.99	31.42	22.13	15.71	11.23
	8.08	5.85	4.25	3.10	2.27	1.67	1.23	.90					
STRESS	-26.75	-34.03	-34.37	-22.08	-12.64	-5.86	-.96	2.79	5.35	7.10	8.30	9.13	9.70
	10.11	10.39	10.60	10.75	10.85	10.93	10.99	11.03					
TIME = 9	SECONDS												
TEMP	950.00	733.86	488.78	349.83	252.80	182.34	131.40	94.31	65.64	45.76	32.07	22.65	16.11
	11.53	8.31	6.02	4.38	3.20	2.34	1.72	1.27					
STRESS	-1.52	-6.26	-26.24	-34.06	-21.80	-12.61	-5.98	-1.16	2.55	5.12	6.89	8.10	8.94
	9.53	9.94	10.24	10.45	10.60	10.71	10.79	10.85					
TIME = 10	SECONDS												
TEMP	824.02	705.24	535.87	405.65	305.45	227.63	167.95	123.19	89.22	62.93	44.34	31.35	22.29
	15.95	11.47	8.30	6.03	4.40	3.22	2.36	1.74					
STRESS	-0.00	-2.31	-12.65	-32.32	-27.98	-17.97	-10.19	-4.36	.04	3.45	5.85	7.52	8.69
	9.51	10.08	10.49	10.78	10.99	11.14	11.25	11.33					
TIME = 11	SECONDS												
TEMP	647.39	607.07	516.47	421.78	335.00	260.56	198.97	149.86	111.88	81.58	58.35	41.62	29.75
	21.35	15.38	11.14	8.10	5.92	4.33	3.18	2.34					
STRESS	1.89	4.22	-9.94	-27.28	-30.93	-21.50	-13.49	-7.09	-2.15	1.78	4.78	6.94	8.47
	9.55	10.32	10.87	11.26	11.54	11.74	11.89	12.00					
TIME = 12	SECONDS												
TEMP	556.83	535.71	482.70	416.27	346.46	280.65	222.18	172.50	132.01	100.02	73.17	53.02	38.29
	27.66	20.04	14.56	10.62	7.77	5.70	4.20	3.09					
STRESS	6.39	7.93	-5.71	-25.96	-31.67	-23.40	-15.84	-9.36	-4.09	.06	3.54	6.15	8.05
	9.42	10.40	11.10	11.61	11.98	12.24	12.44	12.58					
TIME = 13	SECONDS												
TEMP	497.62	485.30	451.25	402.54	347.09	290.87	237.85	190.23	149.40	115.71	87.78	64.91	47.58

	34.75	25.37	18.55	13.59	9.98	7.35	5.42	4.01					
STRESS	10.42	12.92	-1.90	-24.00	-31.39	-24.34	-17.53	-11.31	-5.99	-1.61	2.01	4.97	7.21
	8.86	10.07	10.95	11.59	12.05	12.39	12.64	12.82					
TIME = 14 SECONDS													
TEMP	457.56	448.77	423.87	386.72	342.14	294.52	247.50	203.25	163.62	129.56	101.28	76.68	57.23
	42.37	31.26	23.04	16.99	12.54	9.28	6.87	5.10					
STRESS	14.96	17.14	1.42	-21.92	-30.58	-24.60	-18.58	-12.81	-7.64	-3.21	.46	3.65	6.16
	8.08	9.51	10.57	11.35	11.92	12.34	12.65	12.88					
TIME = 15 SECONDS													
TEMP	426.32	419.64	400.43	371.12	334.60	294.15	252.74	212.32	174.76	141.32	112.60	87.80	66.82
	50.27	37.56	27.97	20.79	15.45	11.49	8.56	6.38					
STRESS	18.50	20.47	4.16	-20.05	-29.64	-24.55	-19.25	-13.99	-9.09	-4.74	-1.01	2.21	4.92
	7.06	8.70	9.94	10.86	11.55	12.06	12.44	12.72					
TIME = 16 SECONDS													
TEMP	401.00	395.72	380.42	356.51	326.02	291.40	254.94	218.29	183.21	151.00	122.51	97.95	76.03
	58.18	44.08	33.19	24.92	18.67	13.98	10.47	7.84					
STRESS	21.64	23.46	6.72	-18.09	-28.39	-24.02	-19.35	-14.58	-10.01	-5.81	-2.11	1.08	3.92
	6.23	8.05	9.45	10.52	11.32	11.93	12.38	12.72					
TIME = 17 SECONDS													
TEMP	380.05	375.72	363.08	343.10	317.22	287.32	255.07	221.93	189.40	158.78	130.98	106.54	84.62
	65.87	50.66	38.63	29.30	22.14	16.71	12.59	9.49					
STRESS	24.13	25.85	8.81	-16.45	-27.29	-23.50	-19.37	-15.06	-10.82	-6.83	-3.21	-.04	2.81
	5.23	7.20	8.75	9.95	10.88	11.58	12.10	12.50					
TIME = 18 SECONDS													
TEMP	362.21	358.57	347.90	330.88	308.58	282.51	253.84	223.84	193.80	164.91	138.09	113.98	92.44
	73.18	57.12	44.13	33.84	25.83	19.65	14.92	11.31					
STRESS	26.28	27.92	10.67	-14.94	-26.20	-22.89	-19.21	-15.31	-11.39	-7.62	-4.13	-1.00	1.79
	4.29	6.36	8.04	9.37	10.40	11.20	11.81	12.27					
TIME = 19 SECONDS													
TEMP	346.79	343.66	334.47	319.76	300.29	277.37	251.72	224.49	196.78	169.65	143.98	120.44	99.44
	79.97	63.35	49.59	38.47	29.66	22.76	17.42	13.30					
STRESS	28.16	29.75	12.32	-13.55	-25.16	-22.23	-18.94	-15.39	-11.78	-8.24	-4.90	-1.84	.89
	3.41	5.56	7.34	8.77	9.91	10.80	11.48	12.01					
TIME = 20 SECONDS													
TEMP	333.24	330.52	322.51	309.60	292.55	272.13	249.04	224.23	198.65	173.23	148.79	125.99	105.31

	86.19	69.26	54.93	43.11	33.59	26.01	20.06	15.43					
STRESS	29.83	31.37	13.81	-12.28	-24.18	-21.56	-18.59	-15.36	-12.02	-8.71	-5.53	-2.56	.12
	2.60	4.79	6.65	8.17	9.40	10.38	11.14	11.74					
TIME = 21	SECONDS												
TEMP	321.23	318.83	311.76	300.32	285.25	266.90	246.00	223.32	199.67	175.87	152.67	130.70	110.46
	91.82	74.77	60.05	47.68	37.53	29.34	22.82	17.69					
STRESS	31.33	32.83	15.16	-11.11	-23.25	-20.89	-18.19	-15.24	-12.15	-9.05	-6.03	-3.17	-.54
	1.87	4.08	5.98	7.58	8.89	9.95	10.79	11.45					
TIME = 22	SECONDS												
TEMP	310.48	308.34	302.04	291.95	278.39	261.79	242.76	221.94	200.03	177.74	155.76	134.68	114.98
	96.87	79.86	64.91	52.13	41.46	32.73	25.67	20.04					
STRESS	32.68	34.15	16.38	-10.05	-22.38	-20.23	-17.77	-15.06	-12.20	-9.30	-6.43	-3.69	-1.13
	1.22	3.42	5.36	7.01	8.39	9.51	10.42	11.15					
TIME = 23	SECONDS												
TEMP	300.77	298.88	293.30	284.23	271.94	256.84	239.42	220.23	199.89	179.00	158.18	138.00	118.91
	101.28	84.51	69.48	56.42	45.32	36.11	28.57	22.48					
STRESS	33.90	35.34	17.49	-9.07	-21.55	-19.59	-17.34	-14.84	-12.18	-9.46	-6.75	-4.12	-1.64
	.65	2.82	4.77	6.45	7.89	9.08	10.05	10.83					
TIME = 24	SECONDS												
TEMP	292.11	290.40	285.34	277.09	265.88	252.06	236.04	218.30	199.35	179.75	160.05	140.75	122.30
	105.07	88.74	73.74	60.50	49.08	39.47	31.49	24.98					
STRESS	35.00	36.41	18.50	-8.16	-20.78	-18.98	-16.90	-14.58	-12.11	-9.56	-6.99	-4.48	-2.08
	.16	2.27	4.21	5.93	7.40	8.64	9.67	10.51					
TIME = 25	SECONDS												
TEMP	284.20	282.64	278.02	270.47	260.19	247.48	232.68	216.21	198.53	180.11	161.45	143.01	125.22
	108.43	92.57	77.68	64.35	52.71	42.77	34.41	27.50					
STRESS	36.00	37.40	19.43	-7.31	-20.04	-18.38	-16.46	-14.31	-12.01	-9.60	-7.17	-4.77	-2.46
	-.28	1.78	3.70	5.43	6.93	8.22	9.29	10.19					
TIME = 26	SECONDS												
TEMP	276.92	275.49	271.24	264.30	254.83	243.08	229.36	214.03	197.48	180.14	162.45	144.84	127.71
	111.39	96.00	81.30	67.98	56.18	45.97	37.30	30.04					
STRESS	36.75	38.13	20.12	-6.70	-19.53	-18.00	-16.21	-14.21	-12.05	-9.79	-7.49	-5.19	-2.97
	-.85	1.15	3.05	4.78	6.30	7.62	8.74	9.68					
TIME = 27	SECONDS												
TEMP	270.19	268.87	264.96	258.54	249.77	238.87	226.11	211.78	196.26	179.91	163.13	146.31	129.83

	114.00	99.07	84.61	71.36	59.49	49.08	40.14	32.57					
STRESS	37.61	38.98	20.92	-5.96	-18.88	-17.45	-15.79	-13.92	-11.89	-9.76	-7.57	-5.39	-3.24
	-1.19	.75	2.63	4.34	5.88	7.22	8.37	9.35					
TIME = 28 SECONDS													
TEMP	263.95	262.73	259.10	253.14	245.00	234.85	222.93	209.51	194.91	179.47	163.54	147.47	131.62
	116.28	101.73	87.64	74.50	62.61	52.08	42.91	35.08					
STRESS	38.26	39.62	21.53	-5.41	-18.41	-17.07	-15.52	-13.77	-11.86	-9.85	-7.78	-5.69	-3.62
	-1.63	.26	2.09	3.79	5.32	6.68	7.87	8.88					
TIME = 29 SECONDS													
TEMP	258.14	257.00	253.63	248.08	240.48	231.00	219.83	207.23	193.47	178.86	163.72	148.36	133.12
	118.28	104.09	90.38	77.42	65.56	54.94	45.61	37.55					
STRESS	39.01	40.36	22.23	-4.76	-17.82	-16.57	-15.12	-13.47	-11.68	-9.77	-7.80	-5.80	-3.82
	-1.89	-.05	1.73	3.41	4.94	6.31	7.52	8.56					
TIME = 30 SECONDS													
TEMP	252.71	251.65	248.50	243.31	236.20	227.31	216.83	204.96	191.97	178.12	163.70	149.02	134.36
	120.01	106.19	92.86	80.11	68.33	57.67	48.21	39.96					
STRESS	39.54	40.88	22.73	-4.30	-17.44	-16.26	-14.89	-13.34	-11.65	-9.84	-7.97	-6.05	-4.15
	-2.28	-.49	1.24	2.89	4.42	5.79	7.02	8.08					
TIME = 31 SECONDS													
TEMP	247.62	246.64	243.67	238.81	232.14	223.79	213.91	202.72	190.42	177.27	163.54	149.48	135.39
	121.50	108.07	95.11	82.58	70.91	60.26	50.71	42.32					
STRESS	40.20	41.53	23.36	-3.72	-16.91	-15.80	-14.51	-13.05	-11.45	-9.73	-7.94	-6.11	-4.28
	-2.48	-.73	.95	2.57	4.08	5.46	6.69	7.78					
TIME = 32 SECONDS													
TEMP	242.84	241.92	239.13	234.56	228.28	220.41	211.09	200.50	188.84	176.34	163.24	149.78	136.22
	122.79	109.73	97.13	84.85	73.31	62.70	53.11	44.60					
STRESS	40.64	41.96	23.76	-3.35	-16.59	-15.54	-14.33	-12.94	-11.42	-9.79	-8.09	-6.34	-4.57
	-2.83	-1.13	.50	2.10	3.59	4.96	6.20	7.30					
TIME = 33 SECONDS													
TEMP	238.34	237.46	234.84	230.53	224.61	217.17	208.36	198.32	187.25	175.34	162.82	149.92	136.87
	123.89	111.20	98.96	86.92	75.55	65.01	55.40	46.81					
STRESS	41.23	42.54	24.32	-2.82	-16.11	-15.12	-13.97	-12.66	-11.21	-9.66	-8.03	-6.35	-4.66
	-2.97	-1.32	.27	1.83	3.30	4.66	5.90	7.02					
TIME = 34 SECONDS													
TEMP	234.08	233.26	230.78	226.71	221.11	214.07	205.71	196.18	185.65	174.29	162.32	149.95	137.38

	124.83	112.50	100.58	88.83	77.63	67.18	57.59	48.93					
STRESS	41.59	42.89	24.66	-2.52	-15.84	-14.91	-13.82	-12.57	-11.20	-9.72	-8.16	-6.55	-4.92
	-3.28	-1.68	-.14	1.39	2.84	4.19	5.43	6.55					
TIME = 35 SECONDS													
TEMP	230.05	229.27	226.93	223.07	217.76	211.09	203.15	194.09	184.05	173.21	161.75	149.86	137.75
	125.62	113.65	102.01	90.56	79.56	69.22	59.66	50.97					
STRESS	42.11	43.41	25.16	-2.04	-15.41	-14.52	-13.48	-12.30	-10.99	-9.58	-8.09	-6.54	-4.96
	-3.39	-1.83	-.32	1.16	2.59	3.93	5.16	6.28					
TIME = 36 SECONDS													
TEMP	226.23	225.49	223.27	219.61	214.57	208.23	200.67	192.04	182.46	172.09	161.11	149.69	138.01
	126.27	114.65	103.30	92.15	81.34	71.12	61.62	52.93					
STRESS	42.41	43.70	25.44	-1.79	-15.19	-14.35	-13.36	-12.23	-10.99	-9.64	-8.21	-6.72	-5.20
	-3.67	-2.16	-.69	.76	2.16	3.48	4.71	5.83					
TIME = 37 SECONDS													
TEMP	222.60	221.90	219.79	216.31	211.51	205.47	198.28	190.04	180.88	170.96	160.42	149.43	138.17
	126.81	115.52	104.46	93.59	82.99	72.91	63.48	54.80					
STRESS	42.88	44.17	25.89	-1.36	-14.79	-13.99	-13.05	-11.97	-10.78	-9.49	-8.12	-6.69	-5.22
	-3.74	-2.28	-.84	.57	1.94	3.25	4.47	5.59					
TIME = 38 SECONDS													
TEMP	219.15	218.48	216.47	213.16	208.59	202.83	195.96	188.08	179.32	169.81	159.68	149.11	138.24
	127.24	116.28	105.50	94.90	84.51	74.58	65.24	56.59					
STRESS	43.13	44.41	26.12	-1.16	-14.62	-13.85	-12.95	-11.93	-10.78	-9.54	-8.23	-6.85	-5.44
	-4.01	-2.58	-1.18	.19	1.54	2.82	4.03	5.15					
TIME = 39 SECONDS													
TEMP	215.85	215.22	213.30	210.14	205.78	200.28	193.71	186.17	177.78	168.65	158.92	148.73	138.23
	127.58	116.93	106.42	96.09	85.91	76.14	66.90	58.29					
STRESS	43.56	44.84	26.53	-.76	-14.25	-13.52	-12.66	-11.68	-10.58	-9.39	-8.13	-6.80	-5.43
	-4.05	-2.67	-1.30	.04	1.36	2.62	3.82	4.93					
TIME = 40 SECONDS													
TEMP	212.71	212.10	210.27	207.25	203.08	197.82	191.53	184.31	176.26	167.49	158.12	148.30	138.15
	127.84	117.49	107.24	97.17	87.20	77.59	68.46	59.91					
STRESS	43.76	45.04	26.72	-.60	-14.11	-13.40	-12.59	-11.64	-10.59	-9.45	-8.23	-6.95	-5.63
	-4.29	-2.95	-1.62	-.31	.98	2.23	3.41	4.51					
TIME = 41 SECONDS													
TEMP	209.70	209.12	207.37	204.48	200.49	195.45	189.42	182.50	174.76	166.33	157.30	147.82	138.02

	128.02	117.96	107.97	98.15	88.39	78.94	69.93	61.44					
STRESS	44.15	45.43	27.10	-.23	-13.77	-13.09	-12.31	-11.41	-10.40	-9.30	-8.12	-6.89	-5.6
	-4.31	-3.01	-1.71	-.44	.83	2.05	3.22	4.31					

TIME = 42 SECONDS

TEMP	206.82	206.27	204.59	201.82	198.00	193.16	187.38	180.73	173.29	165.17	156.47	147.32	137.83
	128.13	118.35	108.62	99.03	89.48	80.20	71.31	62.90					
STRESS	44.32	45.59	27.25	-.10	-13.65	-13.00	-12.25	-11.38	-10.41	-9.36	-8.22	-7.03	-5.80
	-4.54	-3.27	-2.00	-.76	.48	1.68	2.83	3.92					

TIME = 43 SECONDS

TEMP	204.06	203.53	201.92	199.26	195.59	190.95	185.40	179.00	171.84	164.02	155.63	146.78	137.59
	128.18	118.67	109.19	99.83	90.48	81.37	72.60	64.28					
STRESS	44.68	45.95	27.60	.24	-13.34	-12.72	-11.99	-11.16	-10.23	-9.21	-8.11	-6.96	-5.77
	-4.55	-3.31	-2.08	-.86	.35	1.53	2.66	3.74					

TIME = 44 SECONDS

TEMP	201.41	200.90	199.35	196.80	193.28	188.82	183.47	177.32	170.42	162.87	154.77	146.21	137.31
	128.18	118.93	109.68	100.53	91.40	82.46	73.82	65.59					
STRESS	44.81	46.08	27.72	.35	-13.25	-12.65	-11.95	-11.15	-10.25	-9.27	-8.21	-7.10	-5.96
	-4.75	-3.55	-2.35	-1.16	.02	1.18	2.30	3.36					

TIME = 45 SECONDS

TEMP	198.86	198.37	196.89	194.44	191.04	186.75	181.61	175.68	169.03	161.74	153.91	145.63	137.00
	128.13	119.13	110.11	101.17	92.24	83.47	74.96	66.83					
STRESS	45.15	46.41	28.05	.66	-12.95	-12.36	-11.71	-10.93	-10.07	-9.12	-8.10	-7.02	-5.90
	-4.75	-3.58	-2.41	-1.25	-.09	1.05	2.15	3.20					

TIME = 46 SECONDS

TEMP	196.41	195.94	194.51	192.15	188.89	184.75	179.80	174.07	167.66	160.62	153.04	145.02	136.66
	128.04	119.28	110.48	101.74	93.01	84.40	76.03	68.00					
STRESS	45.26	46.52	28.15	.75	-12.88	-12.32	-11.68	-10.93	-10.10	-9.18	-8.19	-7.15	-6.06
	-4.94	-3.80	-2.66	-1.53	-.40	.72	1.80	2.84					

TIME = 47 SECONDS

TEMP	194.05	193.60	192.22	189.95	186.80	182.82	178.03	172.51	166.31	159.51	152.18	144.41	136.29
	127.91	119.38	110.80	102.25	93.71	85.27	77.03	69.11					
STRESS	45.57	46.83	28.45	1.04	-12.61	-12.07	-11.45	-10.73	-9.92	-9.04	-8.08	-7.07	-6.01
	-4.93	-3.82	-2.70	-1.59	-.49	.61	1.67	2.70					

TIME = 48 SECONDS

TEMP	191.78	191.34	190.02	187.82	184.79	180.94	176.32	170.99	165.00	158.41	151.31	143.78	135.89

	127.75	119.44	111.06	102.70	94.36	86.07	77.97	70.15					
STRESS	45.66	46.91	28.53	1.11	-12.55	-12.03	-11.43	-10.74	-9.96	-9.10	-8.17	-7.19	-6.17
	-5.11	-4.03	-2.94	-1.86	-.77	.30	1.35	2.36					
TIME = 49	SECONDS												
TEMP	189.59	189.17	187.89	185.77	182.84	179.12	174.66	169.50	163.70	157.33	150.45	143.14	135.48
	127.56	119.46	111.28	103.11	94.94	86.81	78.85	71.14					
STRESS	45.94	47.20	28.81	1.38	-12.30	-11.80	-11.22	-10.54	-9.79	-8.96	-8.06	-7.11	-6.11
	-5.08	-4.03	-2.97	-1.91	-.85	.20	1.23	2.23					
TIME = 50	SECONDS												
TEMP	187.47	187.06	185.83	183.78	180.95	177.36	173.04	168.05	162.44	156.26	149.59	142.49	135.04
	127.34	119.44	111.46	103.46	95.47	87.50	79.67	72.07					
STRESS	46.02	47.27	28.87	1.43	-12.25	-11.77	-11.21	-10.56	-9.82	-9.02	-8.15	-7.23	-6.26
	-5.26	-4.23	-3.20	-2.16	-1.12	-.09	.93	1.91					
TIME = 100	SECONDS												
TEMP	129.59	129.46	129.06	128.39	127.46	126.28	124.84	123.16	121.24	119.10	116.74	114.18	111.42
	108.49	105.40	102.17	98.82	95.39	91.85	88.20	84.47					
STRESS	49.73	50.95	32.44	4.82	-9.11	-8.94	-8.76	-8.54	-8.29	-8.01	-7.70	-7.37	-7.01
	-6.63	-6.23	-5.81	-5.38	-4.93	-4.47	-4.00	-3.52					
TIME = 150	SECONDS												
TEMP	105.35	105.27	105.06	104.70	104.20	103.56	102.78	101.87	100.83	99.67	98.42	97.05	95.56
	93.96	92.24	90.43	88.52	86.51	84.42	82.25	80.00					
STRESS	50.75	51.96	33.43	5.77	-8.22	-8.12	-8.02	-7.90	-7.76	-7.61	-7.45	-7.27	-7.08
	-6.87	-6.65	-6.42	-6.17	-5.91	-5.64	-5.36	-5.07					
TIME = 200	SECONDS												
TEMP	91.45	91.40	91.27	91.04	90.73	90.32	89.83	89.25	88.58	87.83	87.00	86.08	85.09
	84.01	82.86	81.64	80.35	78.99	77.57	76.08	74.54					
STRESS	51.12	52.33	33.79	6.11	-7.90	-7.83	-7.77	-7.69	-7.61	-7.51	-7.40	-7.28	-7.16
	-7.02	-6.87	-6.71	-6.54	-6.37	-6.18	-5.99	-5.79					
TIME = 250	SECONDS												
TEMP	82.11	82.07	81.96	81.81	81.58	81.29	80.93	80.51	80.02	79.47	78.86	78.20	77.47
	76.68	75.84	74.94	73.99	72.98	71.93	70.83	69.68					
STRESS	51.31	52.51	33.97	6.28	-7.74	-7.69	-7.64	-7.59	-7.52	-7.45	-7.37	-7.29	-7.19
	-7.09	-6.98	-6.86	-6.74	-6.61	-6.48	-6.33	-6.18					
TIME = 300	SECONDS												
TEMP	75.19	75.16	75.08	74.96	74.79	74.56	74.28	73.96	73.58	73.16	72.69	72.17	71.61

	71.00	70.35	69.65	68.91	68.13	67.31	66.44	65.55					
STRESS	51.43	52.63	34.08	6.39	-7.64	-7.60	-7.56	-7.52	-7.47	-7.41	-7.35	-7.29	-7.21
	-7.13	-7.05	-6.96	-6.86	-6.76	-6.66	-6.55	-6.43					
TIME = 350	SECONDS												
TEMP	69.80	69.78	69.72	69.62	69.48	69.30	69.08	68.81	68.51	68.17	67.80	67.38	66.93
	66.43	65.91	65.34	64.75	64.11	63.45	62.75	62.02					
STRESS	51.50	52.71	34.16	6.46	-7.58	-7.53	-7.51	-7.47	-7.43	-7.39	-7.34	-7.29	-7.23
	-7.16	-7.10	-7.02	-6.95	-6.86	-6.78	-6.69	-6.59					
TIME = 400	SECONDS												
TEMP	65.45	65.43	65.38	65.30	65.18	65.03	64.85	64.63	64.38	64.10	63.79	63.44	63.07
	62.66	62.22	61.76	61.26	60.74	60.18	59.60	58.99					
STRESS	51.56	52.76	34.21	6.51	-7.53	-7.49	-7.47	-7.44	-7.41	-7.37	-7.33	-7.29	-7.24
	-7.18	-7.13	-7.07	-7.00	-6.94	-6.86	-6.79	-6.71					
TIME = 450	SECONDS												
TEMP	61.83	61.82	61.78	61.71	61.60	61.48	61.33	61.14	60.93	60.70	60.43	60.14	59.82
	59.47	59.10	58.71	58.29	57.94	57.37	56.88	56.36					
STRESS	51.60	52.80	34.25	6.55	-7.49	-7.46	-7.44	-7.42	-7.39	-7.36	-7.32	-7.29	-7.24
	-7.20	-7.15	-7.10	-7.05	-6.99	-6.93	-6.86	-6.80					
TIME = 500	SECONDS												
TEMP	58.77	58.76	58.72	58.66	58.57	58.46	58.33	58.17	57.99	57.79	57.56	57.31	57.03
	56.74	56.42	56.08	55.71	55.33	54.92	54.49	54.05					
STRESS	51.63	52.83	34.28	6.58	-7.47	-7.43	-7.42	-7.40	-7.37	-7.35	-7.32	-7.28	-7.25
	-7.21	-7.17	-7.13	-7.08	-7.03	-6.98	-6.92	-6.86					
TIME = 550	SECONDS												
TEMP	56.12	56.11	56.08	56.02	55.96	55.86	55.74	55.61	55.45	55.27	55.07	54.85	54.61
	54.35	54.07	53.77	53.45	53.12	52.76	52.39	52.00					
STRESS	51.65	52.85	34.30	6.60	-7.45	-7.41	-7.40	-7.38	-7.36	-7.34	-7.31	-7.28	-7.25
	-7.22	-7.18	-7.15	-7.10	-7.06	-7.01	-6.97	-6.92					
TIME = 600	SECONDS												
TEMP	53.81	53.80	53.78	53.73	53.66	53.58	53.48	53.36	53.22	53.06	52.88	52.69	52.48
	52.25	52.00	51.73	51.45	51.16	50.84	50.51	50.16					
STRESS	51.67	52.87	34.32	6.62	-7.43	-7.40	-7.39	-7.37	-7.35	-7.33	-7.31	-7.28	-7.26
	-7.23	-7.20	-7.16	-7.12	-7.09	-7.05	-7.00	-6.96					
TIME = 650	SECONDS												
TEMP	51.77	51.76	51.74	51.69	51.63	51.56	51.47	51.36	51.24	51.10	50.94	50.77	50.58

	50.37	50.15	49.92	49.66	49.40	49.12	48.82	48.51					
STRESS	51.69	52.89	34.33	6.63	-7.41	-7.39	-7.38	-7.36	-7.34	-7.33	-7.31	-7.28	-7.26
	-7.23	-7.20	-7.17	-7.14	-7.11	-7.07	-7.03	-6.99					
TIME = 700	SECONDS												
TEMP	49.95	49.94	49.92	49.88	49.82	49.76	49.67	49.58	49.47	49.34	49.20	49.04	48.87
	48.69	48.49	48.28	48.05	47.81	47.56	47.29	47.01					
STRESS	51.70	52.90	34.35	6.65	-7.40	-7.38	-7.37	-7.35	-7.34	-7.32	-7.30	-7.28	-7.26
	-7.24	-7.21	-7.18	-7.16	-7.12	-7.09	-7.06	-7.02					
TIME = 750	SECONDS												
TEMP	48.31	48.30	48.28	48.25	48.20	48.14	48.06	47.98	47.87	47.76	47.63	47.49	47.34
	47.17	46.99	46.79	46.59	46.37	46.14	45.90	45.64					
STRESS	51.71	52.91	34.36	6.66	-7.39	-7.37	-7.36	-7.35	-7.33	-7.32	-7.30	-7.28	-7.26
	-7.24	-7.22	-7.19	-7.17	-7.14	-7.11	-7.08	-7.05					
TIME = 800	SECONDS												
TEMP	46.82	46.81	46.79	46.77	46.72	46.66	46.60	46.51	46.43	46.32	46.20	46.08	45.93
	45.78	45.62	45.44	45.25	45.05	44.84	44.62	44.39					
STRESS	51.72	52.92	34.37	6.66	-7.38	-7.36	-7.35	-7.34	-7.33	-7.31	-7.30	-7.28	-7.27
	-7.25	-7.22	-7.20	-7.18	-7.15	-7.12	-7.10	-7.07					
TIME = 850	SECONDS												
TEMP	45.46	45.46	45.44	45.42	45.37	45.32	45.26	45.19	45.10	45.00	44.90	44.78	44.65
	44.51	44.36	44.20	44.03	43.85	43.65	43.45	43.24					
STRESS	51.73	52.93	34.38	6.67	-7.38	-7.35	-7.35	-7.34	-7.32	-7.31	-7.30	-7.28	-7.27
	-7.25	-7.23	-7.21	-7.19	-7.16	-7.14	-7.11	-7.08					
TIME = 900	SECONDS												
TEMP	44.22	44.22	44.20	44.17	44.14	44.09	44.04	43.97	43.89	43.80	43.70	43.59	43.47
	43.35	43.21	43.06	42.90	42.73	42.55	42.36	42.17					
STRESS	51.74	52.94	34.38	6.68	-7.37	-7.35	-7.34	-7.33	-7.32	-7.31	-7.30	-7.28	-7.27
	-7.25	-7.23	-7.21	-7.19	-7.17	-7.15	-7.12	-7.10					
TIME = 950	SECONDS												
TEMP	43.08	43.07	43.06	43.03	43.00	42.96	42.90	42.84	42.77	42.69	42.59	42.50	42.39
	42.27	42.14	42.00	41.85	41.70	41.53	41.36	41.18					
STRESS	51.75	52.95	34.39	6.68	-7.37	-7.34	-7.34	-7.33	-7.32	-7.31	-7.30	-7.28	-7.27
	-7.25	-7.24	-7.22	-7.20	-7.18	-7.16	-7.14	-7.11					
TIME = 1000	SECONDS												
TEMP	42.02	42.01	42.00	41.98	41.95	41.91	41.86	41.80	41.73	41.66	41.57	41.48	41.37

	41.27	41.15	41.02	40.88	40.74	40.58	40.42	40.25				
STRESS	51.75	52.95	34.39	6.69	-7.36	-7.34	-7.33	-7.32	-7.32	-7.31	-7.29	-7.28	-7.27
	-7.26	-7.24	-7.22	-7.21	-7.19	-7.17	-7.15	-7.12					
TIME = 6000	SECONDS												
TEMP	17.50	17.50	17.50	17.49	17.49	17.49	17.49	17.48	17.48	17.47	17.46	17.46	17.45
	17.44	17.43	17.42	17.41	17.40	17.39	17.38	17.36					
STRESS	51.93	53.13	34.57	6.86	-7.19	-7.18	-7.18	-7.17	-7.17	-7.17	-7.17	-7.17	-7.17
	-7.17	-7.17	-7.17	-7.17	-7.16	-7.16	-7.16	-7.16					
TIME = 11000	SECONDS												
TEMP	12.98	12.98	12.98	12.97	12.97	12.97	12.97	12.97	12.97	12.97	12.96	12.96	12.96
	12.95	12.95	12.95	12.94	12.94	12.93	12.93	12.92					
STRESS	51.84	53.04	34.49	6.78	-7.28	-7.26	-7.26	-7.26	-7.26	-7.26	-7.26	-7.26	-7.26
	-7.26	-7.26	-7.25	-7.25	-7.25	-7.25	-7.25	-7.25					
TIME = 16000	SECONDS												
TEMP	10.78	10.78	10.78	10.78	10.78	10.78	10.78	10.78	10.78	10.77	10.77	10.77	10.77
	10.77	10.77	10.76	10.76	10.76	10.76	10.75	10.75					
STRESS	51.83	53.03	34.47	6.77	-7.29	-7.27	-7.27	-7.27	-7.27	-7.27	-7.27	-7.27	-7.27
	-7.27	-7.27	-7.27	-7.27	-7.27	-7.27	-7.27	-7.27					
TIME = 21000	SECONDS												
TEMP	9.42	9.42	9.42	9.42	9.42	9.42	9.42	9.42	9.42	9.42	9.42	9.42	9.41
	9.41	9.41	9.41	9.41	9.41	9.41	9.40	9.40					
STRESS	51.83	53.03	34.47	6.76	-7.29	-7.28	-7.28	-7.27	-7.27	-7.27	-7.27	-7.27	-7.27
	-7.27	-7.27	-7.27	-7.27	-7.27	-7.27	-7.27	-7.27					
TIME = 26000	SECONDS												
TEMP	8.48	8.48	8.48	8.48	8.47	8.47	8.47	8.47	8.47	8.47	8.47	8.47	8.47
	8.47	8.47	8.47	8.47	8.46	8.46	8.46	8.46					
STRESS	51.83	53.03	34.47	6.76	-7.29	-7.28	-7.28	-7.28	-7.28	-7.28	-7.28	-7.28	-7.28
	-7.28	-7.28	-7.28	-7.28	-7.28	-7.28	-7.28	-7.28					
TIME = 31000	SECONDS												
TEMP	7.77	7.77	7.77	7.77	7.77	7.77	7.77	7.77	7.77	7.76	7.76	7.76	7.76
	7.76	7.76	7.76	7.76	7.76	7.76	7.76	7.76					
STRESS	51.92	53.12	34.56	6.85	-7.20	-7.19	-7.19	-7.19	-7.19	-7.19	-7.19	-7.19	-7.19
	-7.19	-7.19	-7.19	-7.18	-7.18	-7.18	-7.18	-7.18					
TIME = 36000	SECONDS												
TEMP	7.21	7.21	7.21	7.21	7.21	7.21	7.21	7.21	7.21	7.21	7.21	7.21	7.21

	7.21	7.21	7.21	7.21	7.20	7.20	7.20	7.20					
STRESS	51.83	53.03	34.47	6.76	-7.29	-7.28	-7.28	-7.28	-7.27	-7.27	-7.27	-7.27	-7.27
	-7.27	-7.27	-7.27	-7.27	-7.27	-7.27	-7.27	-7.27					
T=INFINITY													
STRESS	51.81	53.01	34.45	6.75	-7.31	-7.29	-7.29	-7.29	-7.29	-7.29	-7.29	-7.29	-7.29
	-7.29	-7.29	-7.29	-7.29	-7.29	-7.29	-7.29	-7.29					

EXAMPLES OF GRAPHICAL COMPUTER OUTPUT PLOTS

This section of the appendix presents computer-plotted figures of typical results calculated by the program for six sets of welding parameters shown in Table III (Section IV). Each figure has pertinent information listed to describe the conditions used for a particular calculation. All calculations are for 2014-T6 aluminum plates of infinite length and an effective plate width of 8 inches or the half width of 4 inches.

The first 14 figures use the same conditions as specified by NASA for their experiments, and thus theoretically simulate these same conditions.

The first 10 figures (5 pairs) illustrate the temperature and stress distributions across the plate at the instantaneous time given on each pair of figures. Figures A-1, A-3, A-5, A-7, and A-9 show the temperature distributions at 7, 9, 15, 50, and 1000 seconds, respectively. Figures A-2, A-4, A-6, A-8, and A-10 show the stress distributions at these instances. For this sequence of figures the heat source is located at the 9-second time position.

Figures A-11, A-15, A-19, A-23, A-27, and A-31 illustrate the temperature (of above ambient) distributions for six sets of conditions in the x-direction along planes down the center line of the weld, 1 inch out from and parallel to the center line, and down the edge of the plate parallel to the center line. Figures A-12, A-16, A-20, A-24, A-28, and A-32 illustrate the corresponding stress (ksi) distributions.

Figures A-13, A-17, A-21, A-25, A-29, and A-33 plot temperature (°F) distributions as they appear out across the plate.

Figures A-14, A-18, A-22, A-26, A-30, and A-34 plot corresponding stress (ksi) distributions. These contours are essentially the isotherms and isostress lines of the plate assuming constant temperature through the thickness of the plate. These stress contours are unique to this study and provide an enlightening picture.

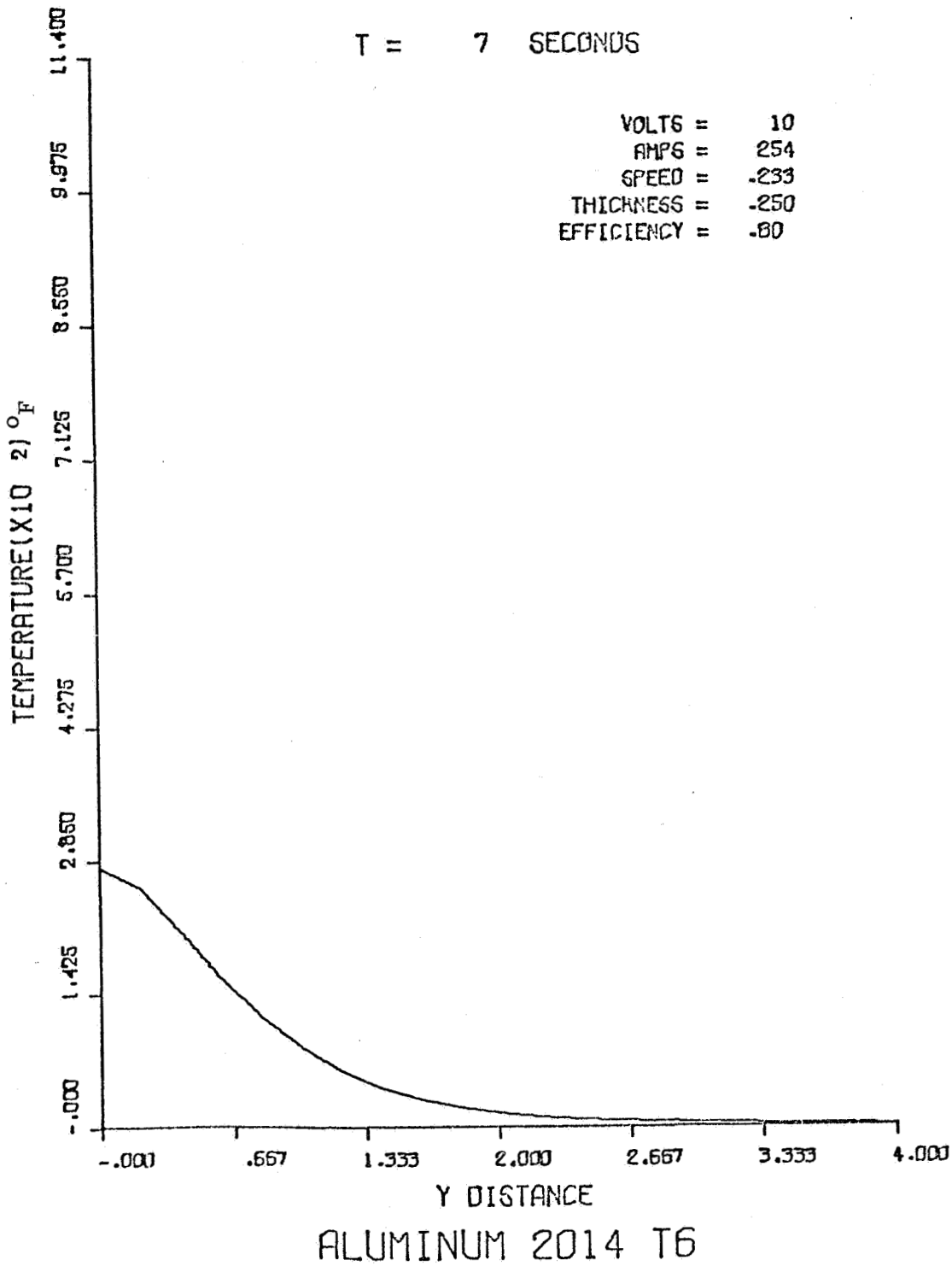

FIGURE A-1. TEMPERATURE DISTRIBUTION ALONG THE SECTION AT T = 7, CONDITION 1

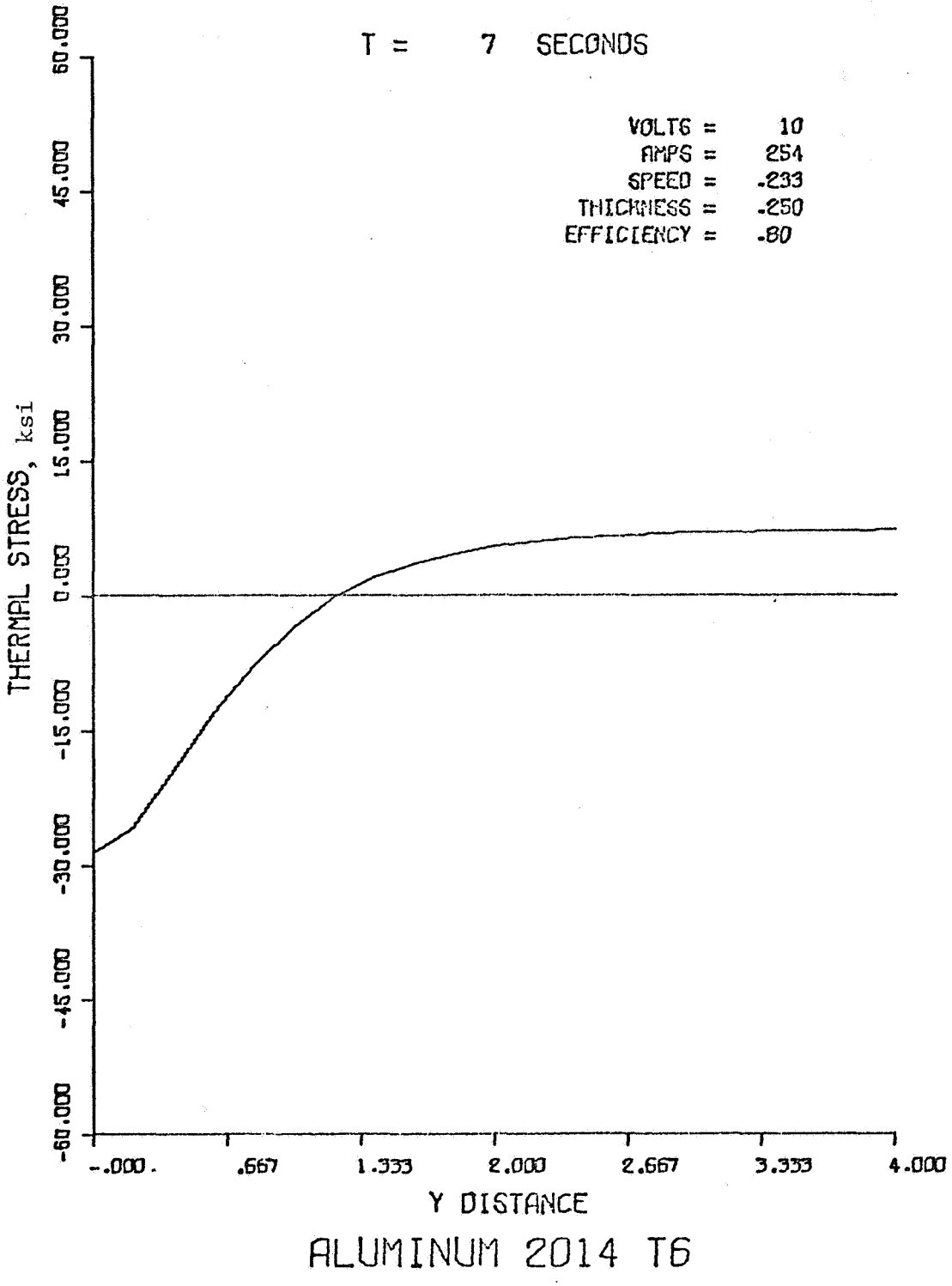

FIGURE A-2. STRESS DISTRIBUTION ALONG THE SECTION AT T = 7, CONDITION 1

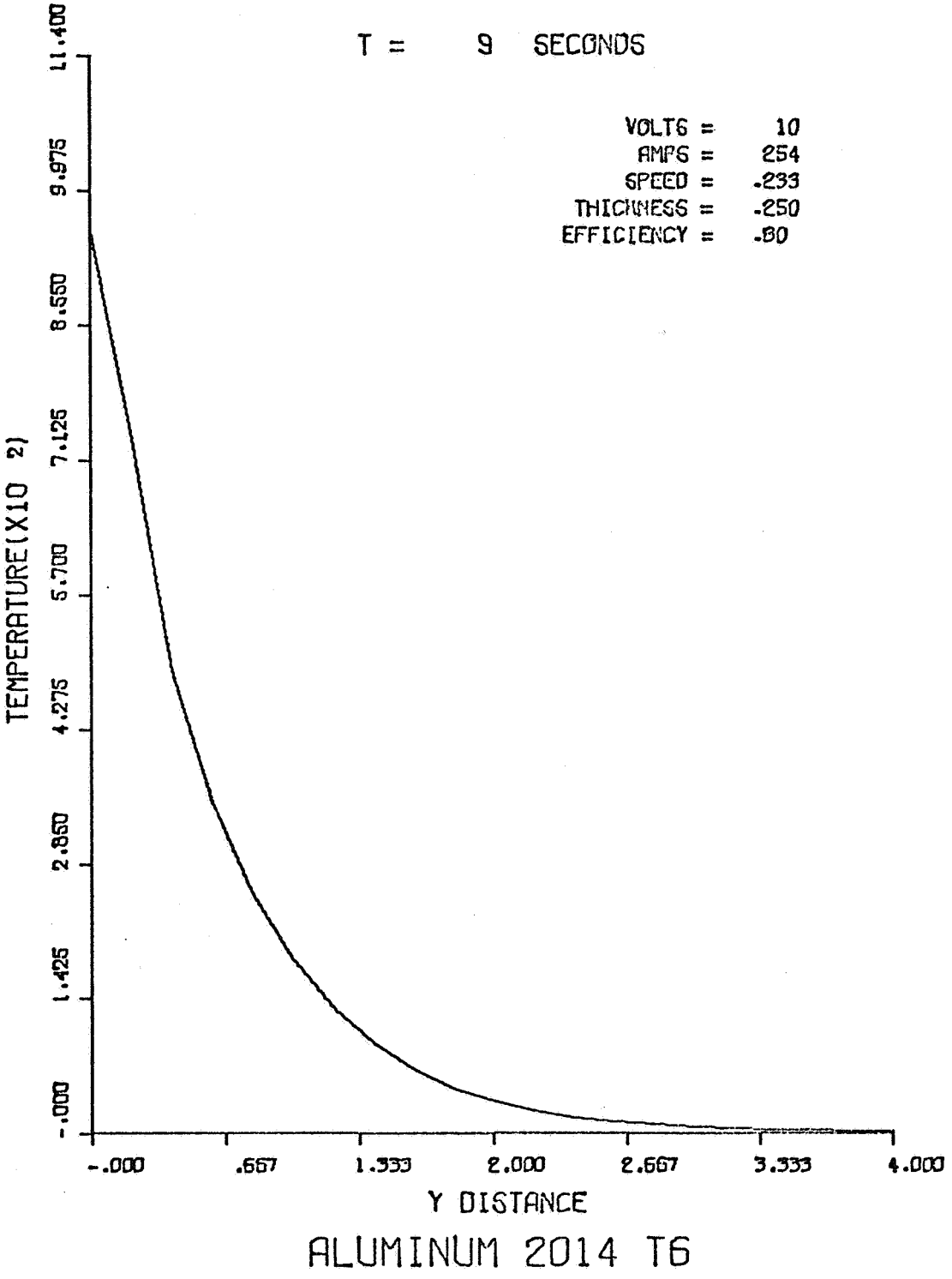

FIGURE A-3. TEMPERATURE DISTRIBUTION ALONG THE SECTION AT T = 9, CONDITION 1

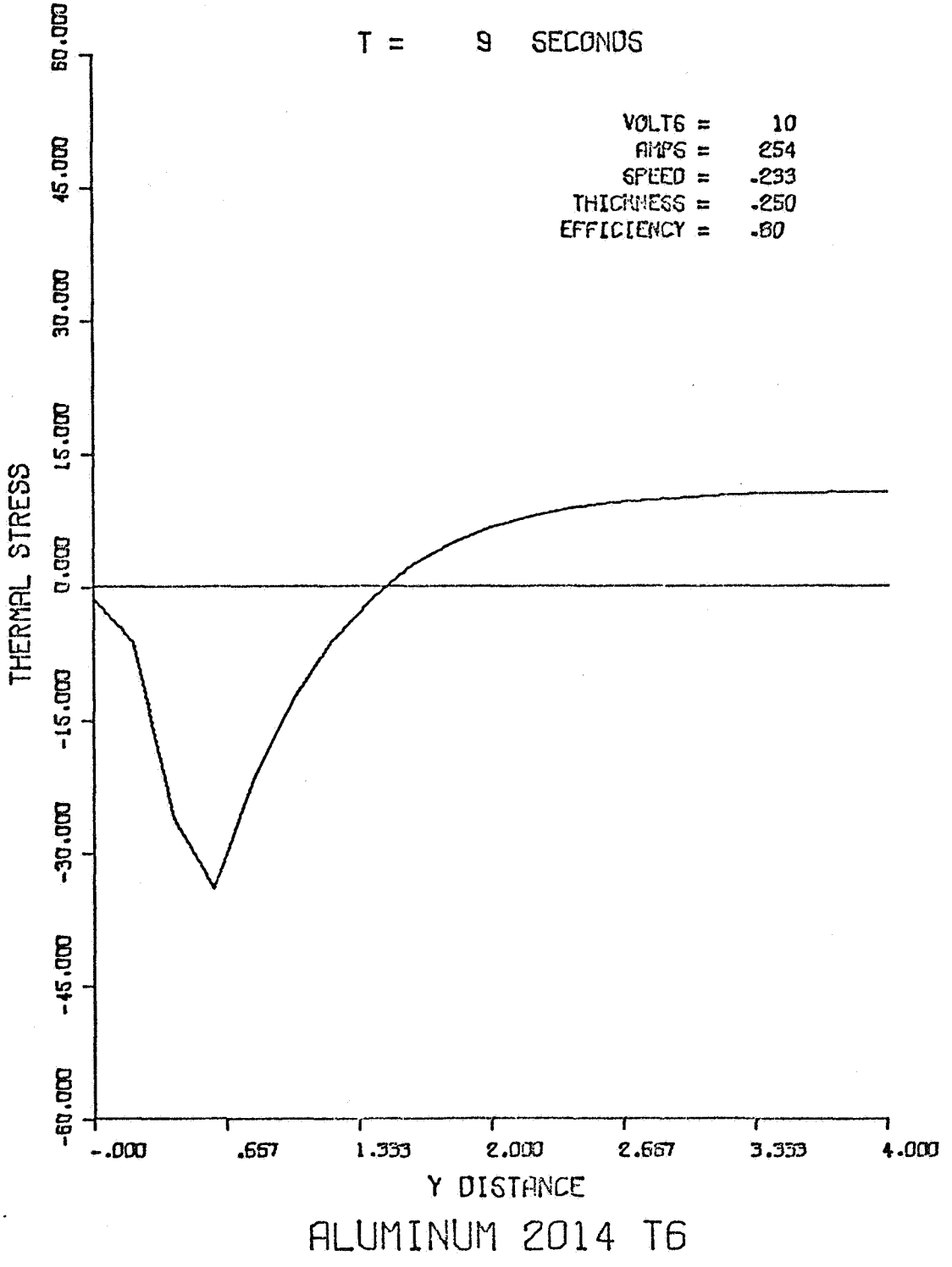

FIGURE A-4. STRESS DISTORTION ALONG THE SECTION AT T = 9, CONDITION 1

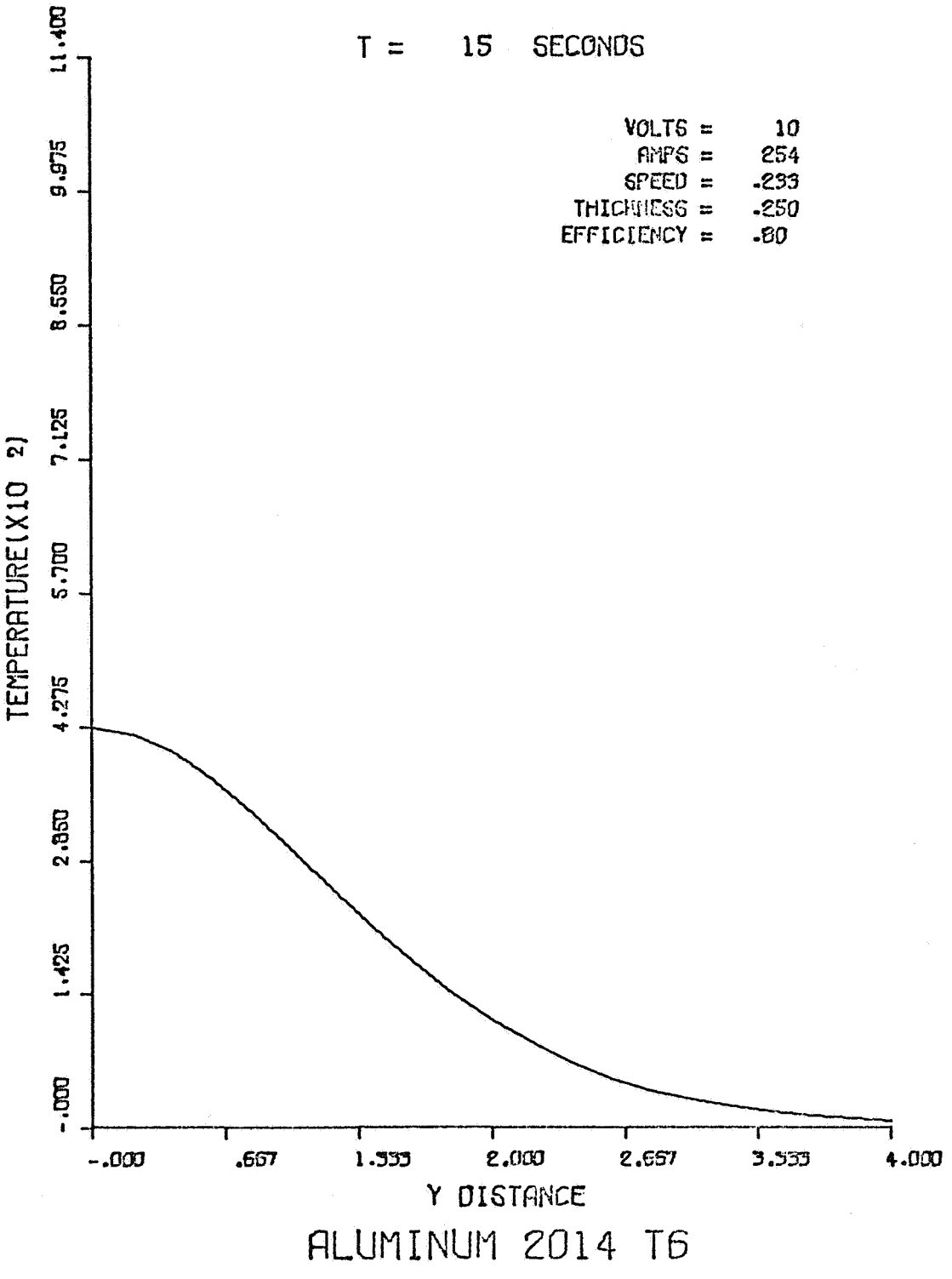

FIGURE A-5. TEMPERATURE DISTRIBUTION ALONG THE SECTION AT T = 15, CONDITION 1

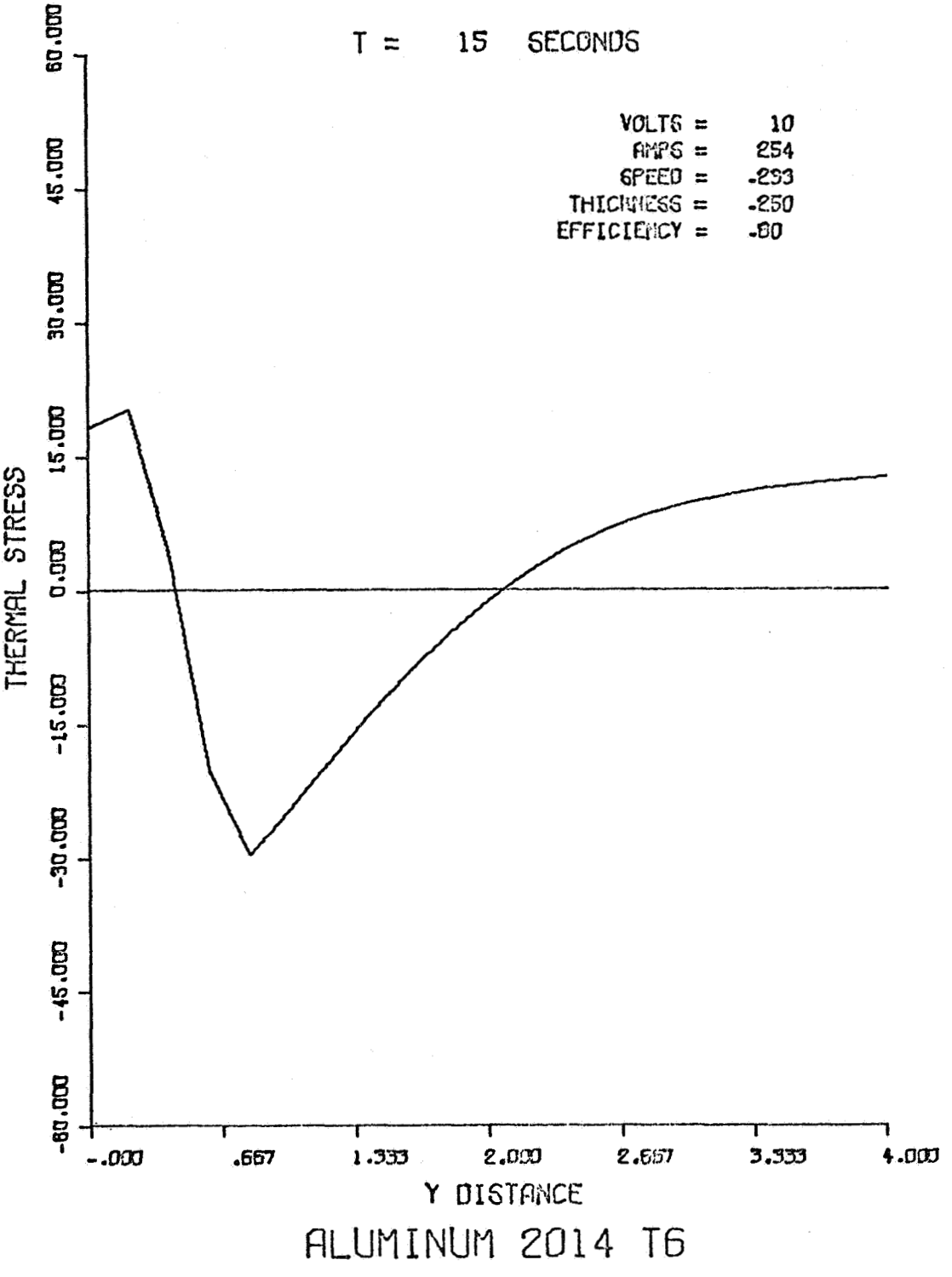

FIGURE A-6. STRESS DISTRIBUTION ALONG THE SECTION AT T = 15, CONDITION 1

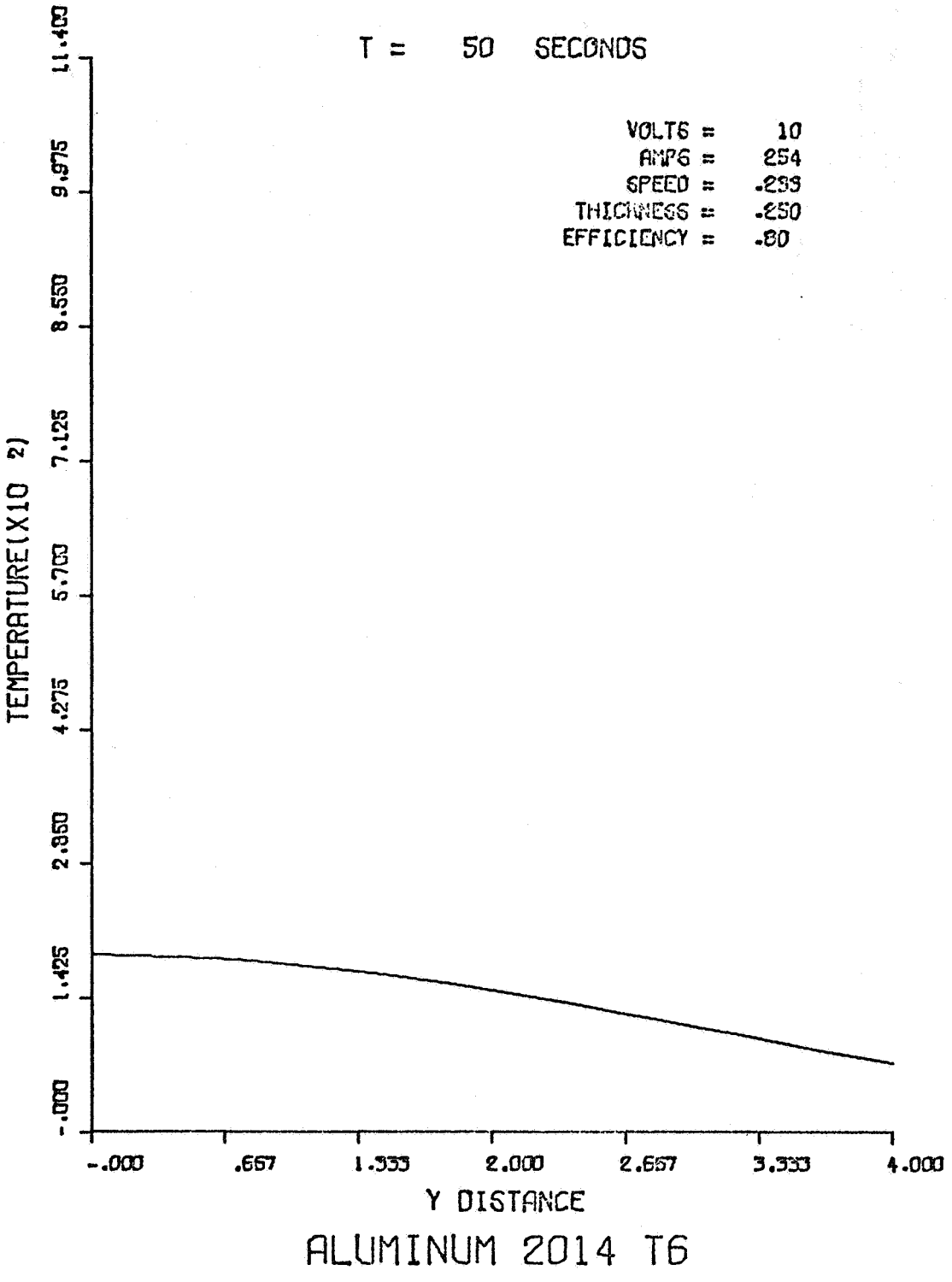

FIGURE A-7. TEMPERATURE DISTRIBUTION ALONG THE SECTION AT T = 50, CONDITION 1

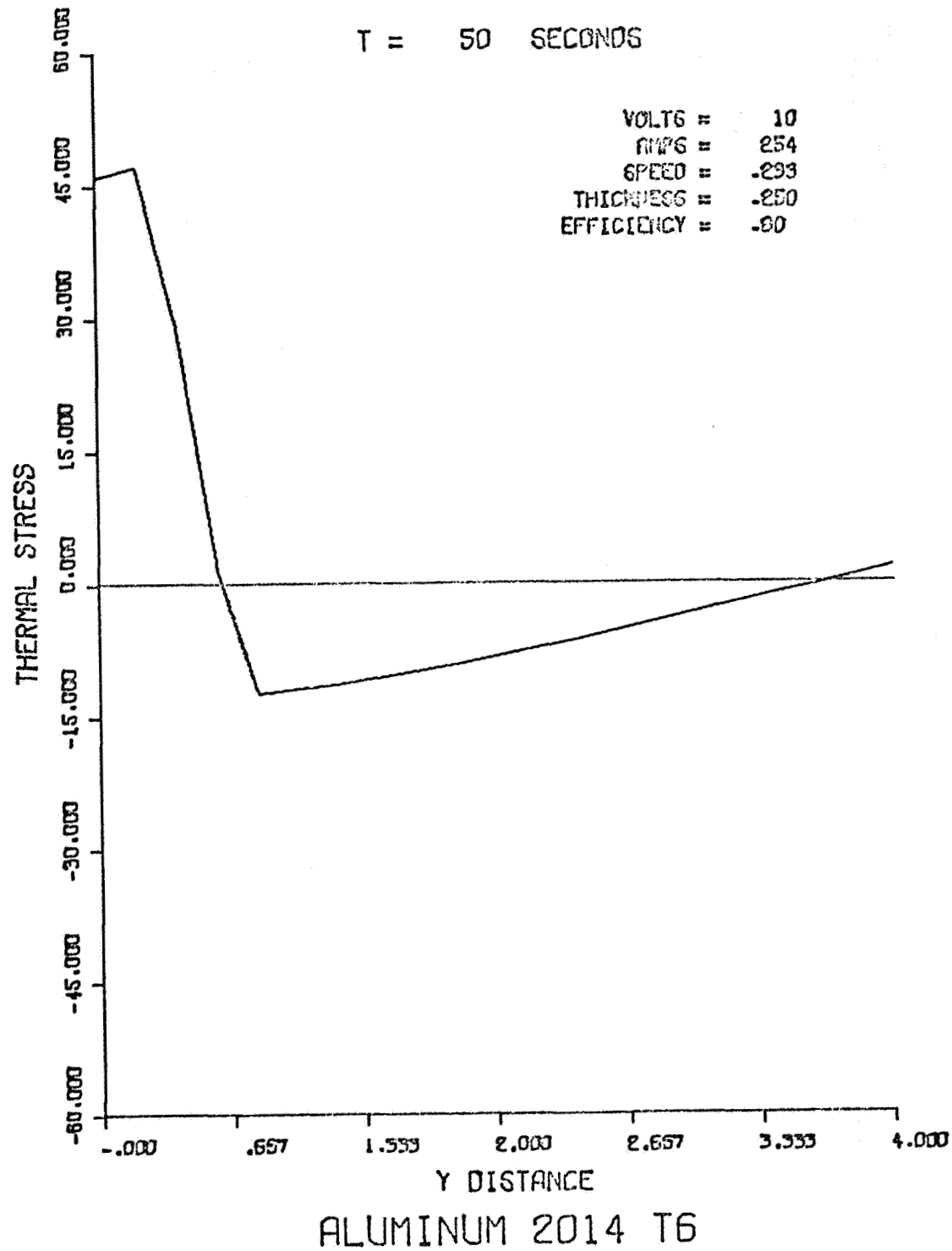

FIGURE A-8. STRESS DISTRIBUTION ALONG THE SECTION AT T = 50, CONDITION 1

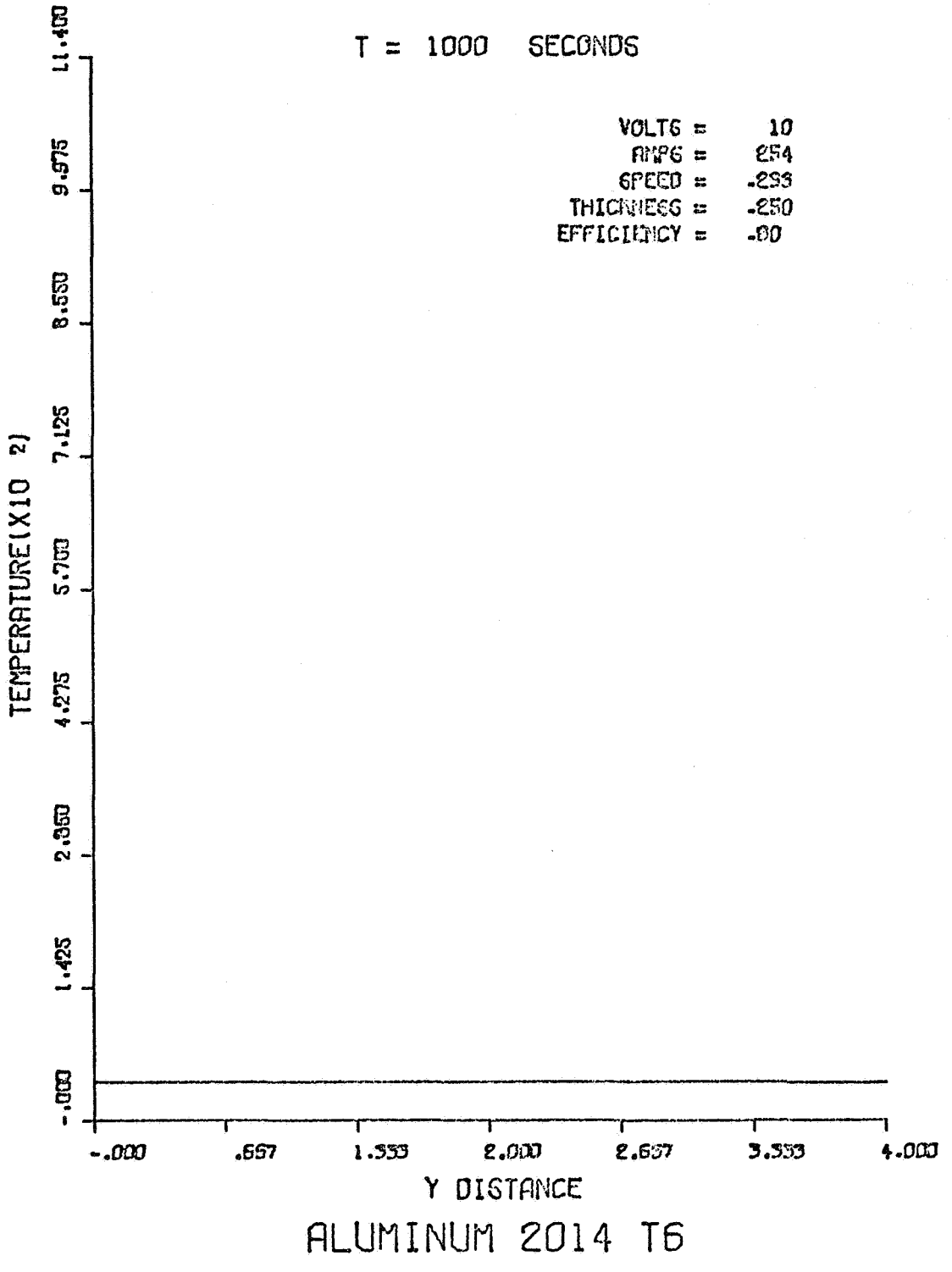

FIGURE A-9. TEMPERATURE DISTRIBUTION ALONG THE SECTION AT T = 1000, CONDITION 1

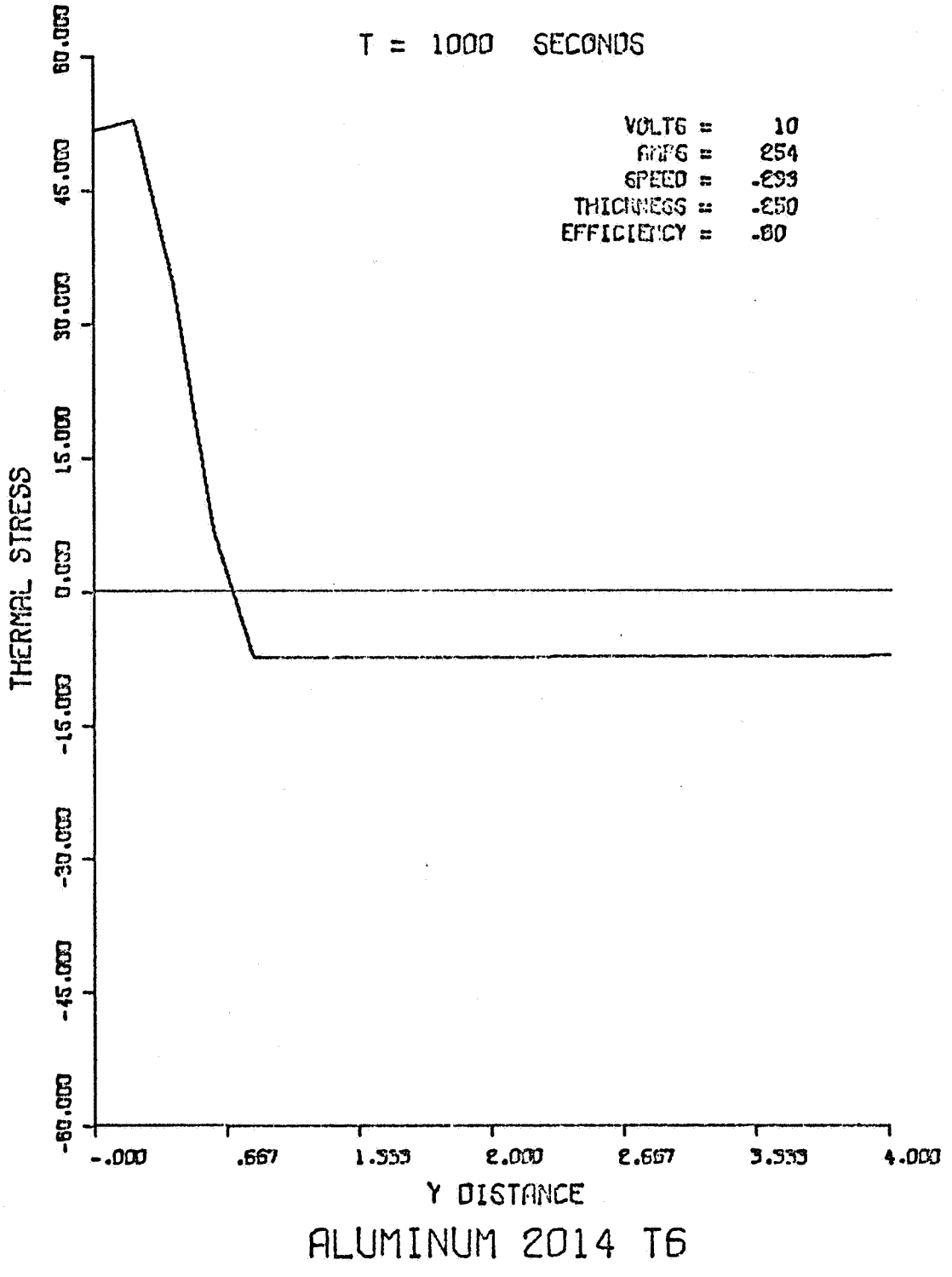

FIGURE A-10. STRESS DISTRIBUTION ALONG THE SECTION AT T = 1000, CONDITION 1

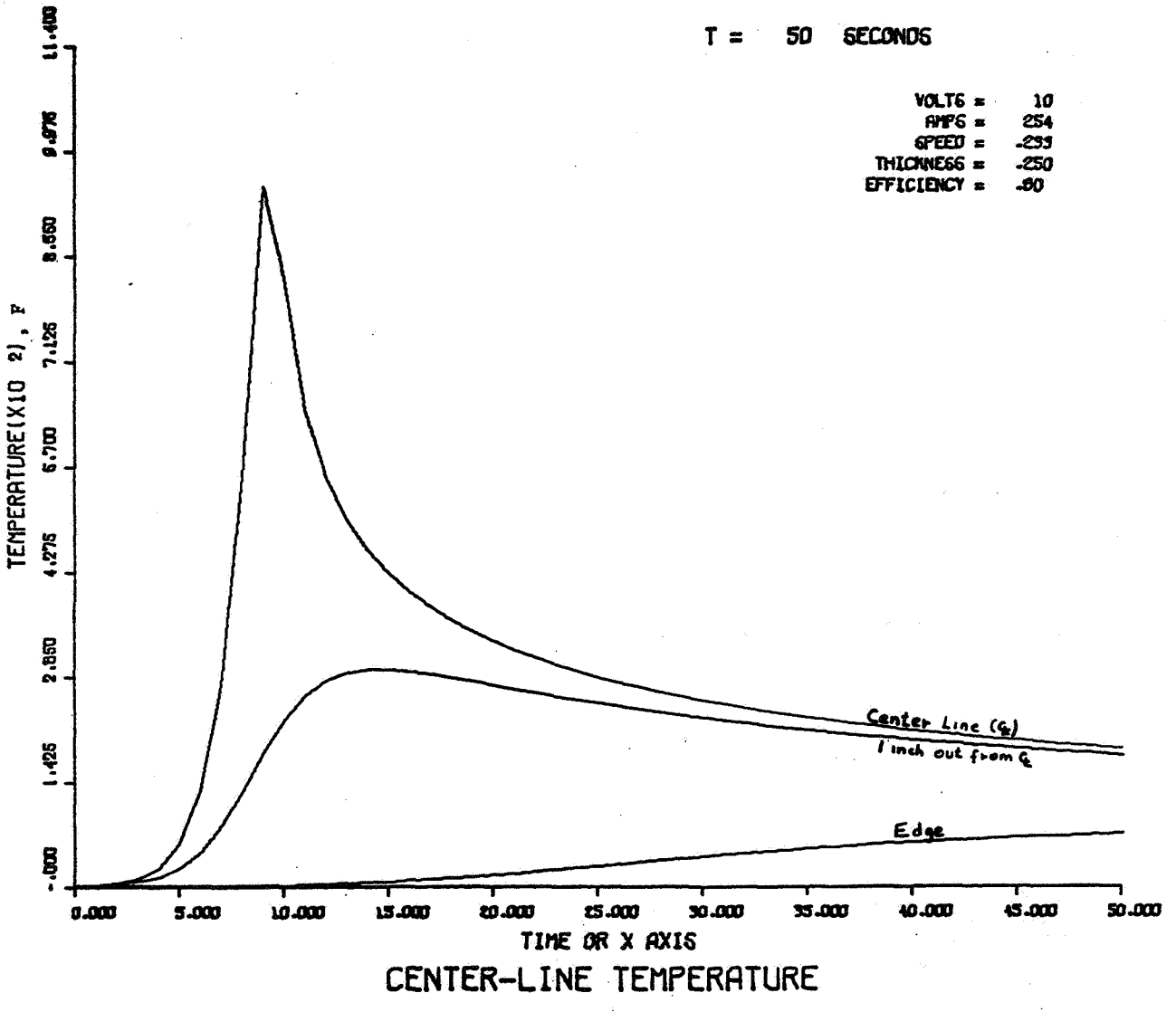

FIGURE A-11. TEMPERATURE CHANGES ALONG THREE LONGITUDINAL LINES, CONDITION 1

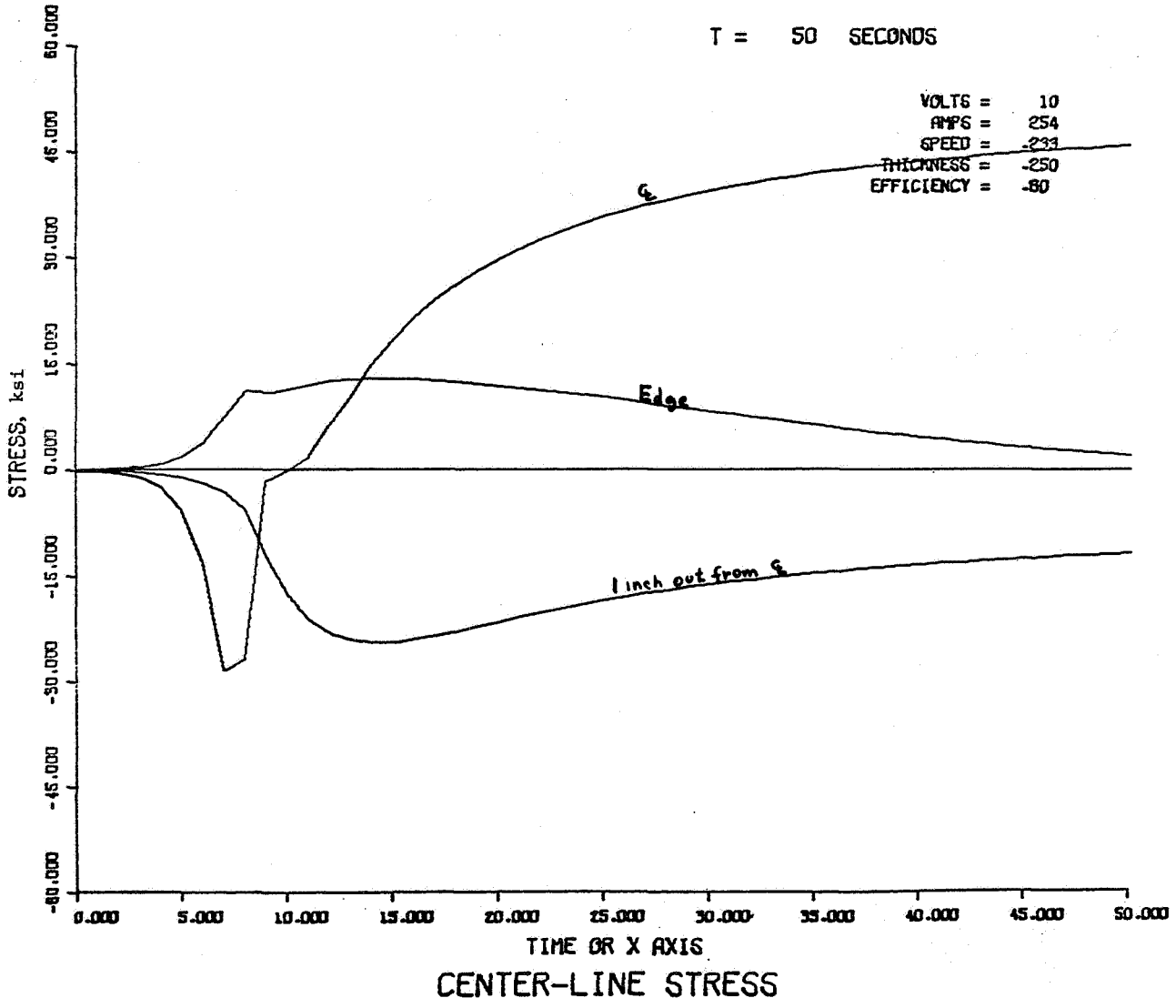

FIGURE A-12. STRESS CHANGES ALONG THREE LONGITUDINAL LINES, CONDITION 1

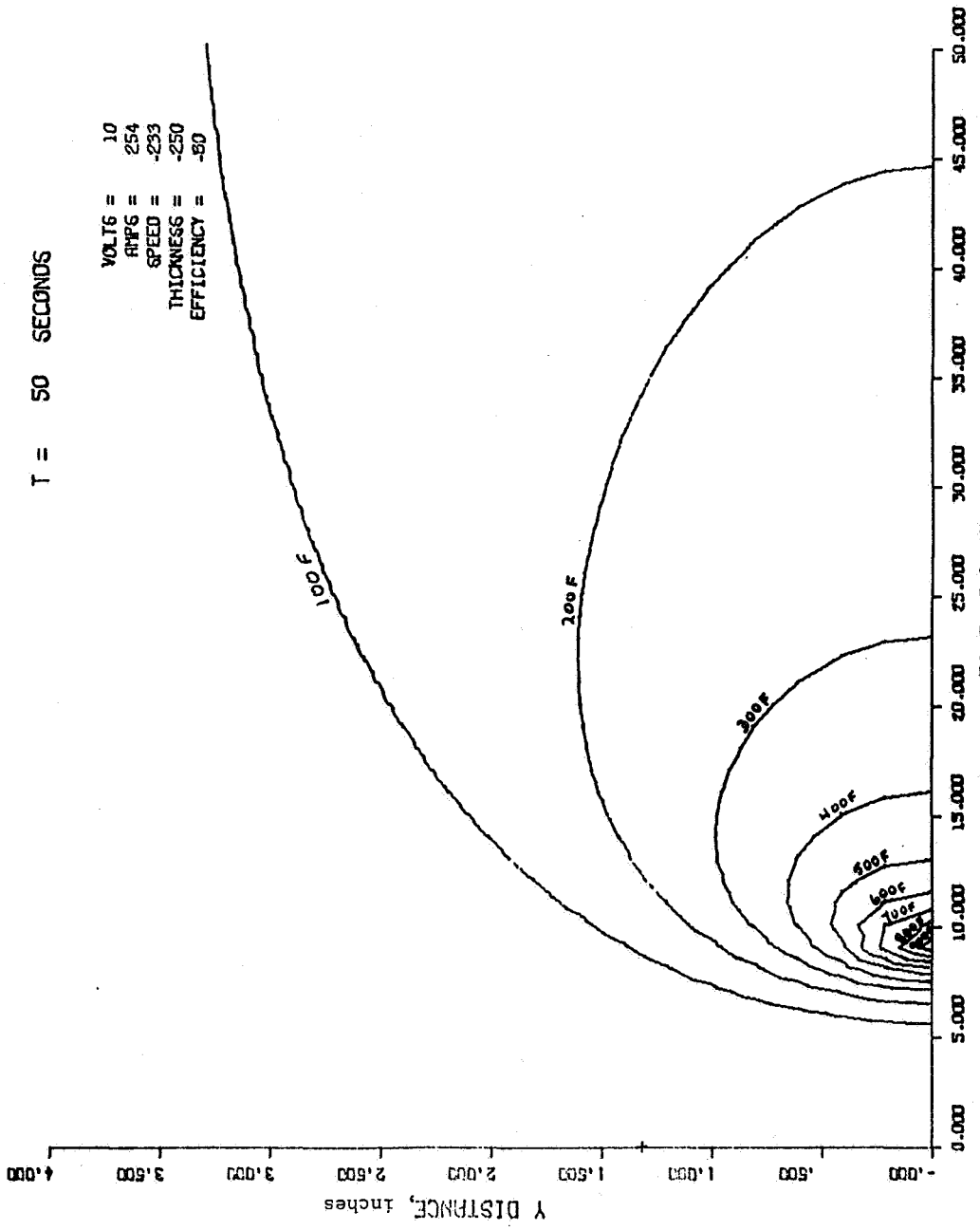

FIGURE A-13. ISOTHERM PATTERN, CONDITION 1

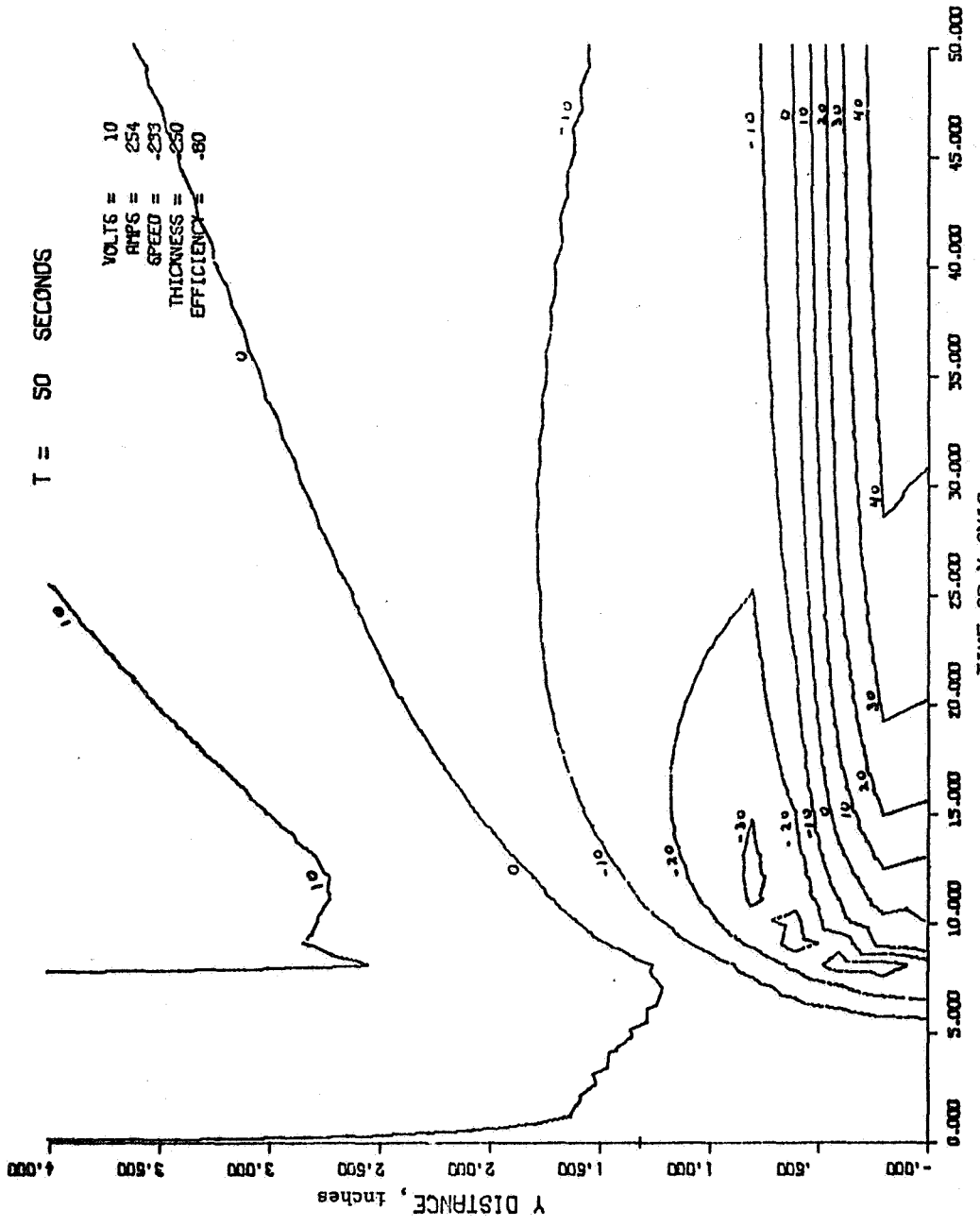

FIGURE A-14. ISOSTRESS PATTERN, CONDITION 1

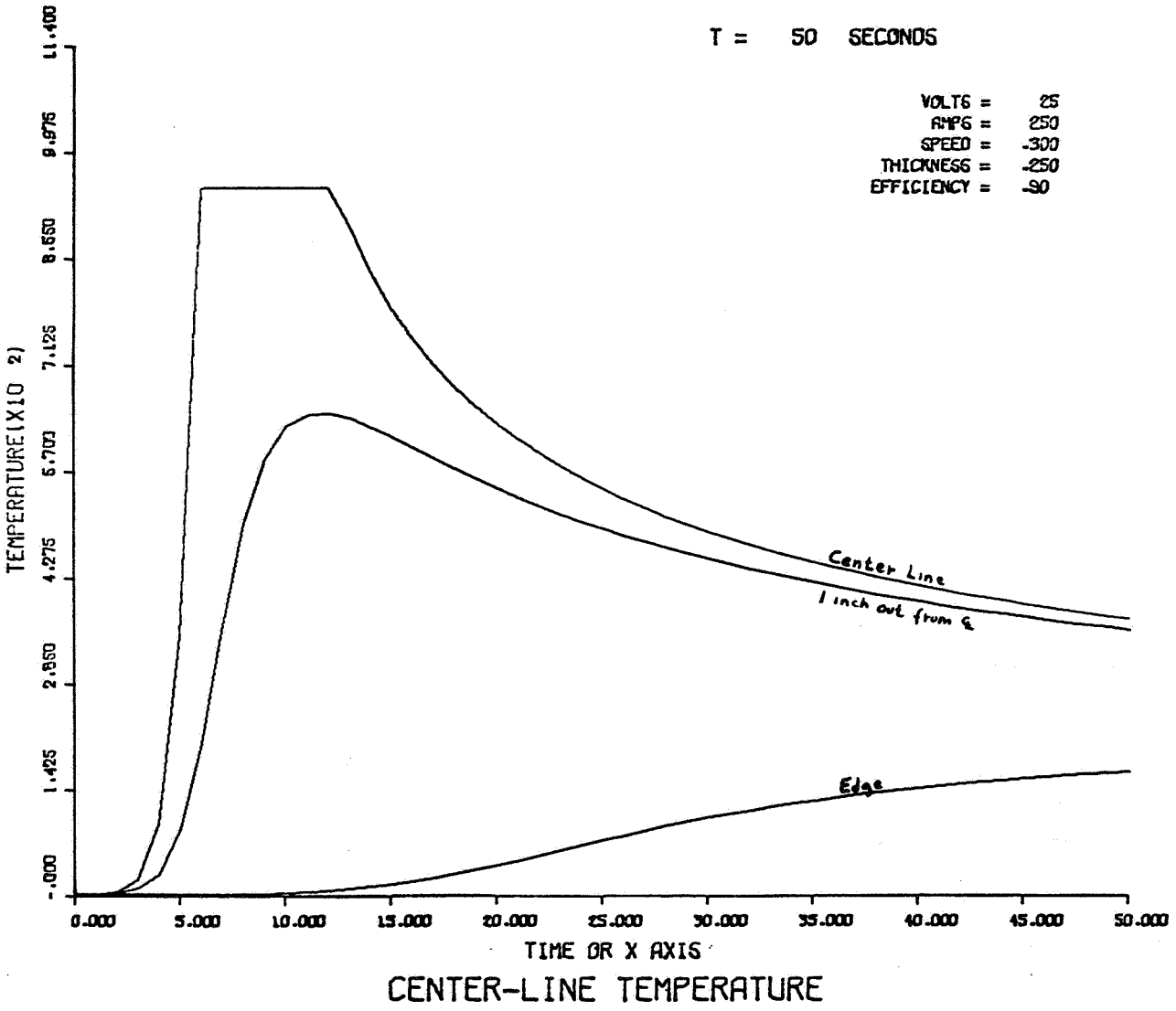

FIGURE A-15. TEMPERATURE CHANGES ALONG THREE LONGITUDINAL LINES, CONDITION 2

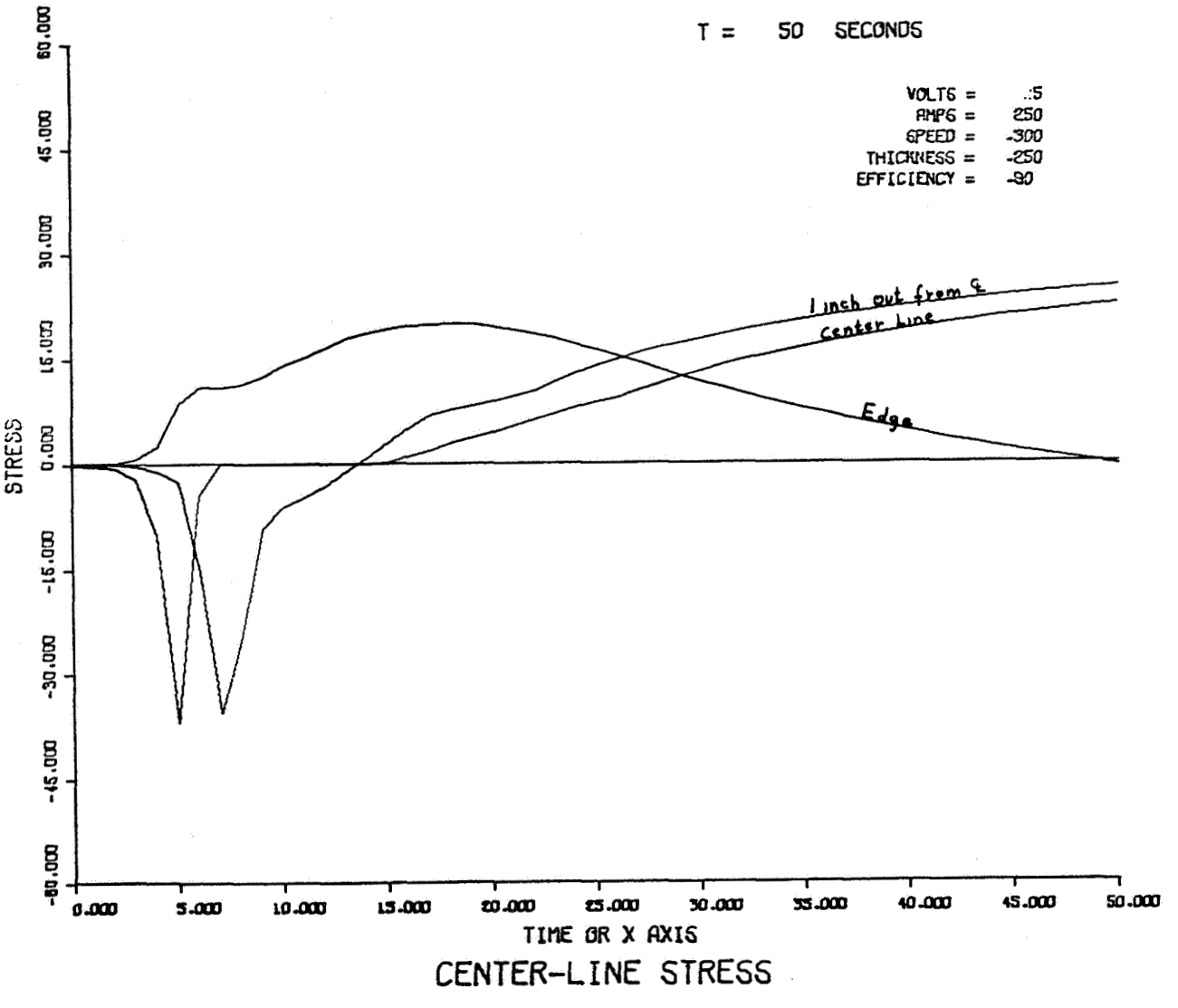

FIGURE A-16. STRESS CHANGES ALONG THREE LONGITUDINAL LINES, CONDITION 2

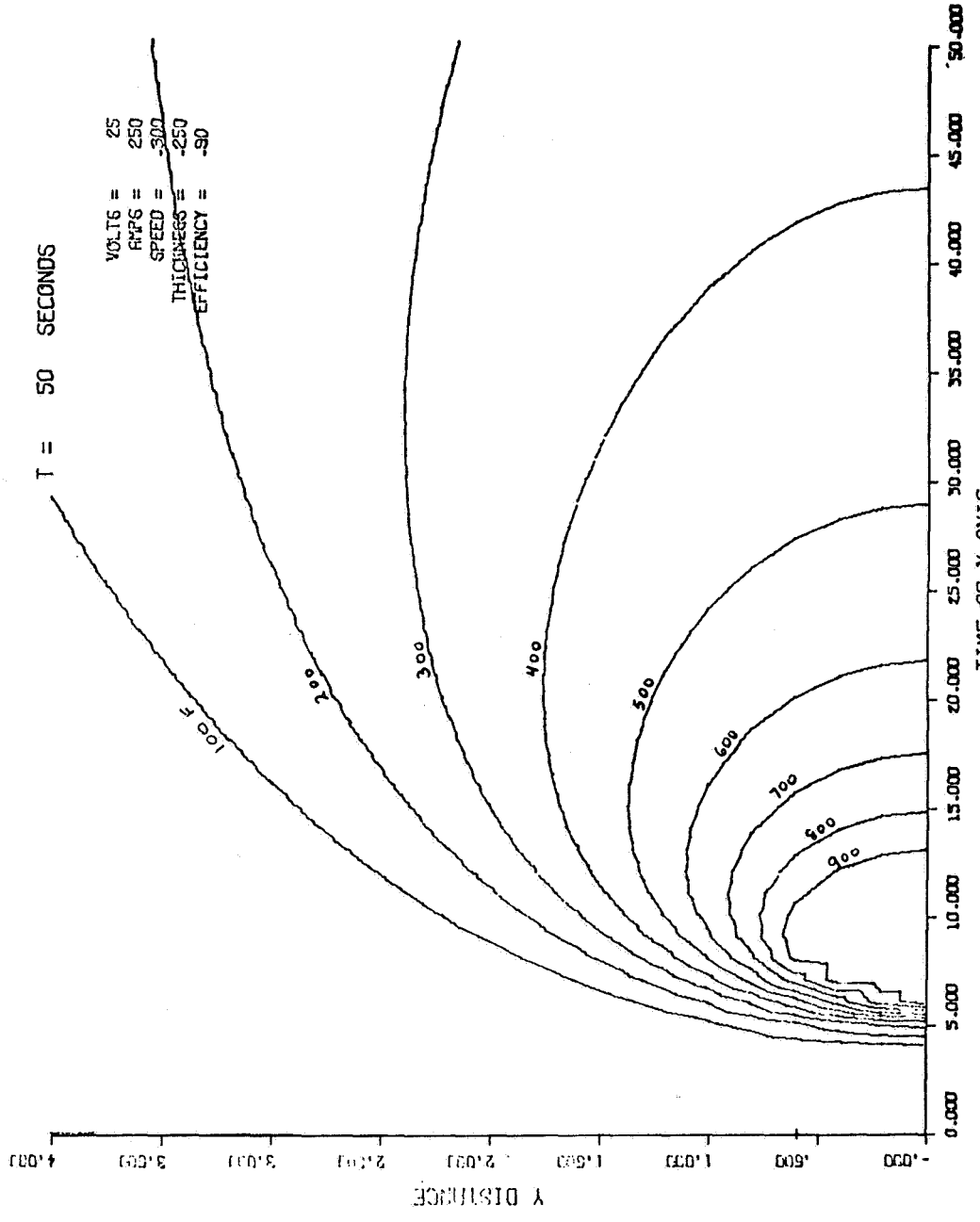

FIGURE A-17. ISOTHERM PATTERN, CONDITION 2

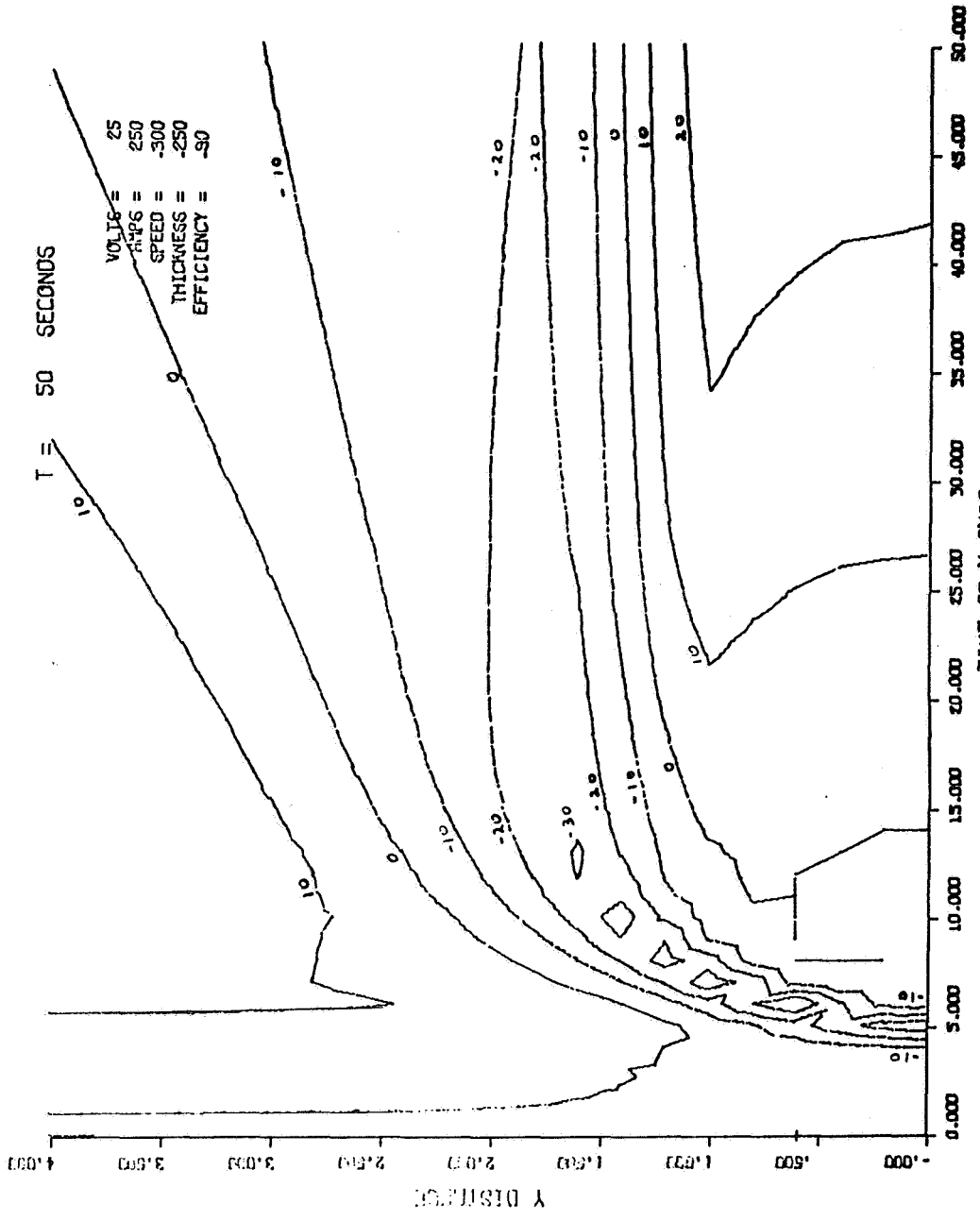

FIGURE A-18. ISOSTRESS PATTERN, CONDITION 2

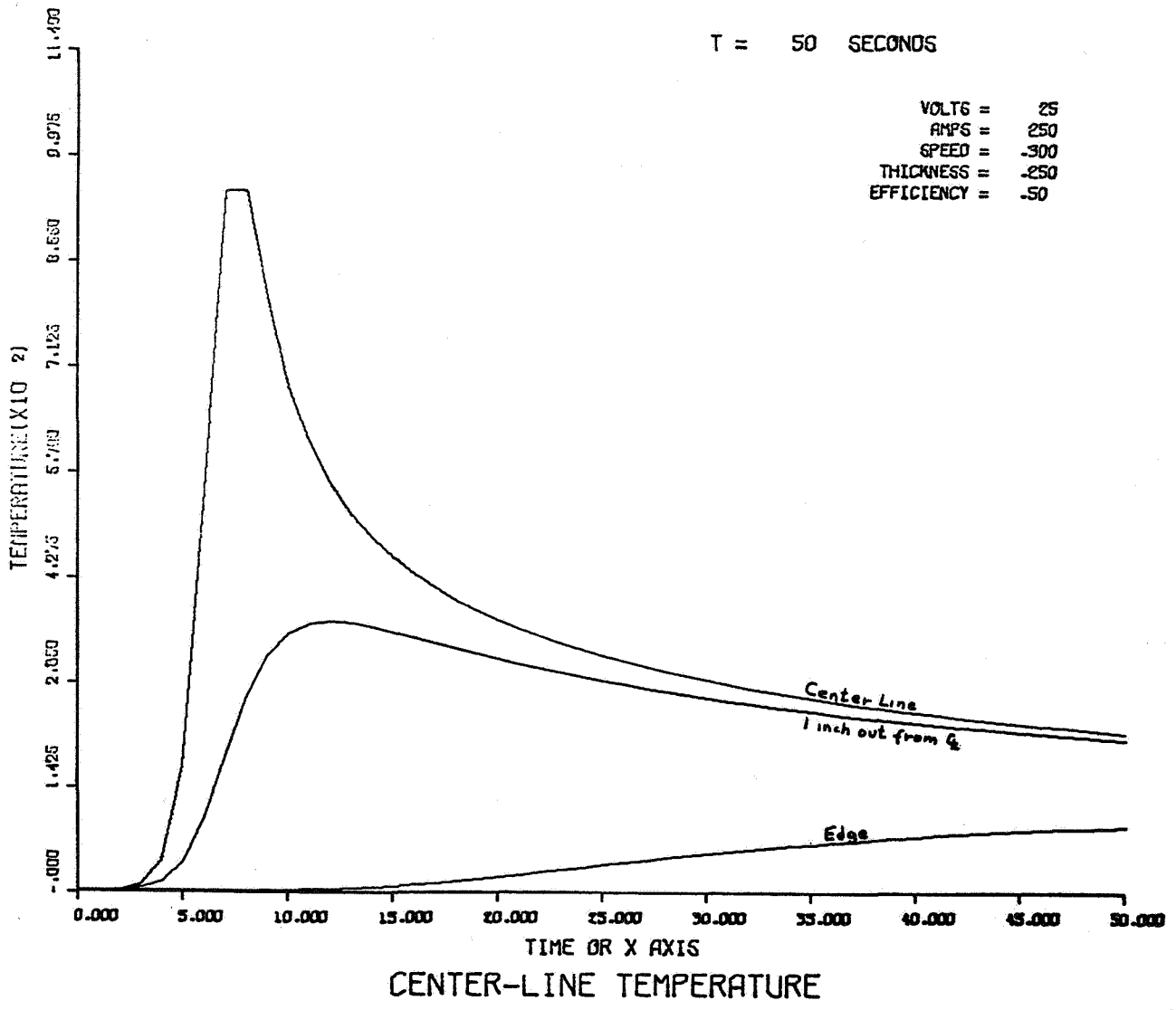

FIGURE A-19. TEMPERATURE CHANGES ALONG THREE LONGITUDINAL LINES, CONDITION 3

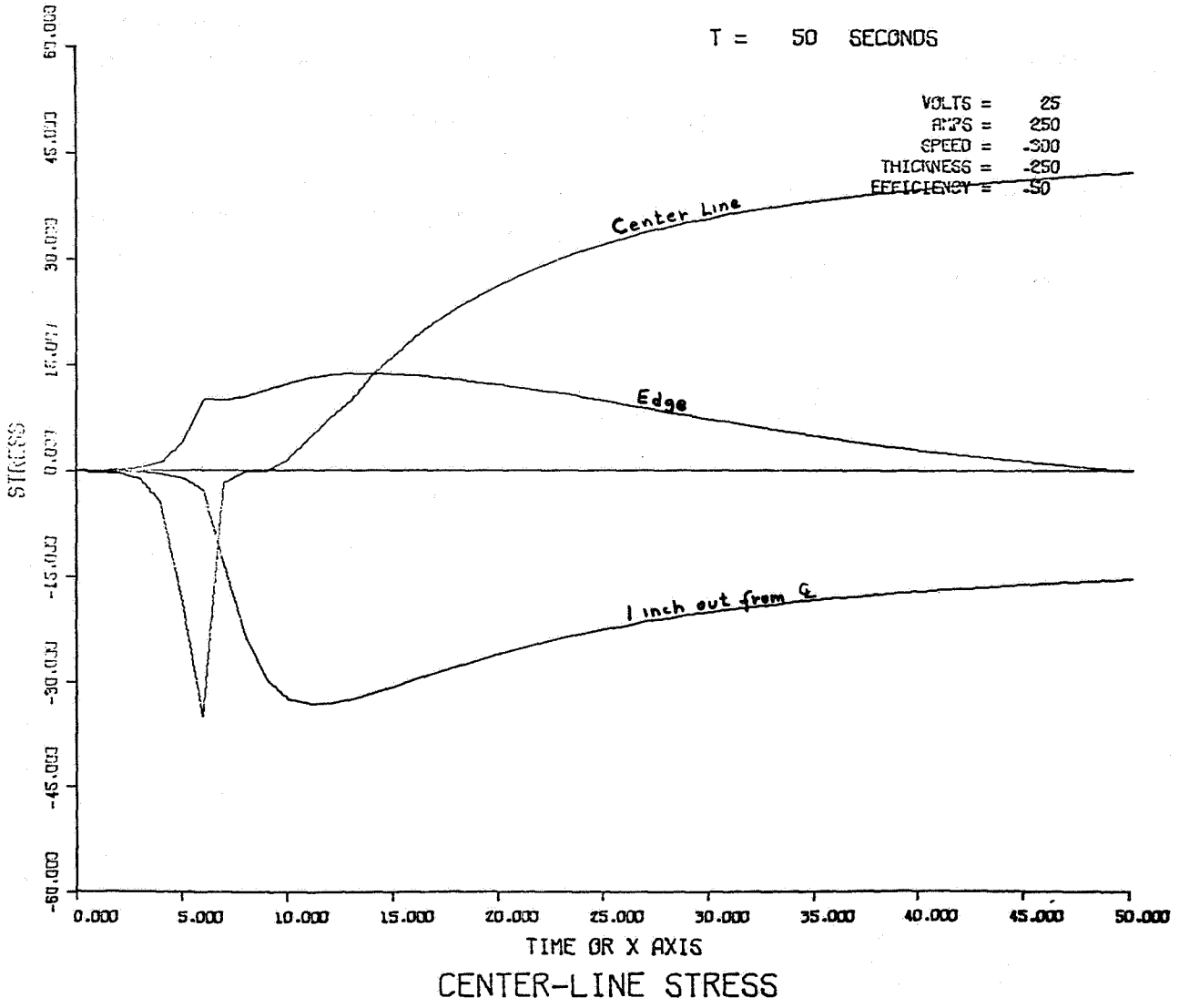

FIGURE A-20. STRESS CHANGES ALONG THREE LONGITUDINAL LINES, CONDITION 3

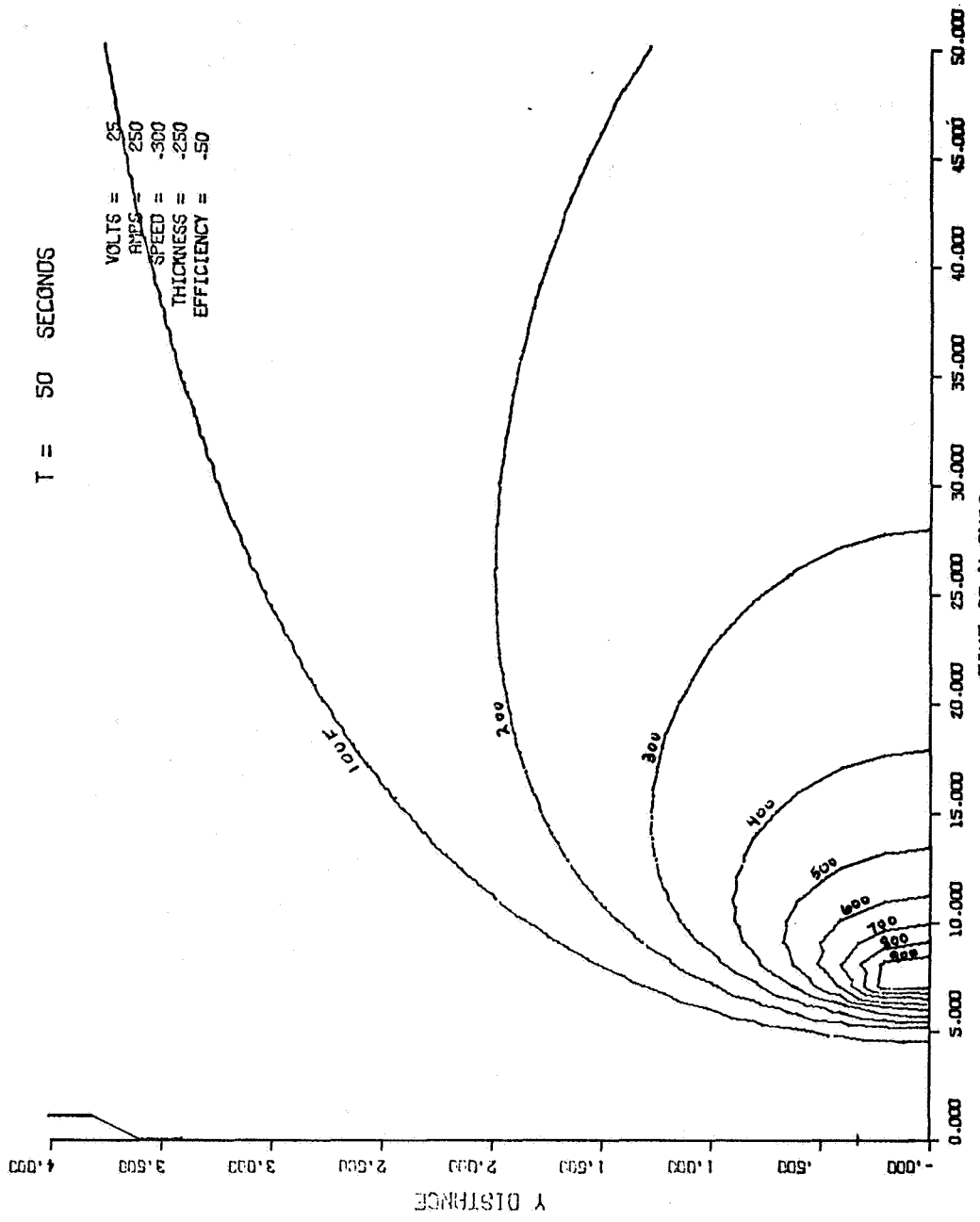

TEMPERATURE ISOTHERMS

FIGURE A-21. ISOTHERM PATTERN, CONDITION 3

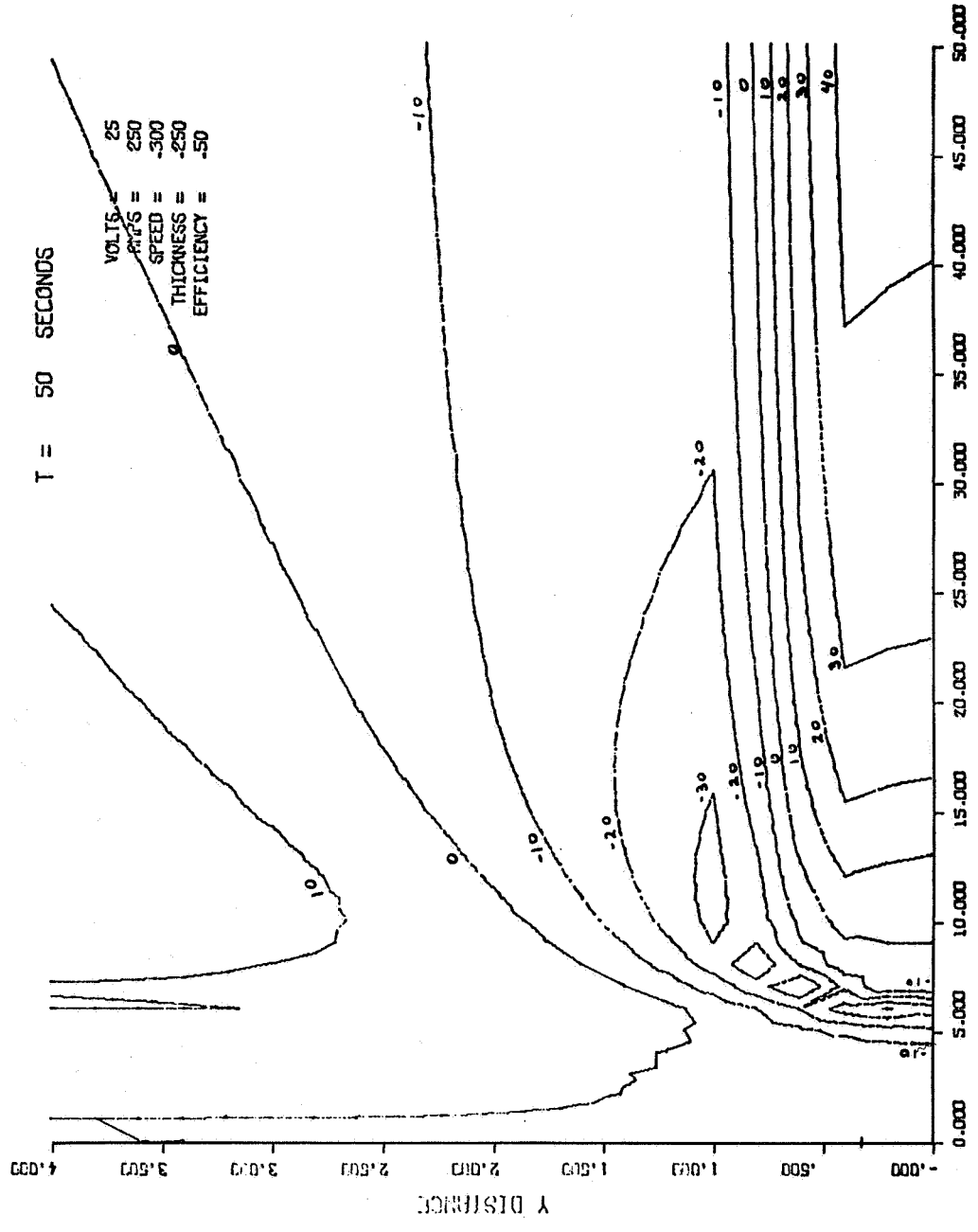

FIGURE A-22. ISOSTRESS PATTERN, CONDITION 3

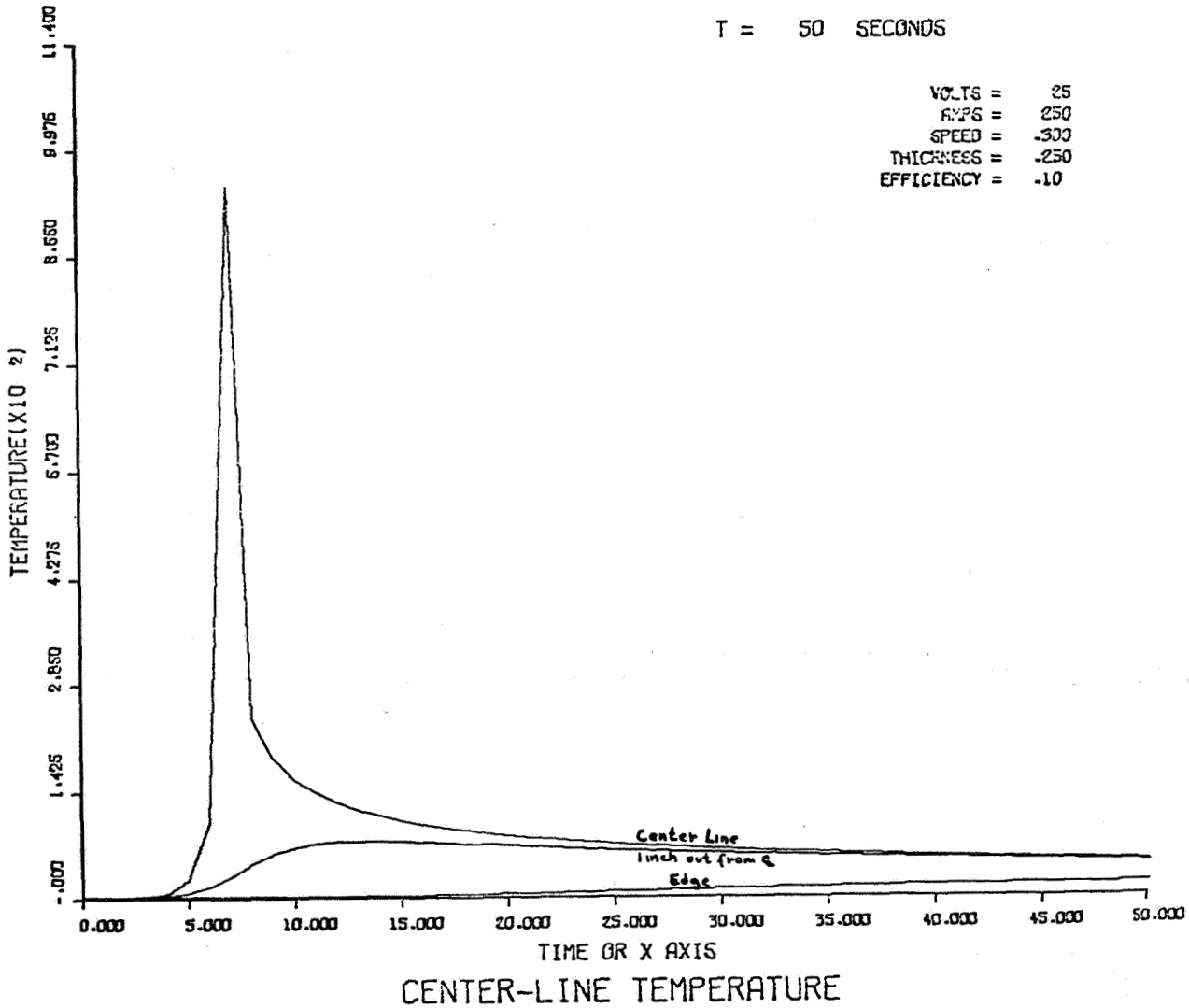

FIGURE A-23. TEMPERATURE CHANGES ALONG THREE LONGITUDINAL LINES, CONDITION 4

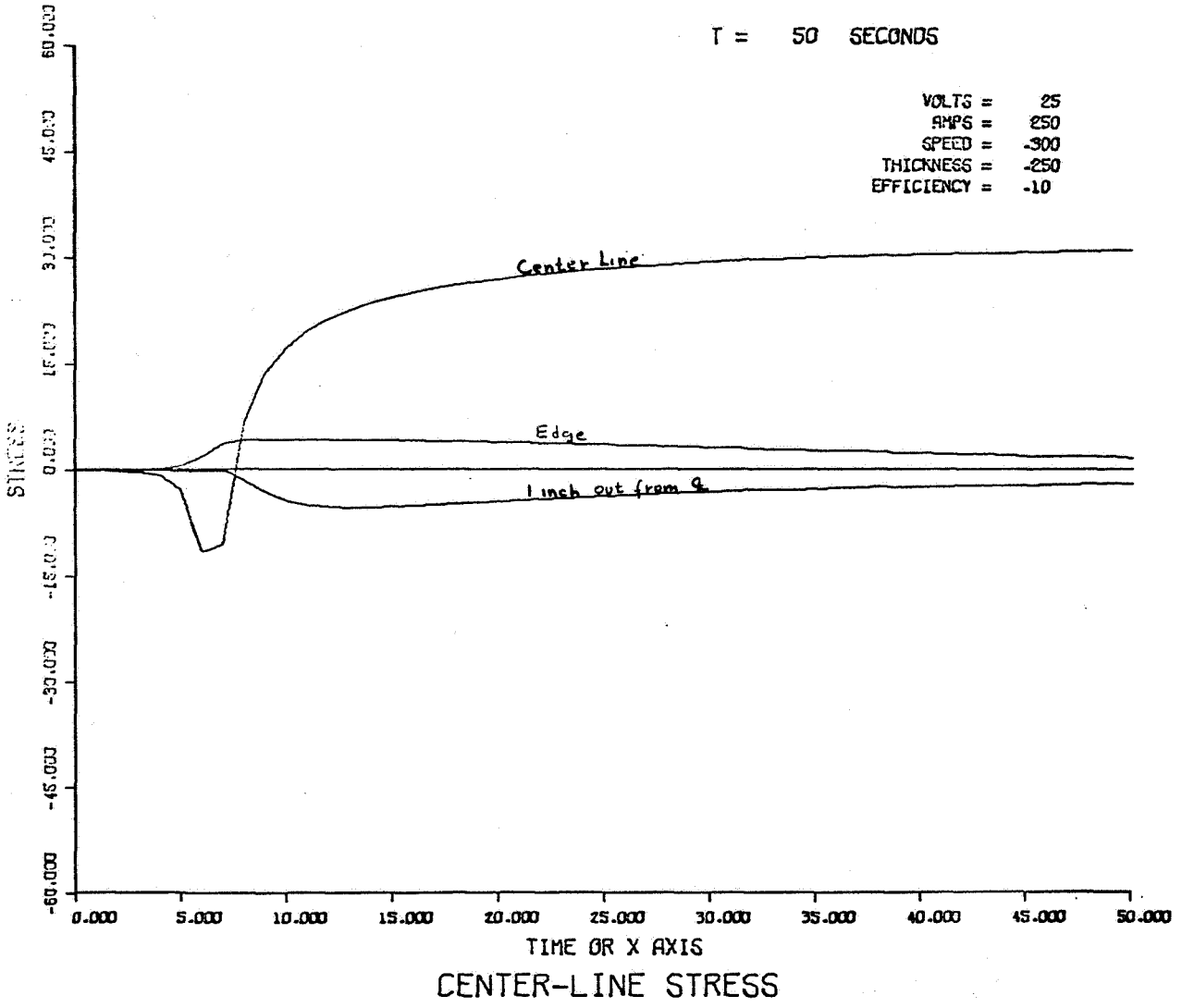

FIGURE A-24. STRESS CHANGES ALONG THREE LONGITUDINAL LINES, CONDITION 4

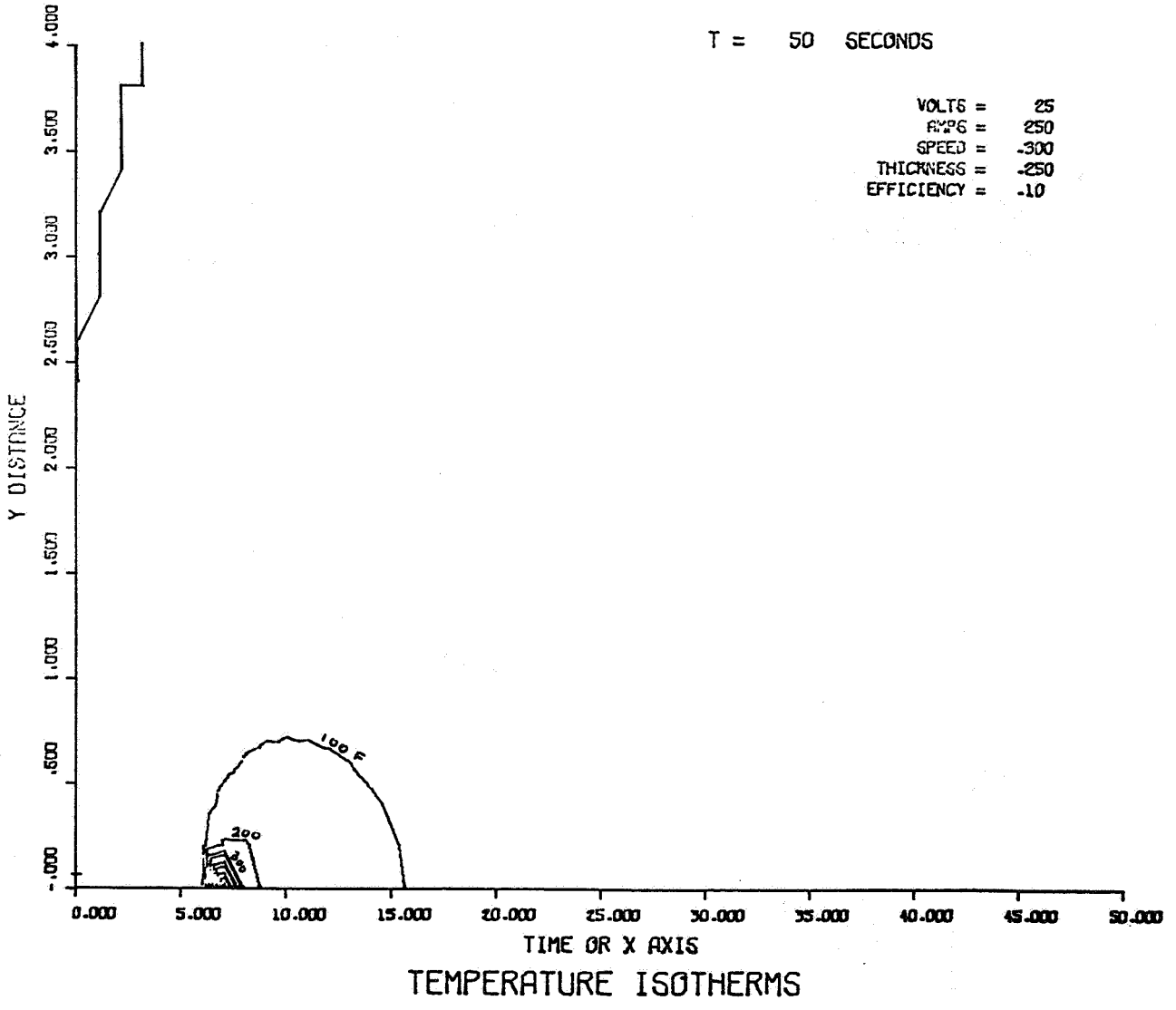

FIGURE A-25. ISOTHERM PATTERN, CONDITION 4

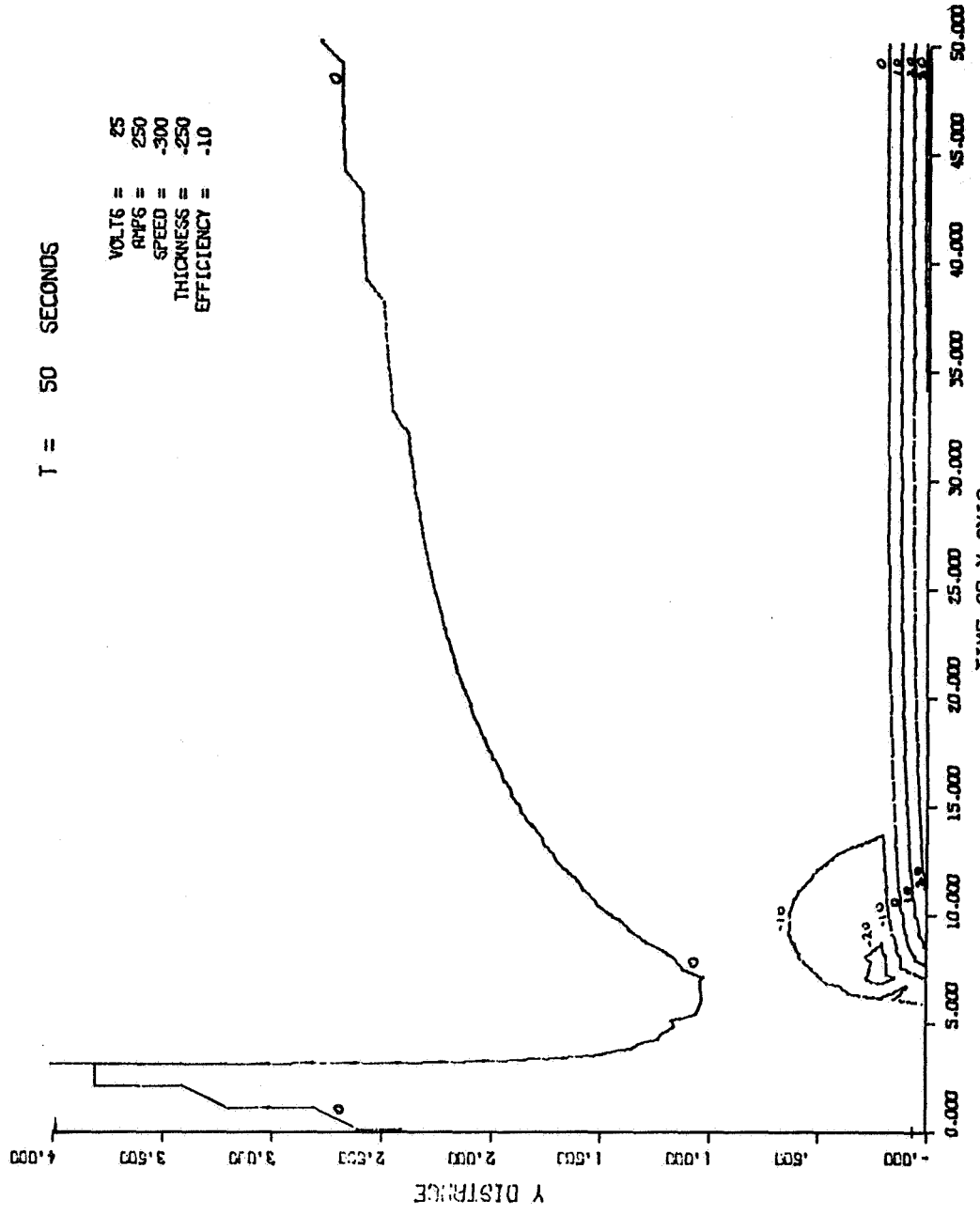

FIGURE A-26. ISOSTRESS PATTERN, CONDITION 4

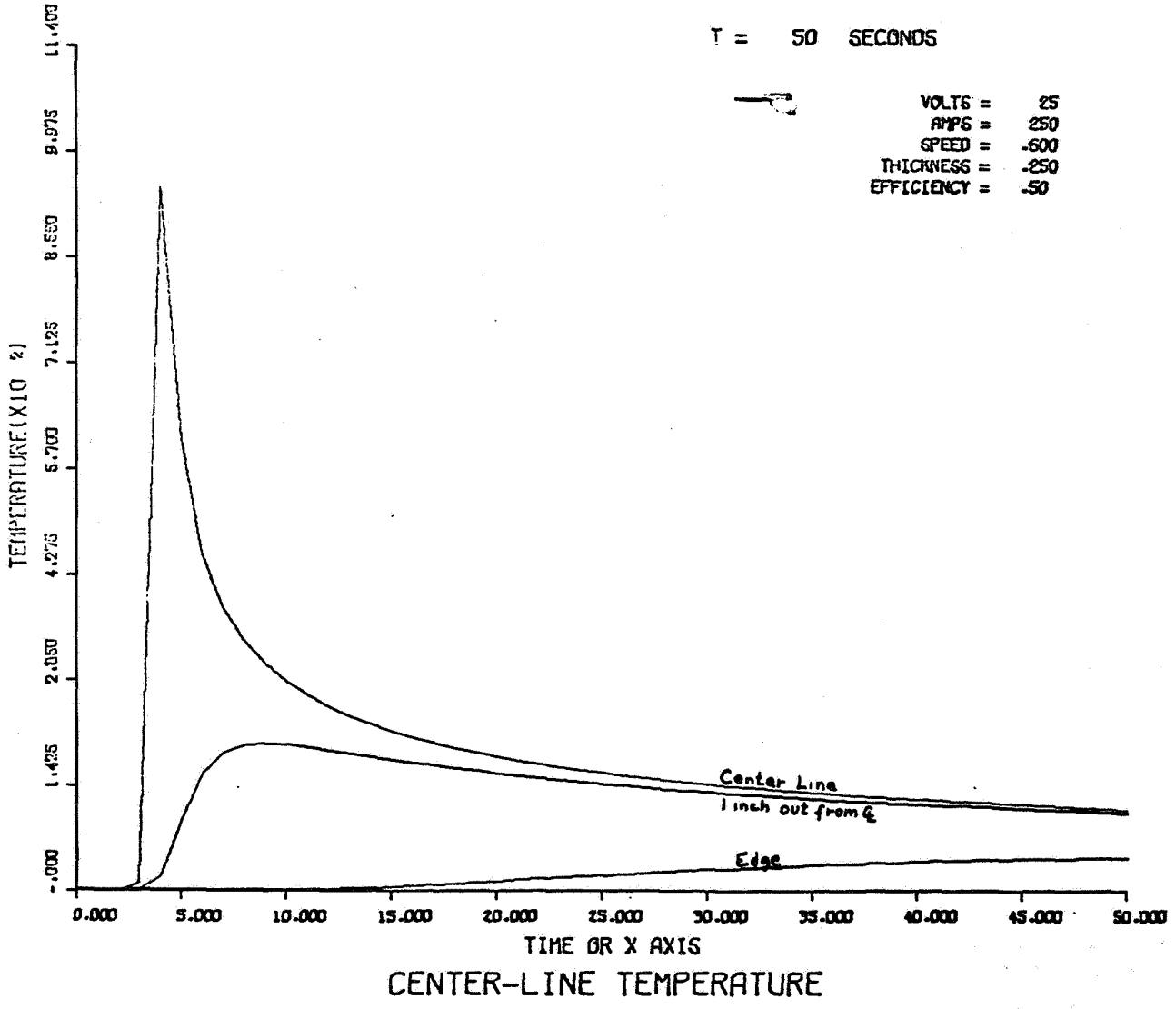

FIGURE A-27. TEMPERATURE CHANGES ALONG THREE LONGITUDINAL LINES, CONDITION 5

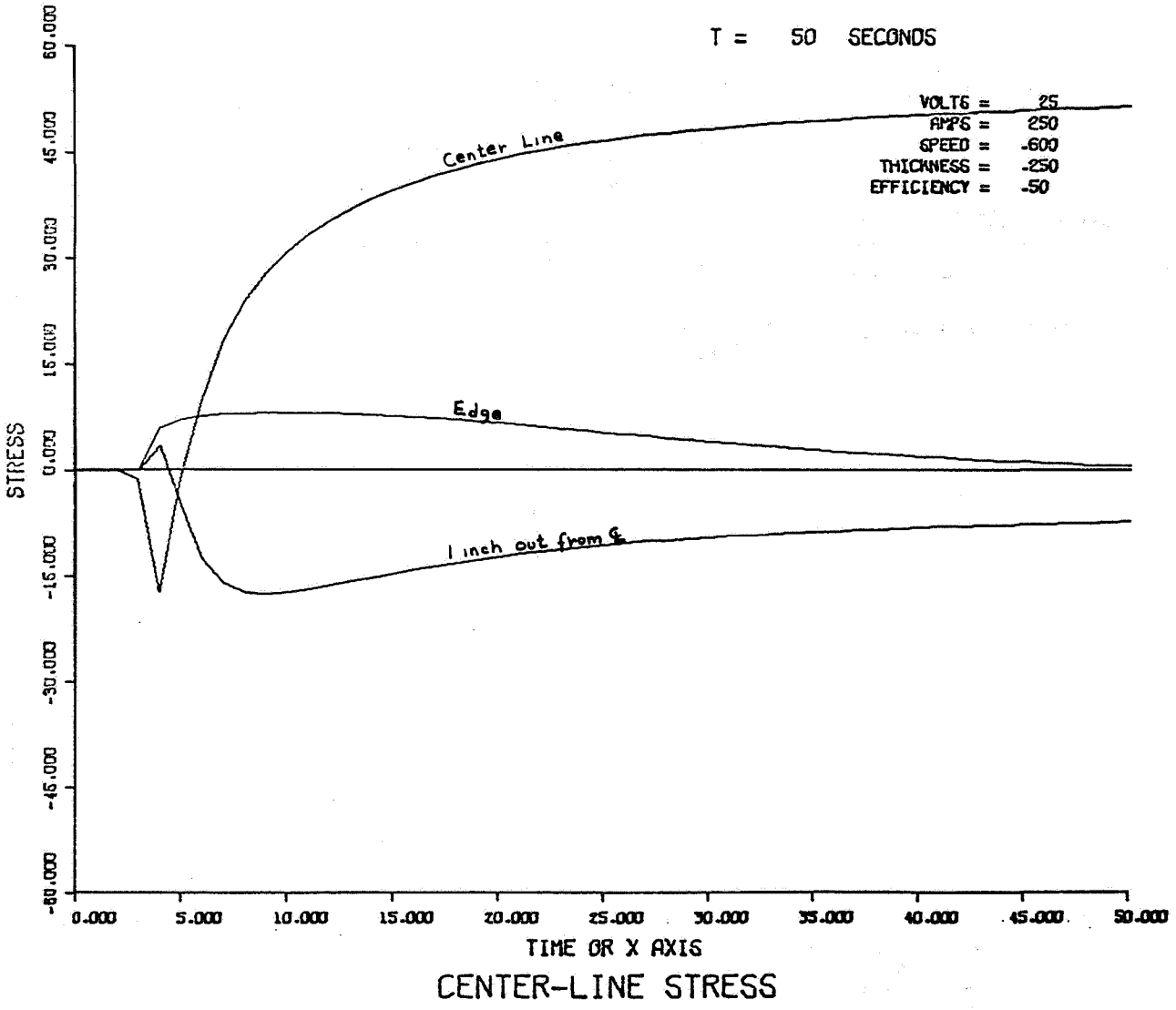

FIGURE A-28. STRESS CHANGES ALONG THREE LONGITUDINAL LINES, CONDITION 5

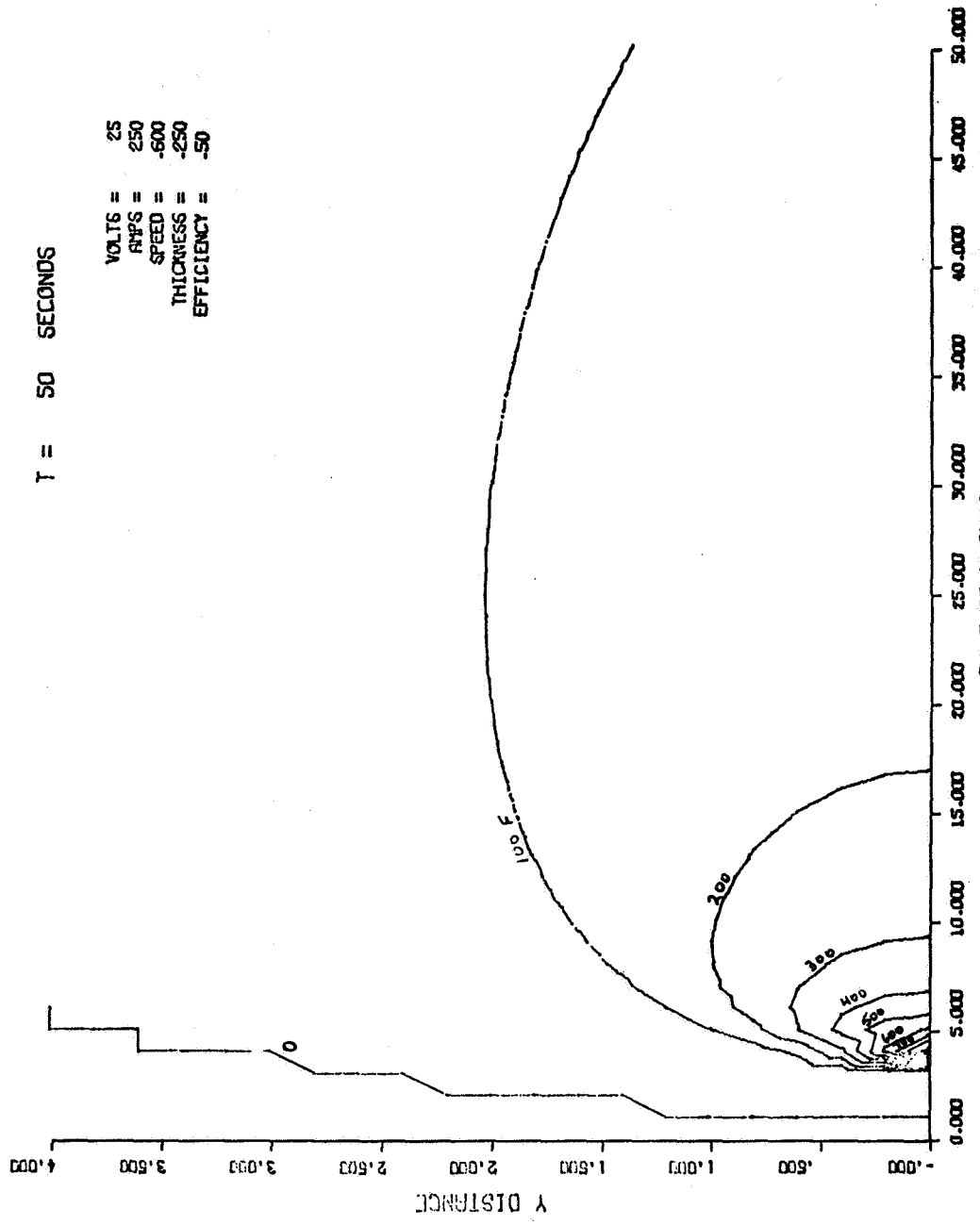

FIGURE A-29. ISOTHERM PATTERN, CONDITION 5

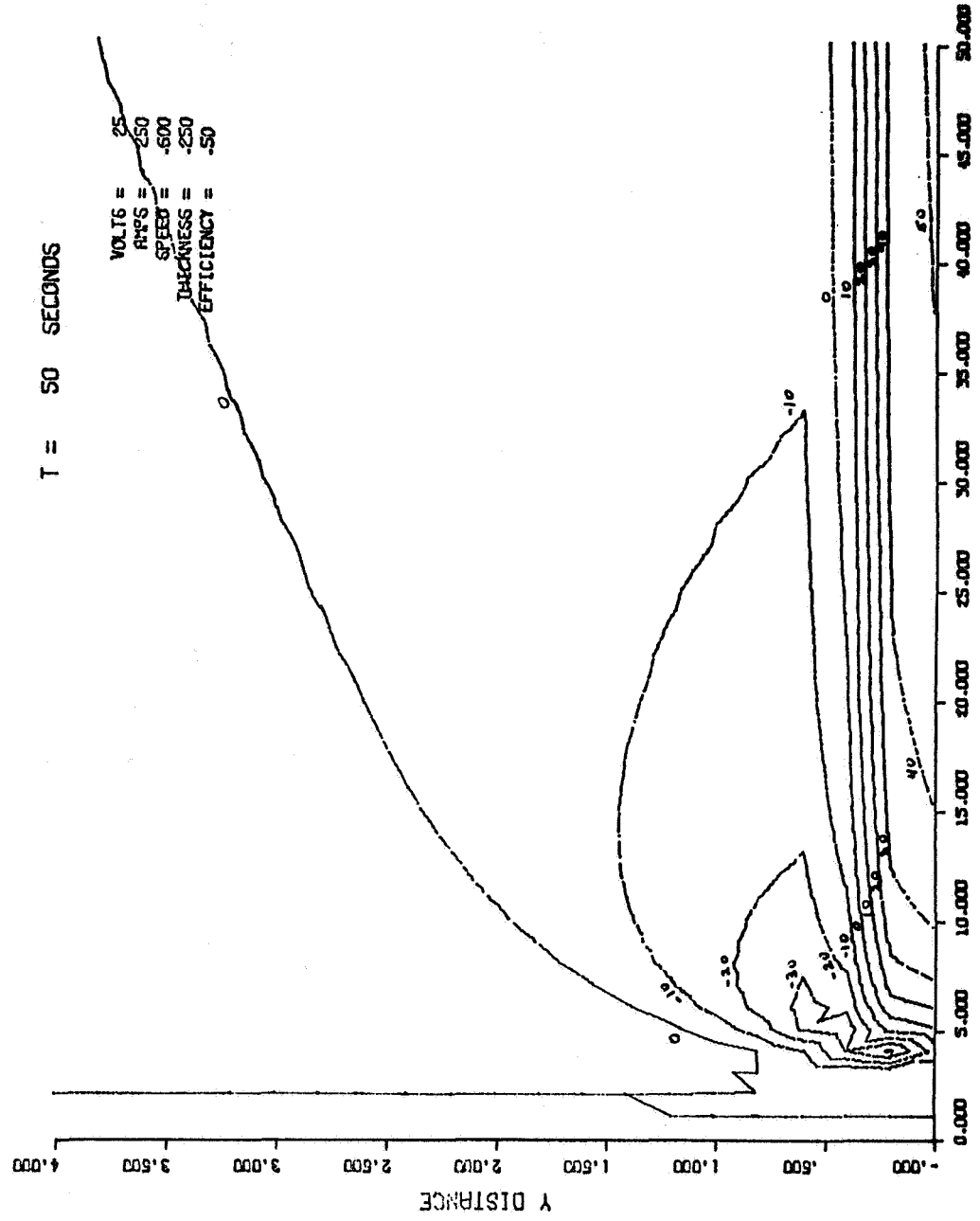

FIGURE A-30. ISOSTRESS PATTERN, CONDITION 5

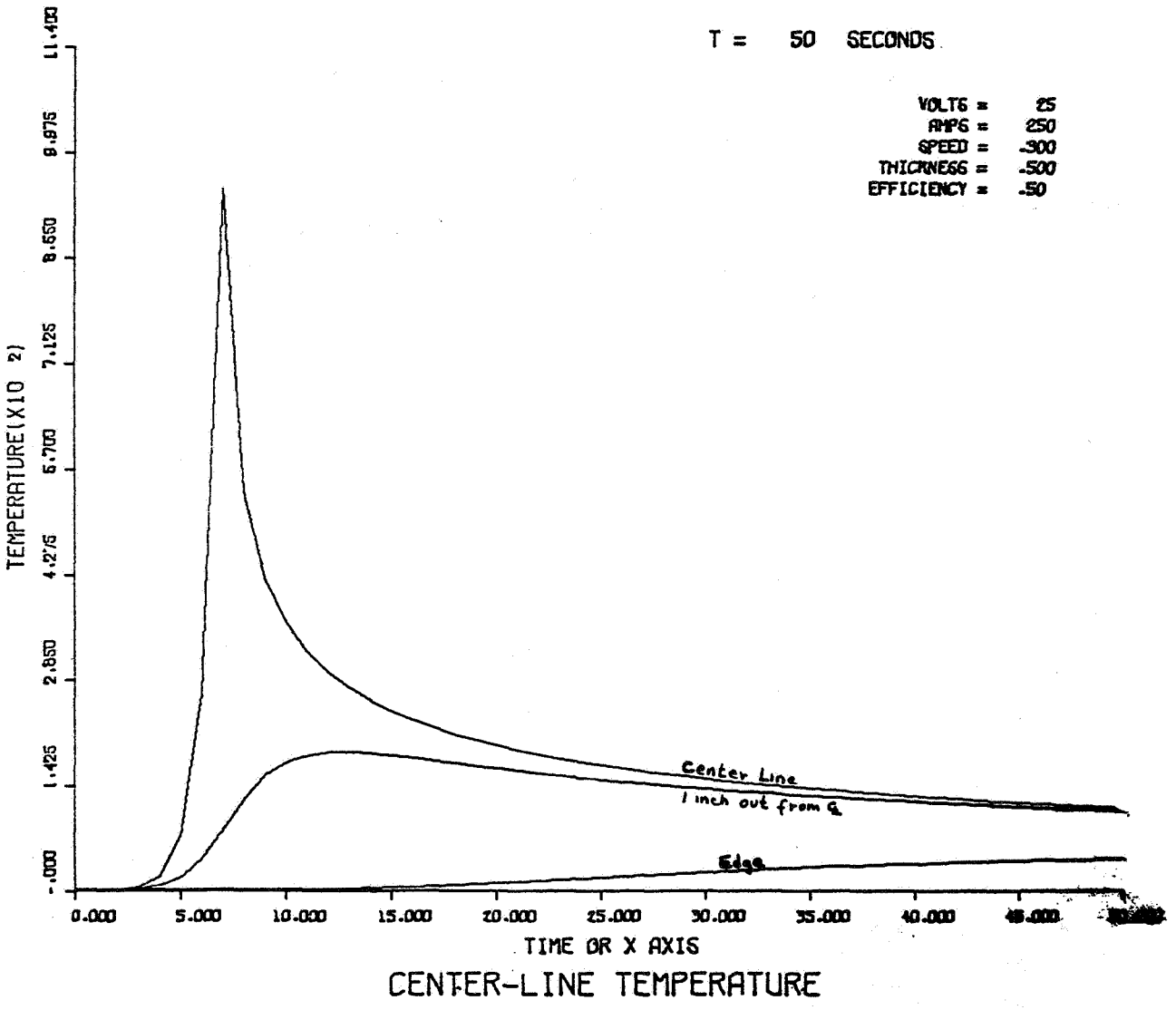

FIGURE A-31. TEMPERATURE CHANGES ALONG THREE LONGITUDINAL LINES, CONDITION 6

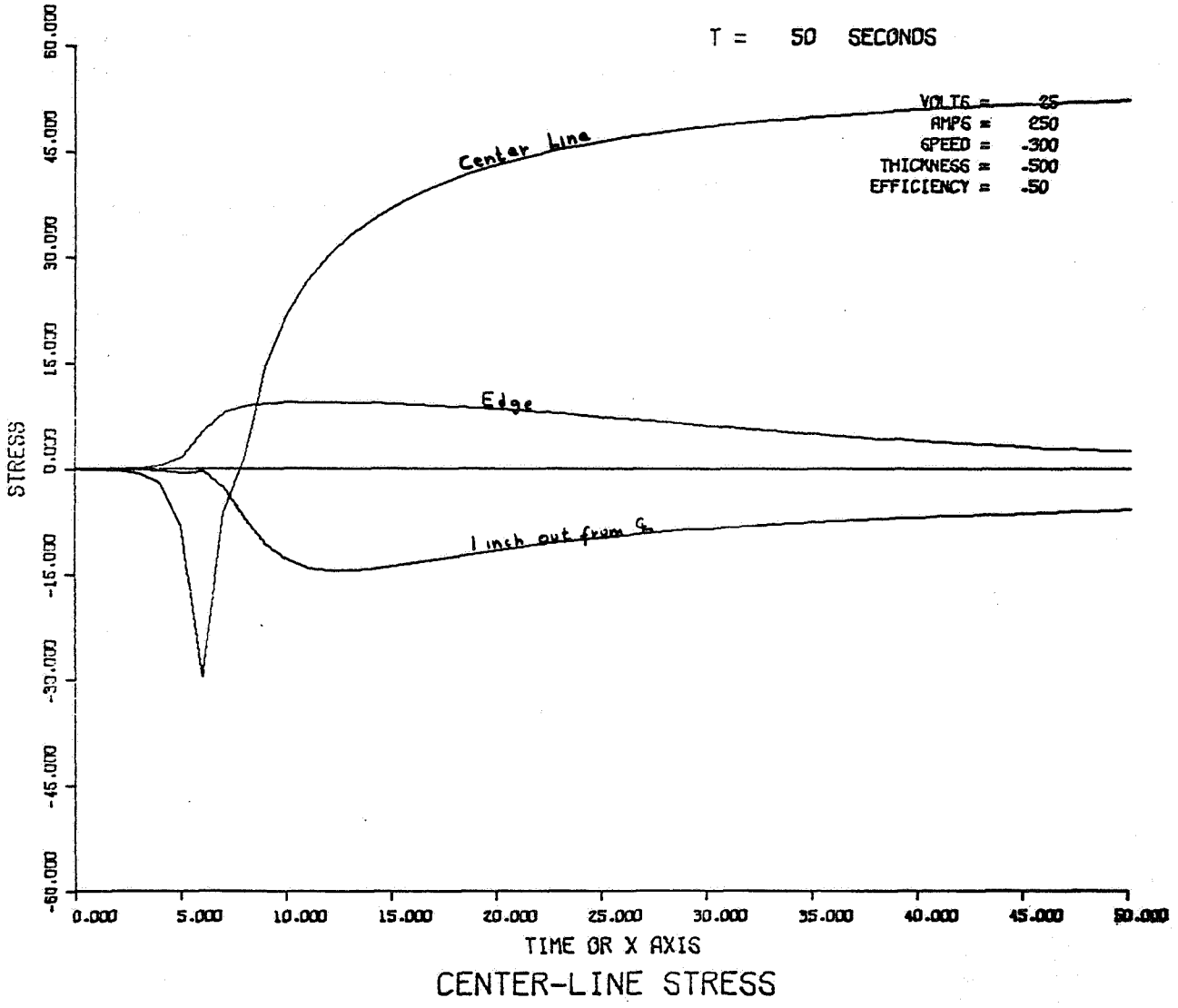

FIGURE A-32. STRESS CHANGES ALONG THREE LONGITUDINAL LINES, CONDITION 6

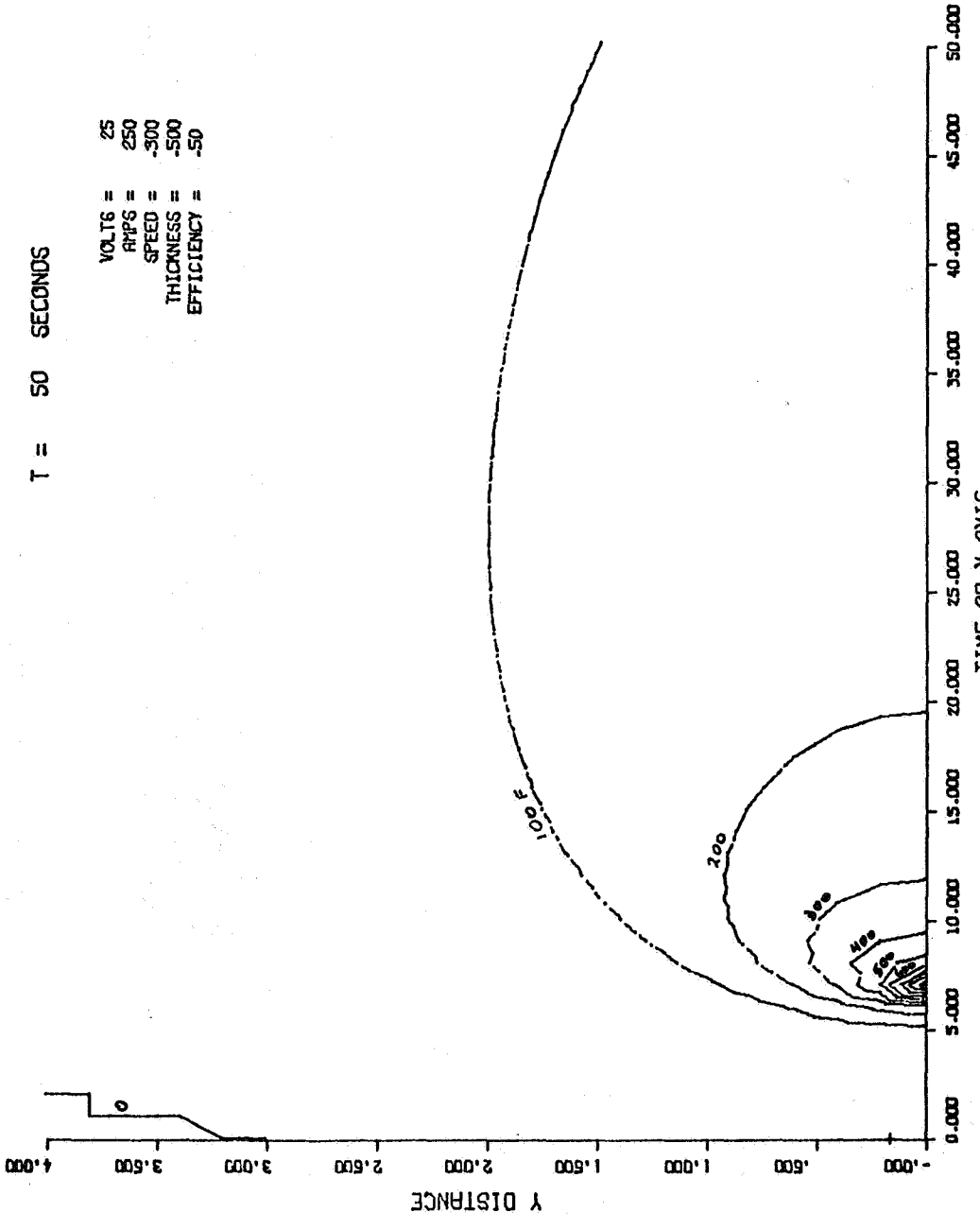

FIGURE A-33. ISOTHERM PATTERN, CONDITION 6

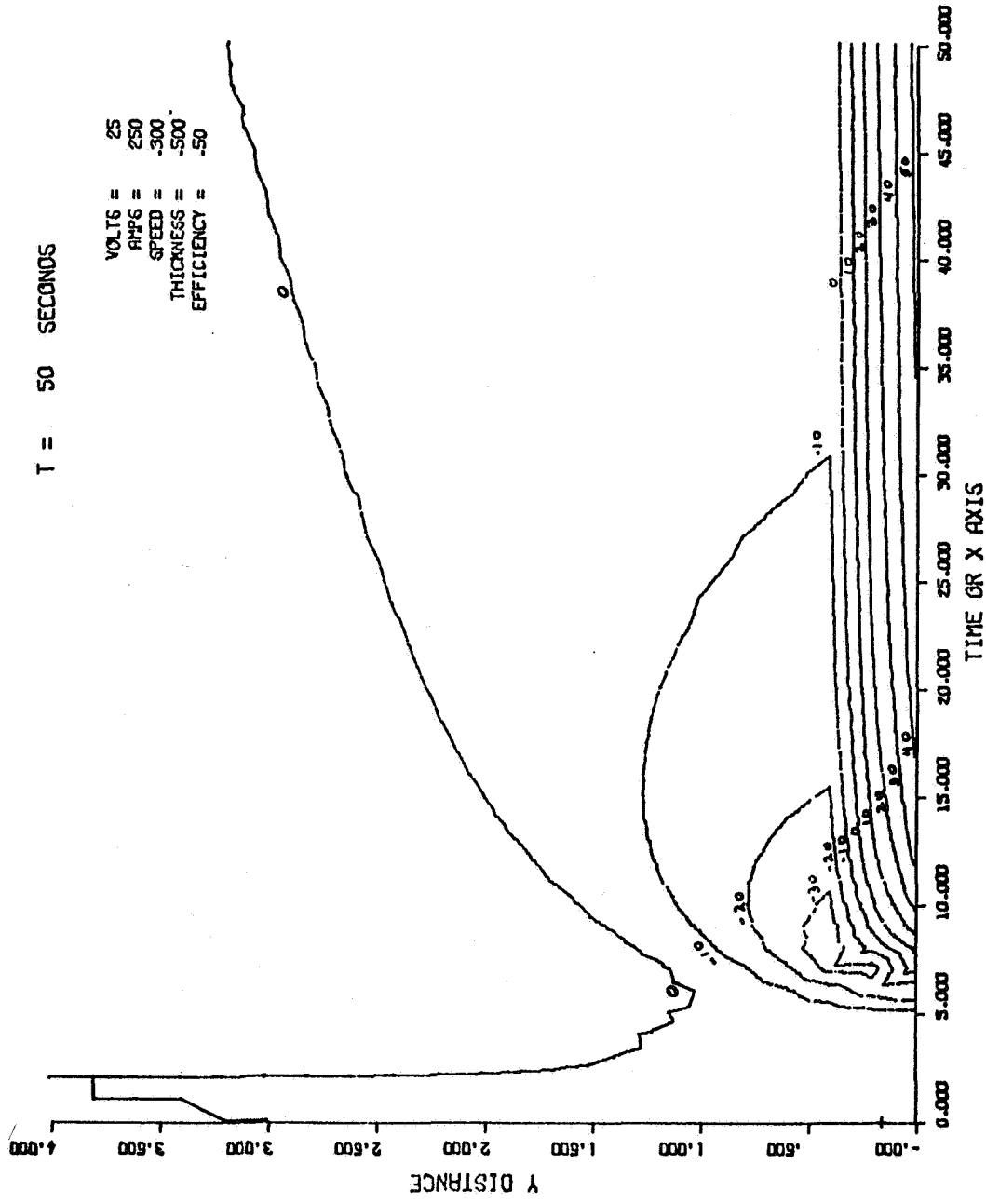

FIGURE A-34. ISOSTRESS PATTERN, CONDITION 6

LITERATURE CITED

1. George C. Marshall Space Flight Center, Huntsville, Alabama, PROCESSING OF BULKHEAD SEGMENTS FOR SATURN V VEHICLES, by E. A. Hasemeyer, R. B. Williams, and W. J. Travis, 22 April 1964, Report No. NASA TM X-53033.

2. T. B. Jefferson, MAN ON MOON: VIA WELDING TECHNOLOGY, Welding Engineer, 51, No. 4, 1966, pp. 49-52.

3. H. H. Dixon, STRUCTURAL RESEARCH AND DEVELOPMENT FOR CRYOGENIC UPPER STAGES, PART 1, Cryogenic Technology, 4, No. 2, 1968, pp. 44-51.

4. H. B. Farner and T. R. Rutkay, FABRICATING THE S-1C SPACE BOOSTER, The Welding Journal, 44, No. 1, 1965, pp. 29-34.

5. NASA USED TIG ON THE ALUMINUM SATURN V, Welding Design and Fabrication, 50, No. 5, 1965, pp. 62-63.

6. W. Spraragen and G. E. Claussen, SHRINKAGE DISTORTION IN WELDING, A REVIEW OF THE LITERATURE TO JANUARY 1, 1937, The Welding Journal, Research Supplement, 16, No. 7, 1937, pp. 21-40.

7. W. Spraragen and M. A. Corvi, SHRINKAGE DISTORTION IN WELDING, The Welding Journal, Research Supplement, 23, No. 11, 1944, pp. 545s-559s.

8. W. Spraragen and W. G. Ettinger, SHRINKAGE DISTORTION IN WELDING, The Welding Journal, Research Supplement, 29, Nos. 6 and 7, 1950, pp. 292s-294s, 323s-335s.

9. W. R. Osgood, RESIDUAL STRESSES IN METALS AND METAL CONSTRUCTION, New York, Reinhold Publishing Company, 1954.

10. Redstone Scientific Information Center, Redstone Arsenal, Alabama, NONDESTRUCTIVE MEASUREMENT OF RESIDUAL STRESSES IN METALS AND METAL STRUCTURES by K. Masubuchi, April 1965, Report No. RSIC 410.

11. T. Naka, SHRINKAGE AND CRACKING IN WELDS, Tokyo, Komino Publishing Company, 1950.

LITERATURE CITED (Continued)

12. H. Kihara and K. Masubuchi, DISTORTIONS AND RESIDUAL STRESSES DUE TO WELDING, Tokyo, The Sampo Publishing Company, 1955.

13. The Society of Naval Architects of Japan, Tokyo, RESEARCH ON WELDING STRESS AND DISTORTION IN JAPAN by H. Kihara, M. Watanable, K. Masubuchi, and K. Satoh, 1959.

14. M. Watanabe and K. Satoh, WELDING MECHANICS AND ITS APPLICATION, Tokyo, Asakura Publishing Company, 1965.

15. N. O. Okerblom, THE CALCULATION OF DEFORMATIONS OF WELDED METAL STRUCTURES, London, Her Majesty's Stationery Office, 1958.

16. R. Gunnert, RESIDUAL STRESSES, METHOD FOR MEASURING RESIDUAL STRESS AND ITS APPLICATION TO A STUDY OF RESIDUAL WELDING STRESSES, Stockholm, Almquist E. Wicksell, 1955.

17. W. S. Hall, H. Kihara, W. Soete, and A. A. Wells, BRITTLE FRACTURE OF WELDED PLATE, Englewood Cliffs, New Jersey, Prentice-Hall, Inc., 1967.

18. K. Masubuchi, CONTROL OF DISTORTION IN WELDED STRUCTURES, Commission X of the International Institute of Welding, April 1, 1968, Document X-456-68.

19. I. N. Artem'eva, STRESSES AND STRAINS AS INFLUENCED BY THE WELDING OF DURALUMIN D16T, Svarchnoe Proizvodatvo, 6, No. 2, 1960, pp. 15-19.

20. H. N. Hill, RESIDUAL WELDING STRESSES IN ALUMINUM ALLOYS, Metal Progress, 80, No. 2, 1961, pp. 92-96.

21. L. Capel, ALUMINUM WELDING PRACTICE, British Welding Journal, 8, No. 5, 1961, pp. 245-257.

22. A. A. Kazimirov and A. Ya. Nedoseka, THE RESIDUAL STRESSES AND DISTORTION WHICH DEVELOP WHEN THE AMg5V ALLOY IS WELDED, Avtomaticheskaya Svarka, 15, No. 10, 1962, pp. 16-21.

LITERATURE CITED (Continued)

23. K. Masubuchi and D. C. Martin, INVESTIGATION OF RESIDUAL STRESSES BY USE OF HYDROGEN CRACKING, PARTS I AND II, Welding Journal, Research Supplement, 40, No. 12, 1961, pp. 553s-563s, 45, No. 9, 1966, pp. 401s-418s.

24. S. Moriguchi, FUNDAMENTAL THEORY OF ELASTIC DISLOCATION IN ELASTIC SOLIDS, Applied Mathematics and Mechanics, 1, 1948, pp. 29-36 and 87-90.

25. K. Masubuchi, ANALYTICAL INVESTIGATION OF RESIDUAL STRESSES AND DISTORTION DUE TO WELDING, Welding Journal, Research Supplement, 39, No. 12, 1960, pp. 525s-537s.

26. N. S. Boulton and H. E. Lance Martin, RESIDUAL STRESSES IN ARC WELDED PLATES, Proc, Institution of Mechanical Engineers, 133, 1936, pp. 295-339.

27. O. E. Rodgers, and J. R. Fetcher, THE DETERMINATION OF INTERNAL STRESSES FROM THE TEMPERATURE HISTORY OF BUTT-WELDED PLATE, The Welding Journal, Research Supplement, 17, No. 11, 1938, pp. 4s-7s.

28. D. Rosenthal and J. Zabrs, TEMPERATURE DISTRIBUTION AND SHRINKAGE STRESSES IN ARC WELDING, Welding Journal, Research Supplement, 19, No. 9, 1940, pp. 323s-331s.

29. N. N. Prokhorov, and N. Nikeloevich Prokhorov, CALCULATING THE DEFORMATION CAUSED BY DEPOSITING A BEAD ON THE EDGE OF A PLATE, Automatic Welding, 17, No. 5, 1964, pp. 54-62.

30. A. A. Kazimirov and A. Ya. Nedoseka, THE RESIDUAL STRESSES CREATED WHEN A BEAD IS DEPOSITED ON THE LONGITUDINAL EDGE OF AN A1Mg5V ALLOY PLATE, Automatic Welding, 18, No. 1, 1965, pp. 28-32.

31. L. Tall, THE STRENGTH OF WELDED BUILT-UP COLUMNS, Lehigh University, Ph. D. Dissertation, 1961.

32. L. Tall, RESIDUAL STRESSES IN WELDED PLATES - A THEORETICAL STUDY, Welding Journal, Research Supplement, 43, No. 1, 1964, pp. 10s-23s.

LITERATURE CITED (Continued)

33. I. Tuzi, STUDIES ON ELASTOPLASTIC THERMAL STRESSES IN RECTANGULAR PLATES WITH UNIVERSAL TEMPERATURE VARIATION (Second Report), Journal of the Society of Naval Architects of Japan, 116, December 1964, pp. 78-89.

34. I. Tuzi, STUDIES ON ELASTOPLASTIC THERMAL STRESSES IN RECTANGULAR PLATES WITH UNIAXIAL TEMPERATURE VARIATION (First Report), Journal of the Society of Naval Architects of Japan, 115, June 1964, pp. 116-128.

35. I. Tuzi, STUDIES ON ELASTOPLASTIC THERMAL STRESSES IN RECTANGULAR PLATES WITH UNIAXIAL TEMPERATURE VARIATION (Fourth Report) — TRANSIENT AND RESIDUAL STRESSES DUE TO BUTT WELDING, Journal of the Society of Naval Architects of Japan, 118, November 1965, pp. 307-317.

36. I. Tuzi, STUDIES ON ELASTOPLASTIC THERMAL STRESSES IN RECTANGULAR PLATES WITH UNIAXIAL TEMPERATURE VARIATION (Third Report) — ON THE LOW-TEMPERATURE STRESS RELIEVING TREATMENT OF WELDMENTS, Journal of the Society of Naval Architects of Japan, 117, June 1965, pp. 244-255.

37. N. N. Prokhorov and N. Nikeloevich Prokohorov, THE INTERNAL DEFORMATION OF WELD METAL, Automatic Welding, 19, No. 3, 1966, pp. 15-20.

38. V. I. Makhnenko and E. A. Velikowanenko, THE STUDY BY COMPUTER OF THE STRESSED AND DEFORMED STATES IN STRUCTURES MADE OF WELDED NARROW PLATES, Automatic Welding, 19, No. 7, 1966, pp. 28-32.

39. H. Kihara and K. Masubuchi, THEORETICAL STUDIES ON THE RESIDUAL WELDING STRESS, Report of Transportation Technical Research Institute, No. 6, 1953.

40. S. Moriguchi, ANALOGY BETWEEN THE THEORY OF RESIDUAL WELDING STRESS AND THE WING THEORY, Proc. of the 5th Japan National Congress for Applied Mechanics, 1955.

41. W. F. Durand, AERODYNAMIC THEORY, 3 and 7, Berlin, Julius Springer, 1934.

LITERATURE CITED (Continued)

42. M. Watanabe and K. Satoh, ON THE TYPE OF DISTORTION IN VARIOUS WELDED JOINTS, Journal of Japan Welding Society, 26, 1957, pp. 399-405.

43. M. Watanabe and K. Satoh, FUNDAMENTAL STUDY ON BUCKLING OF THIN STEEL PLATE DUE TO BEAD-WELDING, Journal of Japan Welding Society, 27, 1958, pp. 313-320.

44. Koichi Masubuchi, BUCKLING TYPE DEFORMATION OF THIN PLATE DUE TO WELDING, Proc. of the 3rd Japan National Congress for Appl. Mech., 1955, pp. 107-111.

45. Toshio Mura, ON THE BUCKLING DEFORMATION OF THIN PLATES DUE TO WELDING, Proc. of the 3rd Japan National Congress for Appl. Mech., 1955, pp. 103-106.

46. D. Rosenthal, MATHEMATICAL THEORY OF HEAT DISTRIBUTION DURING WELDING AND CUTTING, Welding Journal, Research Supplement, 20, No. 5, 1941, pp. 220s-234s.

47. C. M. Adams, Jr., COOLING RATES AND PEAK TEMPERATURES IN FUSION WELDING, The Welding Journal, Research Supplement, 37, No. 5, 1958, pp. 210s-215s.

48. J. M. Barry, Z. Paley, and C. M. Adams, Jr., HEAT CONDUCTION FROM MOVING ARCS IN WELDING, The Welding Journal, Research Supplement, 42, No. 3, 1963, pp. 97s-104s.

49. K. Masubuchi, TEMPERATURE DISTRIBUTION OF WELDED PLATES, PART I, PLANE PROBLEM, Monthly Report of Transportation Technical Research Institute, Tokyo, 2, No. 2, 1953, pp. 47-56.

50. N. Christensen, V. Davis, deL, and K. Gjermundsen, DISTRIBUTION OF TEMPERATURES IN ARC WELDING, British Welding Journal, 12, No. 2, 1965, pp. 54-75.

51. N. N. Rykalin, CALCULATION OF HEAT PROCESS IN WELDING, Moscow, 1960.

LITERATURE CITED (Continued)

52. Defense Metals Information Center, Battelle Memorial Institute, Columbus, Ohio, BACKGROUND FOR THE DEVELOPMENT OF MATERIALS TO BE USED IN HIGH-STRENGTH-STEEL STRUCTURAL WELDMENTS, July 1962, DMIC Report No. 172.

53. H. S. Carslaw and J. C. Jaeger, CONDUCTION OF HEAT IN SOLIDS, Oxford University Press, 1959.

54. Wright Air Development Division, Wright-Patterson Air Force Base, Ohio, THERMAL PROPERTIES OF SOLID MATERIALS, VOL, 2 ALLOYS by A. Goldsmith, H. J. Hirschhorn, and T. E. Waterman, November 1960, WADC Technical Report No. 58-476.

55. R. J. Grosh, E. A. Trabant, and G. A. Hawkins, TEMPERATURE DISTRIBUTION IN SOLIDS OF VARIABLE THERMAL PROPERTIES HEATED BY MOVING HEAT SOURCES, Quarterly of Applied Mathematics, 13, No. 2, July 1955, pp. 161-167.

56. N. S. Boulton, and H. E. Lance-Martin, RESIDUAL STRESSES IN ARC WELDED PLATES, Proc. Institution of Mechanical Engineers, 133, 1936, pp. 295-339.

57. D. Rosenthal and R. Schmerber, THERMAL STUDY OF ARC WELDING, Welding Journal, Research Supplement, 17, No. 4, 1938, pp. 2-8.

58. G. N. Watson, THEORY OF BESSEL FUNCTIONS, Cambridge, New York and London, 1922.

59. N. W. McLochlan, BESSEL FUNCTIONS FOR ENGINEERS, Oxford University Press, 1955.

60. Manufacturing Engineering Laboratory, George C. Marshall Space Flight Center, Huntsville, Alabama, A SUMMARY OF MEASUREMENTS OF METAL MOVEMENT RESULTING FROM WELDING IN THE HORIZONTAL POSITION by R. W. Jackson, 15 August 1967, MEL Report No. WD-70-67.

61. Manufacturing Engineering Laboratory, George C. Marshall Space Flight Center, Huntsville, Alabama, AN ENGINEERING EVALUATION OF METAL MOVEMENT MEASUREMENTS ON A 2014-T6 ALUMINUM ALLOY BEAD-ON-PLATE WELDMENT, 21 February 1968, MEL Report No. WD-79-68.

LITERATURE CITED (Concluded)

62. S. Timoshenko, STRENGTH OF MATERIALS, New York, D. Von Nostrand Company, Inc., 1956 (3rd Edition).

DISTRIBUTION

EXTERNAL

	No. of Copies
Air University Library ATTN: AUL3T Maxwell Air Force Base, Alabama 36112	1
U. S. Army Electronics Proving Ground ATTN: Technical Library Fort Huachuca, Arizona 85613	1
Naval Weapons Center ATTN: Technical Library, Code 753 China Lake, California 93555	1
Naval Weapons Center, Corona Laboratories ATTN: Documents Librarian Corona, California 91720	1
Lawrence Radiation Laboratory ATTN: Technical Information Division P. O. Box 808 Livermore, California 94550	1
Sandia Corporation ATTN: Technical Library P. O. Box 969 Livermore, California 94551	1
U. S. Naval Postgraduate School ATTN: Library Monterey, California 93940	1
Electronic Warfare Laboratory, USAECOM Post Office Box 205 Mountain View, California 94042	1
Jet Propulsion Laboratory ATTN: Library (TDS) 4800 Oak Grove Drive Pasadena, California 91103	2
U. S. Naval Missile Center ATTN: Technical Library, Code N3022 Point Mugu, California 93041	1
U. S. Army Air Defense Command ATTN: ADSX Ent Air Force Base, Colorado 80912	1
Central Intelligence Agency ATTN: OCR/DD-Standard Distribution Washington, D. C. 20505	4
Harry Diamond Laboratories ATTN: Library Washington, D. C. 20438	1
Scientific & Tech. Information Div., NASA ATTN: ATS Washington, D. C. 20546	1
U. S. Atomic Energy Commission ATTN: Reports Library, Room G-017 Washington, D. C. 20545	1
U. S. Naval Research Laboratory ATTN: Code 2027 Washington, D. C. 20390	1
Weapons Systems Evaluation Group Washington, D. C. 20305	1
John F. Kennedy Space Center, NASA ATTN: KSC Library, Documents Section Kennedy Space Center, Florida 32899	2
APGC (PGBPS-12) Eglin Air Force Base, Florida 32542	1
U. S. Army CDC Infantry Agency Fort Benning, Georgia 31905	1
Argonne National Laboratory ATTN: Report Section 9700 South Cass Avenue Argonne, Illinois 60440	1
U. S. Army Weapons Command ATTN: AMSWE-RDR Rock Island, Illinois 61201	1
Rock Island Arsenal ATTN: SWERI-RDI Rock Island, Illinois 61201	1
U. S. Army Cmd. & General Staff College ATTN: Acquisitions, Library Division Fort Leavenworth, Kansas 66027	1
Combined Arms Group, USACDC ATTN: Op. Res., P and P Div. Fort Leavenworth, Kansas 66027	1
U. S. Army CDC Armor Agency Fort Knox, Kentucky 40121	1
Michoud Assembly Facility, NASA ATTN: Library, I-MICH-OSD P. O. Box 29300 New Orleans, Louisiana 70129	1
Aberdeen Proving Ground ATTN: Technical Library, Bldg. 313 Aberdeen Proving Ground, Maryland 21005	1
NASA Sci. & Tech. Information Facility ATTN: Acquisitions Branch (S-AK/DL) P. O. Box 33 College Park, Maryland 20740	5
U. S. Army Edgewood Arsenal ATTN: Librarian, Tech. Info. Div. Edgewood Arsenal, Maryland 21010	1

	No. of Copies
National Security Agency ATTN: C3/TDL Fort Meade, Maryland 20755	1
Goddard Space Flight Center, NASA ATTN: Library, Documents Section Greenbelt, Maryland 20771	1
U. S. Naval Propellant Plant ATTN: Technical Library Indian Head, Maryland 20640	1
U. S. Naval Ordnance Laboratory ATTN: Librarian, Eva Liberman Silver Spring, Maryland 20910	1
Air Force Cambridge Research Labs. L. G. Hanscom Field ATTN: CRMXLR/Stop 29 Bedford, Massachusetts 01730	1
U. S. Army Materials Research Agency ATTN: AMXMR-ATL Watertown, Massachusetts 02172	1
Strategic Air Command (OAI) Offutt Air Force Base, Nebraska 68113	1
Picatinny Arsenal, USAMUCOM ATTN: SMUPA-VA6 Dover, New Jersey 07801	1
U. S. Army Electronics Command ATTN: AMSEL-CB Fort Monmouth, New Jersey 07703	1
Sandia Corporation ATTN: Technical Library P. O. Box 5800 Albuquerque, New Mexico 87115	1
ORA(RRRT) Holloman Air Force Base, New Mexico 88330	1
Los Alamos Scientific Laboratory ATTN: Report Library P. O. Box 1663 Los Alamos, New Mexico 87544	1
White Sands Missile Range ATTN: Technical Library White Sands, New Mexico 88002	1
Rome Air Development Center (EMLAL-1) ATTN: Documents Library Griffiss Air Force Base, New York 13440	1
Brookhaven National Laboratory Technical Information Division ATTN: Classified Documents Group Upton, Long Island, New York 11973	1
Watervliet Arsenal ATTN: SWEWV-RD Watervliet, New York 12189	1
U. S. Army Research Office (ARO-D) ATTN: CRD-AA-IP Box CM, Duke Station Durham, North Carolina 27706	1
Lewis Research Center, NASA ATTN: Library 21000 Brookpark Road Cleveland, Ohio 44135	1
U. S. Army Artillery & Missile School ATTN: Guided Missile Department Fort Sill, Oklahoma 73503	1
U. S. Army CDC Artillery Agency ATTN: Library Fort Sill, Oklahoma 73504	1
U. S. Army War College ATTN: Library Carlisle Barracks, Pennsylvania 17013	1
U. S. Naval Air Development Center ATTN: Technical Library Johnsville, Warminster, Pennsylvania 18974	1
Frankford Arsenal ATTN: C-2500-Library Philadelphia, Pennsylvania 19137	1
Div. of Technical Information Ext., USAEC P. O. Box 62 Oak Ridge, Tennessee 37830	1
Oak Ridge National Laboratory ATTN: Central Files P. O. Box X Oak Ridge, Tennessee 37830	1
Air Defense Agency, USACDC ATTN: Library Fort Bliss, Texas 79916	1
U. S. Army Air Defense School ATTN: AKBAAS-DR-R Fort Bliss, Texas 79906	1

	No. of Copies
U. S. Army Combat Developments Command Institute of Nuclear Studies Fort Bliss, Texas 79916	1
Manned Spacecraft Center, NASA ATTN: Technical Library, Code BM6 Houston, Texas 77058	1
Defense Documentation Center Cameron Station Alexandria, Virginia 22314	20
U. S. Army Research Office ATTN: STINFO Division 3045 Columbia Pike Arlington, Virginia 22204	1
U. S. Naval Weapons Laboratory ATTN: Technical Library Dahlgren, Virginia 22448	1
U. S. Army Mobility Equipment Res. & Dev. Center ATTN: Tech Doc Center, Bldg. 315, Vault Fort Belvoir, Virginia 22060	2
Langley Research Center, NASA ATTN: Library, MS-185 Hampton, Virginia 23365	1
Research Analysis Corporation ATTN: Library McLean, Virginia 22101	1
U. S. Army Tank Automotive Center ATTN: SMOTA-RTS.1 Warren, Michigan 48090	1
Battelle Memorial Institute ATTN: Mr. Vern Ellzey 505 King Avenue Columbus, Ohio 43201	25

	No. of Copies
INTERNAL	
Headquarters U. S. Army Missile Command Redstone Arsenal, Alabama 35809	
ATTN: AMSMI-D	1
AMSMI-XE, Mr. Lowers	1
AMSMI-Y	1
AMSMI-R, Mr. McDaniel	1
AMSMI-RAP	1
AMSMI-RBLD	10
USACDC-LnO	1
AMSMI-RB, Mr. Croxton	1
AMSMI-RBR	25
AMSMI-R, Mr. Fagan	1
AMSMI-RR, Dr. Hallowes	1
National Aeronautics & Space Administration Marshall Space Flight Center Marshall Space Flt. Ctr., Ala. 35812	
ATTN: R-ME-MW, Mr. Hoppes	100
MS-T, Mr. Wiggins	5
DIR, Mr. Shepherd	1
R-RP-N, Dr. Shelton	1
I-PL-CH, Mr. Goodrum	1
Commanding General U. S. Army Sentinel System Command ATTN: SENSC-XS, Dr. Lange Redstone Arsenal, Alabama 35809	1

DOCUMENT CONTROL DATA - R & D

(Security classification of title, body of abstract and indexing annotation must be entered when the overall report is classified)

1. ORIGINATING ACTIVITY *(Corporate author)*
Battelle Memorial Institute
505 King Avenue
Columbus, Ohio 43201

2a. REPORT SECURITY CLASSIFICATION
Unclassified

2b. GROUP
N/A

3. REPORT TITLE

ANALYSIS OF THERMAL STRESSES AND METAL MOVEMENT DURING WELDING

4. DESCRIPTIVE NOTES *(Type of report and inclusive dates)*
None

5. AUTHOR(S) *(First name, middle initial, last name)*
Koichi Masubuchi
F. B. Simmons
R. E. Monroe

6. REPORT DATE
10 July 1968

7a. TOTAL NO. OF PAGES
155

7b. NO. OF REFS
62

8a. CONTRACT OR GRANT NO.
DA-01-021-AMC-14693(Z)

b. PROJECT NO.

c.

d.

9a. ORIGINATOR'S REPORT NUMBER(S)
RSIC-820

9b. OTHER REPORT NO(S) *(Any other numbers that may be assigned this report)*
AD

10. DISTRIBUTION STATEMENT

This document has been approved for public release and sale; its distribution is unlimited.

11. SUPPLEMENTARY NOTES
None

12. SPONSORING MILITARY ACTIVITY
Redstone Scientific Information Center
Research and Development Directorate
U. S. Army Missile Command
Redstone Arsenal, Alabama 35809

13. ABSTRACT

A literature survey on thermal stresses during welding and buckling after welding is described. From the analyses found, a computer program was developed to calculate thermal stresses and resulting residual stresses due to a moving heat source. This program is included in the appendix.

Studies at Marshall Space Flight Center on three-dimensional movement during welding of flat plate specimens are summarized and interpreted on the basis of the Battelle literature survey and computer analysis. It is concluded that local metal movement during welding appears to be caused by bending moment and that general metal movement is apparently caused by buckling. Future programs to improve the present analysis are recommended.

DD FORM 1 NOV 68 1473 REPLACES DD FORM 1473, 1 JAN 64, WHICH IS OBSOLETE FOR ARMY USE.

14. KEY WORDS	LINK A		LINK B		LINK C	
	ROLE	WT	ROLE	WT	ROLE	WT
Welding						
Distortions						
Stresses						
Metal movement						
Buckling						
Heat flow						
Shrinkage						